Matematisk-fysiske Meddelelser
udgivet af
Det Kongelige Danske Videnskabernes Selskab
Bind **35**, nr. 1

Mat. Fys. Medd. Dan. Vid. Selsk. **35**, no. 1 (1966)

DISTRIBUTION OF OCTUPOLE OSCILLATOR STRENGTH IN EVEN-EVEN SPHERICAL NUCLEI FROM Ni TO Pb

BY

C. J. VEJE

København 1966
Kommissionær: Munksgaard

Synopsis

The distribution of the octupole oscillator strength, arising from one-phonon excitations of density variation modes in even-even spherical nuclei, is analysed on the basis of an interaction consisting of pairing + octupole-octupole force.

Special attention is paid to the isospin structure of the states.

It is found that, in many cases, two or three lines of comparable strength occur in the low-energy spectrum ($\lesssim 5$ MeV).

The experimental evidence on energy and transition probability, which is available almost only for the very lowest state, can be accounted for reasonably well by a strength constant for the octupole-octupole force which varies smoothly with the atomic number.

PRINTED IN DENMARK
BIANCO LUNOS BOGTRYKKERI A-S

CONTENTS

1. Introduction

In recent years, a theory has been developed which gives a description of the density variation modes of nuclear vibrations in terms of single-particle excitations. This represents an improvement upon older, more phenomenological theories, not only by relating the collective and the single-particle aspects, but also by comprising in the same picture all degrees of collectiveness of the spectrum.

In a quantal system like a nucleus, density variations occur due to transitions of one or more particles between different states. When a particle is excited (a particle-hole pair created out of the ground state), the corresponding fluctuations in the nuclear field affect the motion of the other particles and tends to generate other particle-hole excitations.

Thus, because of the interaction between the particles through the field, the randomly distributed fluctuations from different single-particle excitations come in phase, and a more or less collective movement of the particles, a vibration, arises.

The octupole vibrations which we shall study are known from experiment to be less collective than the quadrupole ones. They should be more intimately connected to the details in the single-particle level scheme, and the oscillator strength in the low energy part of the spectrum might be spread over several levels.

The lowest octupole excitation has been studied by YOSHIDA (ref. 1) in a few cases.

In the present work we shall extend the investigation of the octupole excitation of lowest energy to a wider region of the periodic table. This gives information about the way in which the coupling constant for the effective force must vary with the atomic number in order to reproduce the observed energies. We are also going to study the excitations of higher energy and the whole energy distribution of the oscillator strength. It may be mentioned here that from the calculation two rather strong lines appear frequently in the low-energy region (2–5 MeV).

Since the isospin character of the vibrational states has been discussed only briefly before, we pay special attention to this problem and the relation to the isospin dependence of the field producing force (the long-range component).

2. The Hamiltonian

The "microscopic" description of collective excitations of a many-body system was introduced in nuclear physics by several authors, and we meet it under different names (method of linearized equations, random phase approximation, Sawada method, Baranger method, quasi-boson approximation, generalized Tamm-Dancoff method) (refs. 2 and 6). It has been used by several investigators, e.g., by YOSHIDA (ref. 1) in the study of quadrupole and octupole vibrations in some cases of spherical nuclei, by BÈS, by MARSHALEK, and by SOLOVIEV et al. for deformed nuclei (ref. 3), and by KISSLINGER and SORENSEN for quadrupole oscillations in a wide region of the periodic table (ref. 4). Since the theory has been presented repeatedly, we shall only mention here as much as is needed for introducing definitions and notations (which are almost the same as that used by YOSHIDA (ref. 1)). We consider spherical even-even nuclei. The particles are supposed to move in a shell-model potential, interacting by a short-range and a long-range force. Thus, the Hamiltonian is

$$H = H(\text{shell mod.}) + H(\text{short range}) + H(\text{long range}). \tag{2.1}$$

The short-range part of the interaction

The short-range part of the interaction is represented by a pairing force (ref. 5). Only that part of the pairing which influences the particles in the partly filled shells is taken into account, and pairing between neutrons and protons is not included.

The pairing + shell-model part of the Hamiltonian is

$$\left.\begin{aligned} &H(\text{shell model}) + H(\text{short range}) \\ &= \sum_{jmt_0} \varepsilon(j,t_0)a^+(j,m,t_0)a(j,m,t_0) \\ &-\tfrac{1}{4}G(t_0)\sum_{\substack{j',m',\\ j,m,t_0}} a^+(j',m',t_0)a^+(j',-m',t_0)a(j,-m,t_0)a(j,m,t_0) \\ &\qquad\qquad \times(-1)^{j'-m'-j+m}. \end{aligned}\right\} \tag{2.2}$$

Here, t_0 is the z component (or the $\nu = 0$ spherical tensor component) of the isospin of the particle with the convention

$$t_0 = \left\{ \begin{array}{l} \frac{1}{2} \text{ for protons} \\ -\frac{1}{2} \text{ for neutrons,} \end{array} \right\} \quad (2.3)$$

$\varepsilon(j, t_0)$ is the shell-model single-particle energy, $a^+(j, m, t_0)$ and $a(j, m, t_0)$ are creation and annihilation operators for a particle in the state j, m, t_0 (j represents all quantum numbers necessary to specify the state, with the exception of t_0 and the magnetic quantum number m). The force constant in the pairing $G(t_0)$, and the number of particles n in the partly filled shell are inserted into the BCS equations (2.4) and (2.5) which are solved for protons and neutrons separately with respect to the quantities $\lambda(t_0)$ and $\Delta(t_0)$:

$$\sum_j \frac{j + \frac{1}{2}}{E(j, t_0)} = \frac{2}{G(t_0)}, \quad (2.4)$$

$$\sum_j v^2(j, t_0) \times (2j + 1) = n, \quad (2.5)$$

where

$$E(j, t_0) = \left((\varepsilon(j, t_0) - \lambda(t_0))^2 + \Delta^2(t_0)\right)^{1/2}, \quad (2.6)$$

$$v^2(j, t_0) = \tfrac{1}{2}\left(1 - \frac{\varepsilon(j, t_0) - \lambda(t_0)}{E(j, t_0)}\right). \quad (2.7)$$

Here, $E(j, t_0)$ is the quasiparticle energy, $\lambda(t_0)$ the chemical potential or Fermi energy, $\Delta(t_0)$ the gap, $v^2(j, t_0)$ is the probability for the shell-model level jmt_0 to be filled. The probability for it to be empty is

$$u^2(j, t_0) = 1 - v^2(j, t_0). \quad (2.8)$$

The index t_0 is often omitted below.

Since the octupole oscillations involve mainly single-particle transitions between different shells, the pairing has less influence than for the quadrupoles. It has been checked that uncertainty in the pairing strength constant G is less significant than uncertainties in other parameters. Thus, in almost all cases (cf. sect. 14) we have used a standard value for G/A (A is the atomic number).

The long-range part of the interaction

We shall simulate the interaction between the particles through the octupole part of the nuclear field by an effective force of attractive long-range octupole-octupole type, working between all nucleons. Expressed in terms of creation and annihilation operators it takes the form

$$\left.\begin{aligned} & H \text{ (long range)} \\ &= -\tfrac{1}{2}\sum_{\substack{\mu \\ j's \\ m's \\ t_0's}} (-1)^{3-\mu} \langle t_0'(1)\, t_0'(2) \,|\, \varkappa(\vec{t}(1),\vec{t}(2)) \,|\, t_0(1)\, t_0(2)\rangle \\ &\times \langle j_1' m_1' \,|\, i^3 Y_{3\mu}\left(\frac{r}{a}\right)^3 | j_1 m_1\rangle \langle j_2' m_2' \,|\, i^3 Y_{3-\mu}\left(\frac{r}{a}\right)^3 | j_2 m_2\rangle \\ &\times a^+(j_1, m_1', t_0'(1))\, a^+(j_2', m_2', t_0'(2)) \\ &\times a(j_2, m_2, t_0(2))\, a(j_1, m_1, t_0(1)), \end{aligned}\right\} \quad (2.9)$$

where the quantity

$$a = \left(\frac{\hbar}{M\omega_0}\right)^{1/2}, \quad (2.10)$$

M being the nucleon mass and ω_0 the frequency of the harmonic oscillator used in the shell-model potential. (For further details, see below). In the force constant $\varkappa$ we have introduced the isospin of the nucleons $\vec{t}(1)$ and $\vec{t}(2)$.

Assuming the interaction to be invariant under rotations in isospin space, we can write $\varkappa$ in the form

$$\left.\begin{aligned} \varkappa &= \varkappa_0 + \varkappa_1 \,.\, 4\vec{t}(1) \,.\, \vec{t}(2) \\ &= \varkappa_0 + \varkappa_1 \sum_{\nu} 2\, t_\nu(1)\, 2\, t_{-\nu}(2)(-1)^\nu, \end{aligned}\right\} \quad (2.11)$$

where $t_\nu(1)$ and $t_\nu(2)$ are spherical components of the isospins of the particles. Thus, $\varkappa_0$ represents the isoscalar or $\tau = 0$ component of the force, and $\varkappa_1$ the isovector or $\tau = 1$ part. In the following section we come back to the relative magnitude and sign of $\varkappa_1$ and $\varkappa_0$.

Below we concentrate on that part of the field which acts on protons or neutrons, but does not change neutrons into protons, or vice versa. In that case, only the $\nu = 0$ part of the force is working and thus it is the only part which is considered in the treatment below. The $\nu \neq 0$ components are

relevant when exciting vibrations in the neighbouring odd-odd nuclei (cf. sect. 4).

Since the force is introduced to describe the variations in the field, we shall only take into account the field-producing part of the interaction (i.e. the annihilation matrix element in the particle-hole interaction).

The radial dependence in the field is not very well established. Our choice is made mainly for the sake of simplicity, and further investigations would be of great interest.

We shall primarily study the low-lying, strong excitations, which are supposed to be connected to vibrations of the nuclear surface. With our expression for the radial matrix element the surface region obtains a heavy weight. It may be that contributions to the field interaction from single-particle transitions $j \to j'$, involving changes in the principal quantum number of the harmonic oscillator $|\Delta N| = 3$, are not properly weighted in our picture. For instance, particles with a tail far outside the nucleus probably give rise to much smaller polarization of the core than supposed by the r^3 dependence which attributes a great influence to the outermost part of the wave function. A better dependence might be obtained, e.g., by using the radial derivative of a Saxon-Wood potential. The effect should be especially significant for the resulting high-energy modes, whereas the low-energy modes should be less affected. For our choice of force it appears that, for single-particle transitions with $\Delta N = 1$, the radial matrix elements are all of the same order of magnitude, even when squared. (The smallest values are obtained when the change in the number of radial nodes is maximal).

This means that the radial part of the interaction does not give rise to strong cancellation of any of the contributions from the single-particle transitions of low energy. For the $\Delta N = 3$ terms the square of the radial matrix element is fluctuating more strongly, sometimes being quite small when a great change in the number of radial nodes is involved. Roughly speaking, the squares of the $\Delta N = 3$ radial matrix elements are half as large as the $\Delta N = 1$ terms. The angular part of the matrix element is very sensitive to whether spin flip is involved or not. E.g., the square of the reduced matrix element is about 20 times larger for $j_1, j_1' = 7/2, 13/2$ than for $j_1, j_1' = 9/2, 13/2$.

It may finally be mentioned that it is still an unresolved problem whether the isospin independent ($\tau = 0$) field and the isospin dependent field ($\tau = 1$) are of the same radial structure. (For a definition of τ, see sections 3 and4). You might suggest that for the $\tau = 1$ modes volume phenomena play a greater role compared to surface phenomena than for $\tau = 0$ modes and, thus, that the radial dependence of the $\tau = 1$ field is slower than for the $\tau = 0$ field.

3. The excitations

For the total Hamiltonian H (2.1) the quasi-boson approximation is used. We describe the excitation as a superposition of two-quasiparticle creations and annihilations and write the excitation operator $B^+(\alpha)$ in the form

$$\left.\begin{aligned} B^+(\alpha) = \sum_{\substack{j_1 j_2 \\ m_1 m_2 \\ t_0}} \{ & p(\alpha, j_1, j_2, t_0) \langle j_1 m_1 j_2 m_2 \mid 3\mu \rangle \alpha^+(j_1, m_1, t_0) \alpha^+(j_2, m_2, t_0) \\ & + (-)^{\mu} q(\alpha, j_1, j_2, t_0) \langle j_1 m_1 j_2 m_2 \mid 3 - \mu \rangle \alpha(j_2, m_2, t_0) \alpha(j_1, m_1, t_0) \}, \end{aligned}\right\} \quad (3.1)$$

where the quasiparticle creation and annihilation operators are given by

$$\alpha^+(j, m, t_0) = u(j, t_0) a^+(j, m, t_0) - (-1)^{j-m} v(j, t_0) a(j, -m, t_0), \quad (3.2)$$

$$\alpha(j, m, t_0) = u(j, t_0) a(j, m, t_0) - (-1)^{j-m} v(j, t_0) a^+(j, -m, t_0). \quad (3.3)$$

This means that the two-quasiparticle excitations (each having energy $E(j_1) + E(j_2)$), are considered to be elementary oscillators which are coupled by the long-range part of the force. In the expression for $B^+(\alpha)$, j_1 and j_2 run over all possible proton and neutron states, but each pair should only be taken once, i.e. if $j_1 j_2 t_0$ is included, $j_2 j_1 t_0$ should not be.

Now, $B^+(\alpha)$ working on the ground state $|0\rangle$, gives the excited state $|\alpha\rangle$ with energy $\hbar\omega_\alpha$

$$|\alpha\rangle = B^+(\alpha)|0\rangle \quad (3.4)$$

and $B(\alpha)|0\rangle = 0$, where $B(\alpha)$ is the hermitian conjugate to $B^+(\alpha)$. We further have

$$[H, B^+(\alpha)] = \hbar\omega_\alpha B^+(\alpha) \quad (3.5)$$

which, on inserting (3.1), gives the expressions (12.1) and (12.2) for $p(\alpha, j_1 j_2 t_0)$ and $q(\alpha, j_1 j_2 t_0)$ used in sect. 12.

The orthonormality of the states gives (taking as above in eq. (3.1) each pair $j_1 j_2$ only once)

$$\sum_{j_1 j_2 t_0} \{ p(\alpha, j_1, j_2, t_0) p(\alpha', j_1, j_2, t_0) - q(\alpha, j_1, j_2, t_0) q(\alpha', j_1, j_2, t_0) \} = \delta_{\alpha\alpha'}. \quad (3.6)$$

Following the common procedure (ref. 6) we end up by eq. (3.7) the solutions $\hbar\omega$ of which are the resulting energies

$$\left(\frac{\varkappa_p}{7}S^p - 1\right)\left(\frac{\varkappa_n}{7}S^n - 1\right) - \frac{\varkappa_{np}^2}{49}S^pS^n = 0 \tag{3.7}$$

or

$$4\frac{\varkappa_0\varkappa_1}{49}S^pS^n - \frac{\varkappa_0 + \varkappa_1}{7}(S^p + S^n) + 1 = 0. \tag{3.8}$$

Here,

$$S^p = \sum_{jj'}^{p} \frac{\langle l'j' \| i^3 Y_3 \left(\frac{r}{a}\right)^3 \| lj\rangle^2 \big(u(j)v(j') + v(j)u(j')\big)^2 \big(E(j) + E(j')\big)}{\big(E(j) + E(j')\big)^2 - (\hbar\omega)^2}, \tag{3.9}$$

where the sum runs over all possible proton states j and j', which may be coupled to spin and parity 3^-. The analogous neutron quantity is denoted by S^n.

The first term in the numerator in S^p is an ordinary reduced matrix element

$$\left.\begin{aligned} \langle l'j' \| i^3 Y_3 \left(\frac{r}{a}\right)^3 \| lj\rangle &= (4\pi)^{-1/2} i^{l-l'+3}(-1)^{j-1/2} \\ \times \tfrac{1}{2}\big(1 + (-1)^{l'+l-3}\big)\langle j' j \tfrac{1}{2} -\tfrac{1}{2} \mid 30\rangle &\langle l'j' \mid \left(\frac{r}{a}\right)^3 \mid lj\rangle \\ \times \big((2j+1)(2j'+1)\big)^{1/2}&. \end{aligned}\right\} \tag{3.10}$$

In ref. 1 YOSHIDA presents a table showing the matrix elements of $\left(\frac{r}{a}\right)^3$, using harmonic oscillator wave functions. The quantities $\varkappa_p$, $\varkappa_n$ and $\varkappa_{np}$ are the octupole-octupole force constants for the proton-proton, neutron-neutron and neutron-proton force, respectively. For these we have used the expressions (2.11):

$$\varkappa_n = \varkappa_p = \varkappa_0 + \varkappa_1, \tag{3.11}$$

$$\varkappa_{np} = \varkappa_0 - \varkappa_1. \tag{3.12}$$

If $\varkappa_1 = 0$, the equation (3.8) for the determination of $\hbar\omega$ reduces to

$$S^p + S^n = \frac{7}{\varkappa_0} \tag{3.13}$$

which is the usual secular equation, and $\varkappa_0 = 0$ gives

$$S^p + S^n = \frac{7}{\varkappa_1}. \tag{3.14}$$

The analogue to this equation has been discussed for dipoles (ref. 7) for which the opposite sign convention has been used in general.

In order to provide an idea of the variation of the force constant $\varkappa$ with A we may use a simple scaling argument.

If we assume the matrix elements to represent an interaction with a range short compared to the nuclear radius, the interaction matrix elements are inversely proportional to the nuclear volume, i.e. $\sim 1/A$. Since each of the factors $(r_1/a)^3$ and $(r_2/a)^3$ varies proportional to $A^{1/2}$, we expect $\varkappa$ to be proportional to A^{-2}.

In our treatment we look apart from couplings to other modes, although such effects may sometimes be of importance. Thus, the resulting states of excitation energies more than some few MeV appear in regions with large level density. In such a situation the present calculation is only expected to give the gross structure of the 3^- distribution.

For the low-lying states, the most important couplings may be those to modes which involve large amplitudes. Thus the couplings to the strongly collective quadrupole vibrations of very low energy are expected to be of special significance.

In deformed nuclei, we know that this coupling causes a splitting of octupole modes with different K values. In the present calculation the most interesting modification of the results which this effect may cause may be that the strength of the strong octupole line, which in the following calculation is often found in the 4–5 MeV region, may be spread over several states, which may be imagined as arising from the coupling of a 3^- phonon to one or more 2^+ phonons.

The isospin of the excitation

In this section we are going to discuss briefly the isospin properties of the excitations, which properties so far have been neglected.

In the same way as the excitation in ordinary space can be described by the spherical tensor quantum numbers λ, $\mu(\lambda = 3$ in our case), it may in isospin space be characterized by analogous quantities τ, ν, where τ must be either 0 or 1 in the present treatment. The excitation operator $B^+(\tau, \nu; \lambda, \mu)$ may e.g. be of the type

$$M(\tau = 0;\ \lambda = 3, \mu) = \sum_i \tfrac{1}{2} r_i^3 Y_{3\mu}(i) \tag{3.15}$$

or

$$M(\tau = 1, \nu;\ \lambda = 3, \mu) = \sum_i r_i^3 Y_{3\mu} t_\nu(i), \tag{3.16}$$

where i runs over all particles in the nucleus (cf. sect. 4). We shall use the matrix elements of the M operators between the ground state and the excited states to describe the isospin structure of the excitations, as further explained in sect. 4.

The matrix elements of $M(\tau = 1, \nu = 1; 3, \mu)$ are non-vanishing only when the excitation involves creation of a neutron hole, proton pair, i.e. when it leads to another nucleus. Such an excitation may be realized by a (p, n) scattering on the nucleus. In the same way τ, $\nu = 1, -1$ leads to the excitations of a neighbouring nucleus Z, $A \to Z-1$, A, e.g. by an (n, p) process. Such excitations and their relevance to the present treatment are discussed briefly in sect. 4. The $\tau = 0$ or τ, $\nu = 1{,}0$ excitations give rise to states in the target nucleus and, as we shall see below, these two excitations are in general mixed, although the strong low-lying states to a good approximation are $\tau = 0$.

As pointed out by LANE and SOPER (ref. 8) and later utilized and explained in greater detail, e.g., by SLIV (ref. 10) and by BOHR and MOTTELSON (ref. BM), the isospin T of a state in a heavy nucleus is in many respects a very well-conserved quantity. Therefore we must ensure that the states which we find have good (T, T_0). (T_0 is the third component of T).

As long as we only apply $\tau = 0$ excitation operators to the ground state, for which

$$(T, T_0) = (T_1, -T_1) = \left(\frac{N-Z}{2}, \frac{Z-N}{2}\right), \tag{3.17}$$

there is no problem: we reach a state with the same T, while τ, $\nu = 1{,}0$ operators may give rise to some mixture of $T = T_1$ and $T = T_1 + 1$. The $T_1 + 1$ part of the excitation is contained in the isobaric analogue to an excitation of low energy in the neighbouring nucleus with $T_0 = -T_1 - 1$. It has quite another structure than the T_1 states in the same energy region and is only mixed weakly with them (ref. 9).

To illustrate the relation to our calculation let us, for simplicity, assume sharp Fermi surfaces for protons and neutrons. Let $\varepsilon(F, n)$ and $\varepsilon(F, p)$ be the Fermi energies for neutrons and protons, respectively. Let us consider a particle-hole excitation for which the particle (i.e. a proton) is created in a state (j_1, m_1) such that $\varepsilon(j_1, m_1) < \varepsilon(F, n)$ or the hole (i.e. a neutron hole) is created in a state (j_2, m_2) such that $\varepsilon(j_2, m_2) > \varepsilon(F, p)$.

In this case T_- acting on the state gives zero. We cannot further align the state in isospin space and, hence, $T = T_1$.

For our purpose this means that, for single-particle transitions inside partly filled shells and for part of the transitions from one shell to the next, there is no possibility for isospin impurities.

It should be stressed that this does not mean that the excitation is pure $\tau = 0$, since $\tau = 1$ and $T = T_1$ are able to couple to T_1.

For the transitions of higher energy, T is not automatically conserved. Let us consider a definite particle-hole excitation (j_1, j_2) and let $A^+(\tau = 1, \nu = 0)$ create the particle-hole pair, coupled to $(\tau = 1, \nu = 0; \lambda = 3, \mu)$. The resulting state with good quantum numbers $(T, T_0) = (T_1, -T_1)$ is then formed by coupling of the ground state $T = T_1$ and $\tau = 1$:

$$\left.\begin{aligned} &\{A^+(\tau = 1)\,|\,T_1>\}_{(T_1,1)\,T_1,-T_1} \\ &= <10\,T_1 - T_1\,|\,T_1 - T_1>\, A^+(\tau = 1,\ \nu = 0)\,|\,T_1 - T_1> \\ &+ <1 - 1\,T_1 - T_1 + 1\,|\,T_1 - T_1>\, A^+(\tau = 1,\ \nu = -1)\,|\,T_1 - T_1 + 1> \end{aligned}\right\} \quad (3.18)$$

$$\left.\begin{aligned} &= \sqrt{\frac{T_1}{T_1+1}}\, A^+(\tau = 1,\ \nu = 0)\,|\,T_1 - T_1> \\ &- \sqrt{\frac{1}{T_1+1}}\, A^+(\tau = 1,\ \nu = -1)\,|\,T_1 - T_1 + 1> \end{aligned}\right\} \quad (3.19)$$

$$\simeq A^+(\tau = 1,\ \nu = 0)\,|\,T_1 - T_1> \quad \text{for} \quad T_1 >> 1. \quad (3.20)$$

The state is thus a superposition of an excitation, based on the ground state $|\,T_1 - T_1>$, and an excitation based on $|\,T_1 - T_1 + 1>$, which is the isobaric analogue to the ground state. In the following we neglect the last part. The justification for this procedure is, partly, that for the states of low energy which we are most interested in, the effect should be very small and, partly, the assumption of $T_1 \gg 1$, which should be well satisfied, except for the lightest nuclei considered.

When the Fermi surface is smeared out, i.e. when our elementary modes are two-quasiparticle excitations instead of particle-hole excitations, the discussion which was given above contains a slight oversimplification. This is due to the fact that the quasiparticles do not have a definite z component of the isospin in the way we have defined them. Thus, the elementary modes involving the creation of a proton-neutron quasiparticle pair are mixtures of $\nu = \pm 1$.

It shall finally be stressed that in general it is not allowed to treat the

coupling in isospin space between the vibration and the ground state of a heavy nucleus in the weak coupling limit. This means that it is not possible to consider the excitation operator as a definite entity, the isospin of which is coupled to that of the ground state by simple vector coupling, or which may be rotated in isospace without complications.

It is e.g. easy to find a ($\tau = 1$, $\nu = 1$) particle-hole excitation, for which the ($\tau = 1$, $\nu = 0$) partner gives zero when acting on the ground state of a heavy nucleus. This happens whenever the particle or the hole is placed in a level (j,m) which is occupied by neutrons but empty for the protons.

The isospin dependence of the long-range force

The isospin dependence of the long-range force is contained in the isovector component $\varkappa_1$ of which little information is available. It is expected to be negative (to have opposite sign of $\varkappa_0$), since this will push the $\tau = 1$ excitations upwards in energy, as is the case for the giant dipole. (For further details, see sect. 5). This means that the *nn* and *pp* force should be somewhat weaker than the *np* force, or even have opposite sign, if $\varkappa_0 < |\varkappa_1|$.

An estimate of the magnitude of $\varkappa_1$ may be obtained by assuming that the oscillating field has the same isospin dependence as the central nuclear field for which the dependence manifests itself, e.g., in the semi-empirical mass formula and in the real part of the optical potential (ref. 50). This gives

$$\varkappa_1/\varkappa_0 \simeq -1/2. \tag{3.21}$$

A similar result is obtained by assuming that the two-body force responsible for the interaction is approximately of Serber type. Such estimates have been discussed by BOHR and MOTTELSEN (ref. BM).

A determination of $\varkappa_1$ on the basis of a fit to the experimentally determined energies is not possible. This is analogous to the situation for quadrupole vibrations where even many more data are available (ref. KSII). This difficulty is caused by the fact that all the experimental information concerns the low-energy states, and for these the $\tau = 1$ part of the force has only little effect in comparison to the $\tau = 0$ part, and also compared to other parameters, as e.g. the single-particle energies which are not very well known. (We shall see below that a more detailed investigation of the 2–5 MeV part of the spectra, using inelastic scattering with different projectiles and comparing results for different states and for different nuclei, may be one of the best tools for determining $\varkappa_1$, but still a large uncertainty is expected). On the other hand, we are able to obtain a fairly correct picture of the strong lines in the low-energy spectrum without detailed information on $\varkappa_1$, and therefore

we have simply used an isospin independent octupole-octupole force in our general calculations in sect. 15.

By this choice the lines of $\tau = 1$ type are poorly determined but, as we shall see for $\varkappa_1 = -0.5\varkappa_0$, there is no strong tendency to build up very great, individual $\tau = 1$ lines.

A discussion of the influence of $\varkappa_1$ and some examples of spectra, calculated with $\varkappa_1 = -0.5\varkappa_0$ and $\varkappa_1 = -2\varkappa_0$, are presented in sections 5 and 9. For the strong lines of low energy it is possible to give simple rules for the changes in energies and reduced transition probabilities resulting from a finite $\varkappa_1$.

4. Reduced transition probabilities

The coherence and isospin properties of the excitations can be described in terms of the matrix elements of the multipole operators $M(\tau = 0;\ \lambda = 3, \mu)$ and $M(\tau = 1, \nu;\ \lambda = 3, \mu)$ which were given above ((3.15) and (3.16)).

In our treatment only the $\nu = 0$ component of $M(\tau = 1)$ is relevant.

Taking the square of the reduced matrix element from the ground state to the state in question (labelled $3^-, \alpha$), we obtain two new quantities, namely the reduced transition probabilities

$$\left.\begin{aligned} B_0 &\equiv B(\tau = 0;\ 0 \to 3-, \alpha) \\ &= |\langle 3-, \alpha || M(\tau = 0;\ \lambda = 3, \mu) || 0 \rangle|^2, \end{aligned}\right\} \quad (4.1)$$

and

$$\left.\begin{aligned} B_1 &\equiv B(\tau = 1,\ \nu = 0;\ 0 \to 3-, \alpha) \\ &\equiv |\langle 3-, \alpha || M(\tau = 1,\ \nu = 0;\ \lambda = 3, \mu) || 0 \rangle|^2. \end{aligned}\right\} \quad (4.2)$$

In the same way, the ordinary electric transition operator

$$M(E3, \mu) = \sum_i r_i^3 Y_{3\mu}(i)\, e\left(\tfrac{1}{2} + t_0(i)\right) \quad (4.3)$$

gives rise to

$$B \equiv B(E3;\ 0 \to 3-, \alpha) \equiv |\langle 3-, \alpha || M(E3, \mu) || 0 \rangle|^2. \quad (4.4)$$

We see that

$$M(E3, \mu) = e\big(M(\tau = 0;\ \lambda = 3, \mu) + M(\tau = 1,\ \nu = 0;\ \lambda = 3, \mu)\big). \quad (4.5)$$

If for an excitation B_1 vanishes, we shall call it pure $\tau = 0$, whereas $B_0 = 0$ for a pure $\tau = 1$ excitation.

The expressions for B_0 and B_1 can be obtained as special cases from the general formula for B. This has been calculated by KS II under certain conditions. Following their derivation it is easy to get a generalized expression

$$\left.\begin{aligned} B = a^6 \Big\{ & |S^n\Big(1-\frac{\varkappa_n}{7}S^n\Big)|^{1/2} S^p e_p + \mathrm{sign}\Big(\varkappa_{np} S^p\Big(1-\frac{\varkappa_n}{7}S^n\Big)\Big) \\ & \times |S^p\Big(1-\frac{\varkappa_p}{7}S^p\Big)|^{1/2} S^n e_n\Big\}^2 \Big/ \Big\{ |S^n\Big(1-\frac{\varkappa_n}{7}S^n\Big)| \times S'^p \\ & + |S^p\Big(1-\frac{\varkappa_n}{7}S^p\Big)| S'^n \Big\}. \end{aligned}\right\} \quad (4.6)$$

Here,

$$\mathrm{sign}\{x\} = \frac{x}{|x|} \quad (4.7)$$

and S'^p is the derivative of S^p with respect to $\hbar\omega$, the energy of the excited state:

$$\left.\begin{aligned} S'^p = \frac{\partial S^p}{\partial(\hbar\omega)} = \sum_{jj'}^{p} \Big\{ & \frac{2\hbar\omega\,|\langle l'j'||i^3 Y_3\Big(\frac{r}{a}\Big)^3||lj\rangle|^2}{\big((E(j)+E(j'))^2-(\hbar\omega)^2\big)^2} \\ & \times \big(E(j)+E(j')\big)\big(u(j)v(j')+v(j)u(j')\big)^2 \Big\}, \end{aligned}\right\} \quad (4.8)$$

S'^n being the analogous neutron quantity.

The quantities e_n and e_p are the effective charges of neutrons and protons, respectively.

Since we are taking all single-particle transitions into account, the effective charges for an $E3$ transition are the bare charges $e_p = e$ and $e_n = 0$. The expression for B_0, the $\tau = 0$ part of B, is obtained when using $e_p = e_n = 1/2$ in (4.6) while B_1 appears when $e_p = -e_n = 1/2$.

The following relation applies to the three quantities

$$B = e^2\big(\sqrt{B_0} \pm \sqrt{B_1}\big)^2, \quad (4.9)$$

where the minus sign should be used if

$$|S^p\Big(1-\frac{\varkappa_n}{7}S^n\Big)| < |S^n\Big(1-\frac{\varkappa_n}{7}S^p\Big)| \quad (4.10)$$

which, due to the neutron excess, often is the case.

If $\varkappa_1 = 0$ (but $\varkappa_0 \neq 0$) we obtain the simpler expressions

$$B = a^6 e^2 \frac{S^{p2}}{S'^p + S'^n}, \tag{4.11}$$

$$B_0 = a^6 \frac{(S^p + S^n)^2}{4(S'^p + S'^n)}, \tag{4.12}$$

$$B_1 = a^6 \frac{(S^p - S^n)^2}{4(S'^p + S'^n)}. \tag{4.13}$$

If $\varkappa_0 = 0$ and $\varkappa_1 \neq 0$ we get the same formula for B, whereas the expressions for B_0 and B_1 are interchanged because of the sign in the numerator in the general formula (4.6). For an arbitrary $\varkappa_0$, $\varkappa_1$ mixture the sign is sometimes positive, sometimes negative. For the strong states of low energy it is found to be positive in the calculations below.

Inelastic scattering

While B is connected to electromagnetic excitations, B_0 and B_1 are the relevant quantities in inelastic nucleon scattering.

When a particle passes through the nucleus, its motion is changed by the nuclear field and it interacts with the nucleons in a complicated manner.

In a simplified picture we may assume, however, that inside the nucleus the nucleons in a projectile interact with the nuclear field in very much the same way as the other nucleons do, and thus that the interaction essentially is of the form

$$\left.\begin{aligned} &\sum_{j,\mu} \{\varkappa_0 r_j^3 Y^*_{3\mu}(j) M(\tau = 0;\ \lambda = 3, \mu) \\ &+ 2\varkappa_1 \sum_{\nu} r_j^3 Y^*_{3\mu}(j) t^*_\nu M(\tau = 1, \nu;\ \lambda = 3, \mu)\}, \end{aligned}\right\} \tag{4.14}$$

where we sum over the nucleons j in the projectile. The $\tau = 1$, $\nu = \pm 1$ terms govern the charge exchange reactions considered below. For inelastic scattering without charge exchange the reduced transition probability will be proportional to

$$\left(\varkappa_0 \sqrt{B_0} \pm \varkappa_1 \sqrt{B_1} \frac{\sum_j 2t_0(j)}{k}\right)^2 \tag{4.15}$$

or

$$B_0\left(1 + b\sum_j \frac{2t_0(j)}{k}\right)^2, \tag{4.16}$$

where

$$b = \pm\frac{\varkappa_1}{\varkappa_0}\sqrt{\frac{B_1}{B_0}} \tag{4.17}$$

and k is the number of nucleons in the projectile. The plus sign should be used if $B_0 < B$ and the minus sign if $B_0 > B$. We note that we here have utilized the assumption of the simple isospin dependence of the interaction (4.14), whereas the precise dependence on the radial coordinate of the projectile nucleons is of minor importance.

Here, as in the following, we neglect the electromagnetic part of the excitation when we consider inelastic nucleon scattering.

The numerical value of the factor $\sum_j \frac{2t_0(j)}{k}$ in (4.16) is maximal when the projectile contains only one kind of nucleons, i.e. when $k = 1$. If the projectile contains both protons and neutrons, the B_1 part is somewhat washed away, and (4.16) comes closer to B_0.

The expression is simplified if either the total isospin of the projectile is zero, as for α-particles and deuterons, or if the relevant nuclear field with which it interacts is isospin independent ($\varkappa_1 = 0$). Then we get B_0. This means that we are exciting just the $\tau = 0$ part of the vibration.

If the excitation is either pure $\tau = 0$ or $\tau = 1$, only one of the terms survives, but in practice this situation is never reached (cf. sections 7 and 9).

One of the more interesting features in the expression is the interference between the two terms. Even when the state is fairly pure in τ character, i.e. $B_0 >> B_1$ or $B_1 >> B_0$, this interference gives rise to considerable variations in the relative cross sections, using projectiles with different isospin (cf. sect. 11).

Since the experimental material contains mainly measurements of B, and since the underlying theory for electromagnetic processes is more reliable than the theory of direct reactions, we will preferably discuss this quantity. However, we note that inelastic scattering, using different particles, may give in the future most valuable information on the structure of the excitations.

Charge exchange scattering

In the preceding section, we have discussed the inelastic processes connected to $\tau = 0$ and $\tau = 1$, $\nu = 0$ excitations. Now, whereas the $\tau = 0$ part

of the interaction only gives rise to scattering, the $\tau = 1$ part may flip the isospin of an incoming nucleon, i.e. give rise to charge exchange reactions, involving excitations of $\tau = 1$, $\nu = \pm 1$ character. Let us consider a (p,n) process.

We use again the simplified expression (4.14) for the interaction between the incoming particle and the nucleus. For the $\tau = 1$ part the ratio between the nuclear matrix elements for isospin flip to non-isospin flip of the nucleon is given by

$$\left.\begin{aligned} &\frac{\langle T_1 - T_1 + 1, \beta | M(\tau = 1,\ \nu = 1) | T_1 - T_1 \rangle}{\langle T_1 - T_1, \beta | M(\tau = 1,\ \nu = 0) | T_1 - T_1 \rangle} \\ &= \frac{\langle T_1 - T_1 11 | T_1 - T_1 + 1 \rangle \langle T_1 || M(\tau = 1) || T_1 \rangle}{\langle T_1 - T_1 10 | T_1 - T_1 \rangle \langle T_1 || M((\tau = 1 || T_1 \rangle} \\ &= \sqrt{\frac{1}{T_1}}, \end{aligned}\right\} \tag{4.18}$$

$| T_1 - T_1 + 1, \beta \rangle$ being a state in an odd-odd nucleus which is the isobaric analogue to the vibration $| T_1 - T_1, \beta \rangle$ in the target. Thus, by studying the relative probabilities for exciting low-energy states in the target and analogues in the odd-odd nucleus by protons we are able to learn something about the isospin dependence in the interaction between projectile and target.

Scattering via isobaric analogues and stripping

Without going into details we shall briefly sketch how we can obtain information on the structure of the octupole vibrations from stripping experiments and from inelastic proton scattering via isobaric analogue states (states with $T \neq -T_z$). For the sake of simplicity we only consider the last type of experiments. The generalization to stripping is straightforward.

When bombarding a nucleus, say (N_1, Z_1) which has $(T, T_0) = (T_1, -T_1)$, with protons, we are able to form various states $| N_1, Z_1 + 1, \beta \rangle$ with $(T, T_0) = (T_1 + \frac{1}{2}, -T_1 + \frac{1}{2})$ in the compound nucleus $(N_1, Z_1 + 1)$, which are isobaric analogues to states $| N_1 + 1, Z_1, \beta >$ with $(T, T_0) = (T_1 + \frac{1}{2}, -T_1 - \frac{1}{2})$ of low excitation energy in the nucleus $(N, Z) = (N_1 + 1, Z_1)$. The reaction amplitude for the entrance channel is proportional to

$$\langle N_1, Z_1 + 1, \beta | a^+ (\text{proton}) | N_1, Z_1, \text{ ground state} \rangle \tag{4.19}$$

in analogy to

$$\langle N_1 + 1, Z_1, \beta | a^+ (\text{neutron}) | N_1, Z_1, \text{ ground state} \rangle, \tag{4.20}$$

the square of which is a spectroscopic factor for a (d,p) process leading from the target ground state to the low excited state β in the nucleus $(N,Z) = (N_1+1, Z_1)$. Now, the compound state may decay by proton emission to some state in the target. In the decay the amplitude is determined by

$$\langle N_1, Z_1, \gamma \,|\, a\,(\text{proton}) \,|\, N_1, Z_1+1, \beta \rangle, \tag{4.21}$$

which (if β is not the analogue to the ground state) corresponds to a pick-up spectroscopic factor for neutron pick-up from an excited state in the target (N_1+1, Z_1) to a state γ in the final nucleus (N_1, Z_1).

One possibility of learning something about the structure of the octupole oscillations is thus to bombard an even Z odd N target with protons to form a 3^- isobaric analogue state in the compound nucleus. When this state decays through the different proton channels, this "pick-up" process provides information on the occupation of the different single-particle states in the 3^- oscillation.

As a simplified example, let the final state in the target be a single quasiparticle (j',m') + a quasiparticle vacuum, which is assumed to be the same as that in the compound nucleus, and let the emitted proton have quantum numbers j, m. The channel state is

$$\simeq \sum_{\substack{m \\ m'}} a^+(j,m,t_0 = \tfrac{1}{2}) \alpha^+(j',m',t_0' = -\tfrac{1}{2}) \langle jmj'm' \,|\, 3\mu \rangle \,|\, 0 \rangle \tag{4.22}$$

and the decaying state is the isobaric analogue to

$$B^+(3,\mu,\alpha) \,|\, 0' > \tag{4.23}$$

(a one-phonon state with $\lambda = 3$, μ). By $|\,0\rangle$ and $|\,0'\rangle$ we denote the relevant phonon vacua. The overlap is

$$\simeq u(j,m) p(\alpha,j,j'), \tag{4.24}$$

where $p(\alpha,j,j')$ is the amplitude for the j,j' two-quasiparticle excitation in the oscillation α.

When obtaining this result we have neglected the overall reduction factor $2T+1$ which appears in the transition probability for proton decay of an isobaric analogue state. This factor is easily understood, since we imagine that the isobaric analogue state can be formed by applying the isospin raising operator T_+ to the low-energy state in the $(N+1, Z)$ nucleus, i.e. by transforming a neutron into a proton. However, there are $2T+1$ excess neutrons which can be transformed. Thus, the particle with quantum numbers j, m only has the probability $(2T+1)^{-1}$ of having $t_0 = 1/2$ in the decaying analogue state.

Another possibility to learn something about the structure of the octupole oscillations is to study inelastic proton scattering from an even-even target via an isobaric analogue state in the compound system to a 3^- oscillation in the target. In a naive approach we think of using preferably isobaric states which are known (or expected) only to contain to a very small amount a component of a single particle coupled to a 3^- state. In a decay of the analogue state in which a proton is emitted, leaving a hole together with the "last odd particle", we may thus directly gain information on the probability that the target 3^- state contains just this specific particle-hole component.

Let us therefore assume, for simplicity, that the compound state is just the analogue to a single quasiparticle + a quasiparticle vacuum, which is the same as for the target. Let again j, m be the quantum numbers for the emitted particle and j', m' those for the odd nucleon.

The channel state is

$$\sum_{m,\mu} a^+(j,m,t_0 = \tfrac{1}{2}) B^+(3,\mu,\alpha) \langle jm3\mu | j'm' \rangle | 0 > \tag{4.25}$$

and the decaying state the isobaric analogue to

$$\simeq \alpha^+(j',m',t_0' = -\tfrac{1}{2}) | 0' >. \tag{4.26}$$

The overlap is

$$\simeq v(j,m) p(j,j',\alpha) \sqrt{\frac{7}{2j'+1}} \cdot (-1)^{j-j'}. \tag{4.27}$$

Again a reduction factor $(2T+1)^{-1}$ is introduced in the decay probability, when the isospin structure of the states is taken into account.

The major difference between the quadrupole and the octupole vibrations is that, whereas the first ones are in general built up by many two-quasiparticle excitations of roughly the same energy and thus with amplitudes of comparable magnitude, the octupoles are often (cf. sect. 12) formed by some few unperturbed modes. For these modes the amplitudes are rather large (of the order of magnitude of unity) and thus more easy to measure.

Sum rules

In the analysis of transition strengths for multipole excitations the sum rules for reduced transition probabilities play a significant role.

The energy weighted sum of B values is given by the formula (ref. BM).

$$\sum_f (E_f - E_i) B(E3;\ i \to f) = \frac{147\hbar^2}{8\pi M} e^2 \sum_p \langle i | r_p^4 | i \rangle . \tag{4.28}$$

In the first sum we start from a state i, e.g. the ground state, and sum over all states f, which can be reached by an $E3$ excitation. E_f and E_i are the two relevant energies. The last sum runs over all protons p.

From the derivation one immediately generalizes to get the corresponding sums for B_0 and B_1 for the excitations from the ground state:

$$\left.\begin{aligned} &\sum_\alpha (E_\alpha - E_0) B(\tau = 0;\ 0 \to 3-, \alpha) \\ &= \sum_\alpha (E_\alpha - E_0) B(\tau = 1,\ \nu = 0;\ 0 \to 3-, \alpha) \\ &= \frac{147\hbar^2}{8\pi M} \left\{ \tfrac{1}{4} \sum_p \langle r_p^4 \rangle + \tfrac{1}{4} \sum_n \langle r_n^4 \rangle \right\} . \end{aligned}\right\} \tag{4.29}$$

Here, p denotes protons, n neutrons. The index α runs over all available 3^- states in the nucleus. The expectation values of r^4 should be evaluated in the ground state. These expressions are slightly model dependent. In the derivation it is supposed that the multipole operator and the Hamiltonian commute, except for the kinetic energy part. This implies that the shell-model potential is velocity independent and that it is permissible to neglect exchange effects. This is consistent with our approximations when we only consider the $\nu = 0$ excitations. Then we may use an octupole-octupole force which contains only the factor

$$\varkappa_0 + 4\varkappa_1 t_0(i)\, t_0(j) \tag{4.30}$$

which commutes with $M(\tau = 1, \nu = 0)$ as well as with $M(\tau = 0)$.

The single contributions to the sums ((4.28) and (4.29)) and the total sums we call oscillator strengths and total oscillator strengths, respectively. If the protons and neutrons contribute with equal amounts to the sums, then the total B oscillator strength is twice the B_0 strength.

Due to the neutron excess, the contribution from the neutrons is actually often twice as high as that from the protons, which means that the total B strength is 4/3 of the B_0 strength. This is partly due to an oversimplification in our treatment, because we use the same frequency in the harmonic oscillator potential for protons and neutrons. Thus, the protons are kept closer to the nuclear centre, and $\sum_p \langle r_p^4 \rangle$ is too small. A better treatment would be to use, e.g., Saxon-Wood potentials for protons and neutrons.

When making the transformation from the unperturbed two-quasiparticle excitations to the resulting excitations, the total oscillator strengths are unchanged. This is a purely mathematical statement.

Thus the magnitude of the total B,B_0 and B_1 strengths may be calculated, e.g., in a simple model of non-interacting particles in a pure harmonic oscillator potential.

When using a model in which the levels closest to the Fermi energy λ are chosen empirically, as we do below, we introduce an element of inconsistency, due to the fact that we are not sure that these levels can be calculated with the help of any velocity independent potential. It is also immediately seen that, when pushing levels around in a somewhat arbitrary way, the total oscillator strengths cannot be expected to be constant. Since, however, this pushing concerns mainly levels near the Fermi level and some of them move up and others move down, the effect is actually very small (at most some few percent).

Sometimes the so-called isospin zero part of the total B oscillator strength is considered (ref. 11). This quantity is Z/A times the total strength and in our treatment it has not any very distinct meaning.

5. Octupole coupling in simple examples

Before discussing the spectra of real nuclei it may be instructive to consider the simple case of one proton line and one neutron line coupled by the octupole force.

To obtain a measure for the strength of the excitations it is convenient to define

$$F^p = \tfrac{1}{2}\sum_{j_1 j_2}^{p} |\langle l_2 j_2 || i^3 Y_3 \left(\frac{r}{a}\right)^3 || l_1 j_1 \rangle|^2 (u(j_1)v(j_2) + v(j_1)u(j_2))^2 \qquad (5.1)$$

summing over all the proton states j_1 and j_2. The analogous neutron quantity is F^n. The factor $\frac{1}{2}$ is chosen because each term in the sum appears twice.

When the two lines are of equal energy and strength ($F^p = F^n$) the resulting spectrum consists of a pure $\tau = 0$ mode and a pure $\tau = 1$ mode. For the first one, energy and strength are determined only by $\varkappa_0$, the $\tau = 0$ part of the force, and for the second one only by $\varkappa_1$ (fig. 1).

When $F^p \neq F^n$, but the two lines remain in the same position, the resulting modes become of mixed isospin character, but still the low-energy mode

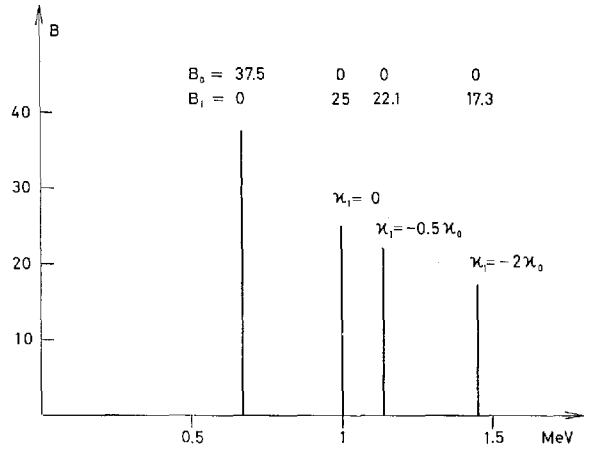

Fig. 1. Position of the two resulting lines for constant $\varkappa_0$ and different values of $\varkappa_1$, when the unperturbed spectrum consists of a protron line $F^p = 50$, and a neutron line $F^n = 50$, both placed at 1 MeV. The line of lowest energy is independent af $\varkappa_1$. B, B_0 and B_1 are given in arbitrary units, obtained when $a = 1$ (cf. equation (4.6)).

is mainly $\tau = 0$, determined by $\varkappa_0$, and the high-energy mode mainly $\tau = 1$, determined by $\varkappa_1$ (fig. 2). This is correct, even if there is rather strong asymmetry in the unperturbed spectrum.

When $\varkappa_0$ is constant and $-\varkappa_1$ increases, the low state becomes purer with respect to isospin. This may be considered in two ways.

1) When $\varkappa_1$ is introduced, it sucks some of the $\tau = 1$ part from the low excitation, which then becomes purer. Thus B_1 decreases while B and B_0 approach each other.
2) When $\varkappa_1$ is introduced, $\varkappa_n$ and $\varkappa_p$ are diminished whereas the proton-neutron force becomes stronger. If, e.g., the state is preferably built up by neutron excitations ($F^n > F^p$), they lose influence and more proton excitations are mixed in. Thus, B increases while B_0 decreases. (The strong component of the excitation is weakened).

It is interesting to note that even when $\varkappa_1 = -2\varkappa_0$ (the *nn* and *pp* forces are repulsive) there is a low-energy collective state. The reason is, that now $\varkappa_{np} = 3\varkappa_0$, i.e. the neutron-proton force is strongly attractive. For the high-lying mode the energy goes up when $-\varkappa_1$ and thus $\varkappa_{np}$ increases, since it becomes more difficult to separate neutrons from protons. From the sum rules it follows immediately that when $F^p \neq F^n$ the two resulting modes cannot at the

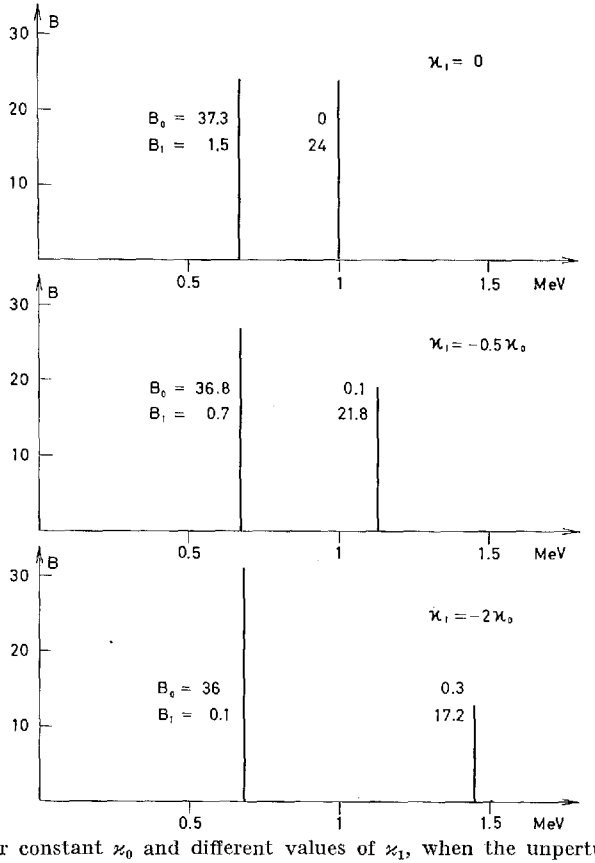

Fig. 2. Spectra for constant $\varkappa_0$ and different values of $\varkappa_1$, when the unperturbed spectrum is $F^p = 40$ in 1 MeV and $F^n = 60$ in 1 MeV. Again $a = 1$ (see fig. 1).

When $\varkappa_1 = -0.5$ times the $\varkappa_0$ value from the figure, but $\varkappa_0 = 0$, a line with $B = B_0 = 24$, $B_1 = 0$ appears in 1 MeV and another one with $B = 14.1$, $B_0 = 0.9$ and $B_1 = 22.1$ in 1.14 MeV.

same time be of pure isospin type. When $\varkappa_1$ is introduced, the low-energy mode becomes of $\tau \simeq 0$ type, but then the high-energy mode must be of mixed isospin character, i.e. $B_0 \neq 0$.

Let us now proceed to the other possibility for asymmetry in the unperturbed spectrum, viz. the case where $F^n = F^p$ but the two lines have different energies (fig. 3). The variations in B are easily understood, when it is remembered that if $\varkappa_1$ is introduced, e.g. more of the high-energy unperturbed mode is mixed into the resulting state of lowest energy. It is obvious that when the forces are so strong that the distance between the two resulting

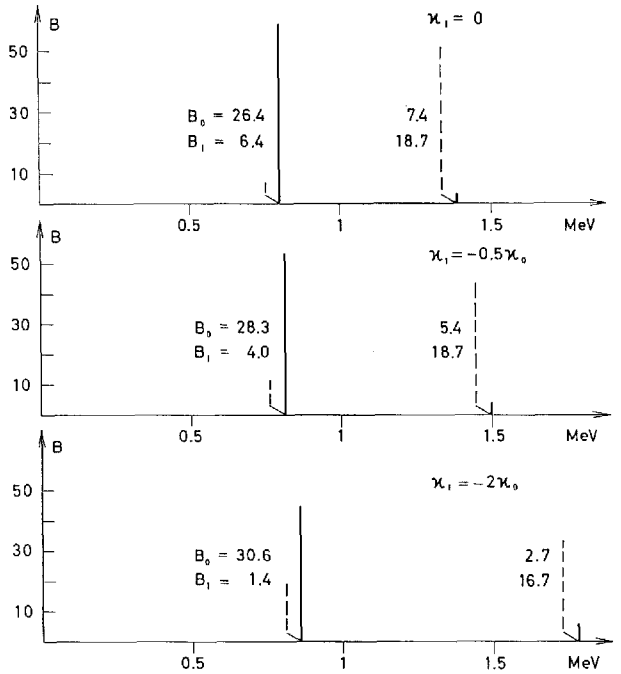

Fig. 3. Spectra for constant $\varkappa_0$ and different values of $\varkappa_1$, when the unperturbed spectrum is $F^p = 50$ in 1 MeV and $F^n = 50$ in 1.5 MeV. When F^p and F^n are interchanged, B gets the values indicated by dashed lines, while B_0 and B_1 are unaffected. Again $a = 1$ (see fig. 1).

modes is much greater than the distance between the unperturbed lines, we are again close to the symmetric case of fig. 1, but we learn that the situation with rather pure modes is reached much earlier.

6. Effects of shell structure

In order to obtain qualitative insight into the manner in which the shell structure affects the resulting spectrum we shall in this section, in some simple examples, study the energy distribution of B oscillator strength, using an isospin independent octupole force.

Let us first consider a system of non-interacting particles in a pure harmonic oscillator potential.

By 3^- excitations a particle can be raised either one or three shells, giving one group of excitations at an energy $\hbar\omega_0$ and another one at $3\hbar\omega_0$.

To find the oscillator strength distribution on these two groups we define, for the proton excitations (cf. (5.1))

$$F_1^p = \tfrac{1}{2} \sum_{|\Delta N = 1|} |\langle l_2 j_2 || Y_3 \left(\frac{a}{r}\right)^3 i^3 || l_1 j_1 \rangle|^2 (u(j_1) v(j_2) + v(j_1) u(j_2))^2, \quad (6.1)$$

$$F_2^p = \tfrac{1}{2} \sum_{|\Delta N = 3|} |\langle l_2 j_2 || Y_3 \left(\frac{a}{r}\right)^3 i^3 || l_1 j_1 \rangle|^2 (u(j_1) v(j_2) + v(j_1) u(j_2))^2, \quad (6.2)$$

where ΔN is the change in principal quantum number from j_1 to j_2.

Analogous quantities F_1^n and F_2^n are defined for neutrons. Apart from a trivial factor, F_1^p is simply the sum of the B values for all the transitions to the states of excitation energy $\hbar\omega_0$, i.e.

$$\sum_{\alpha(\Delta N = 1)} B(E3;\ 0 \to 3-, \alpha) = e^2 a^6 F_1^p. \quad (6.3)$$

It is easy to calculate F_1^p, and F_2^p can then be found from the energy weighted sum of B values (4.28).

For the lightest nuclei $F_1^p = 0$, since a $3\hbar\omega_0$ transition is needed to form a 3^- state. In the limit of very heavy nuclei $F_1^p \simeq F_2^p$.

For $Z = 20$ we get $F_1^p/F_2^p = 70\,\%$, for $Z = 40$ we obtain $76\,\%$ and for $Z = 70$ the ratio is $82\,\%$. This means that in a very large Z interval the sum of B values for excitations of energy $\hbar\omega_0$ is approximately 3/4 of the sum of B values for $3\hbar\omega_0$ excitations. The $\Delta N = 1$ excitations contribute about $20\,\%$ to the total B oscillator strength.

When we introduce an isospin-independent octupole-octupole force between the nucleons, the neutron and proton excitations at $\hbar\omega_0$ couple and give an unshifted line at $\hbar\omega_0$ and a line with lower energy, as explained in the preceding section (cf. fig. 1). The same is the case for the neutron and proton excitations at $3\hbar\omega_0$, and finally there is a coupling between the lines in the two energy regions. This is illustrated by fig. 4. The $\varkappa$ value is taken from the detailed calculation below, where it is fitted by the experimental data. We see that the introduction of the octupole force does not push the lines very far down, and the oscillator strength, placed on the low lines, is almost unchanged. This result is, however, very sensitive to the strength of the octupole force. If $\varkappa$ is increased by about $35\,\%$, the low line comes down to zero energy, i.e. the spherical shape becomes unstable in this model.

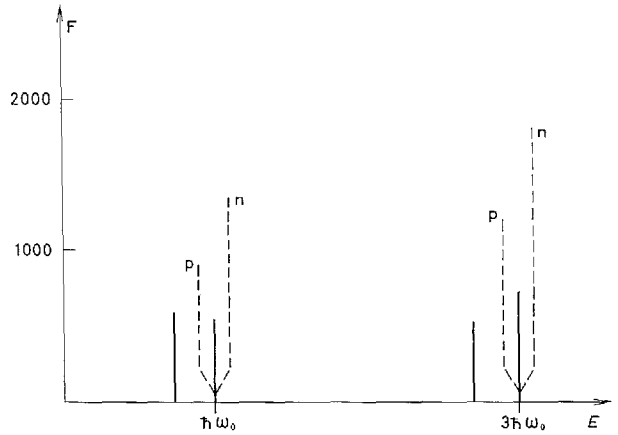

Fig. 4. Resulting spectrum for a simple model of the nucleus $A,Z = 90,40$, when $\varkappa_1 = 0$ and $\varkappa_0 \neq 0$. The unperturbed lines are dashed, the resulting ones fully drawn. The proton and neutron lines are denoted by p and n, respectively. The unperturbed lines are concentrated in $\hbar\omega_0$ (= 9.15 MeV) for $\Delta N = 1$ and in $3\hbar\omega_0$ for $\Delta N = 3$, and they are represented by their strength F, introduced in the text ((5.1) and (6.1)). For the resulting states $F = \frac{(S^p)^2}{S'}$, where $S' = S'^p + S'^n$. The value for $\varkappa_0$ has been taken from the detailed calculation (sect. 15). If S is 35 % smaller, i.e. if $\varkappa_0$ is 35 % greater, the spherical shape becomes unstable. In the unperturbed spectrum the $\Delta N = 1$ lines contribute with 20 % to the total B oscillator strength. The two resulting lines of lowest energy contribute with 21.5 %, the lowest one alone with 9.5 %.

The spectrum is independent of the atom number A under the following conditions: 1) The slow change in the ratio F_1^p/F_2^p with A is neglected, 2) The ratio between neutrons and protons is kept constant, 3) The coupling constant $\varkappa$ varies like $A^{-\frac{5}{3}}$. This $\varkappa$ variation was suggested in section 2 by a simple scaling argument.

The deviation of the actual central nuclear field from that of a harmonic oscillator has important effects on the octupole spectra. Thus, the broadening of the shells leads to a smearing out of the oscillator strengths in the $\hbar\omega_0$ and the $3\hbar\omega_0$ regions.

Of special significance for the low-energy spectra is the spin-orbit splitting which pushes levels down to the shells below. This means that inside the partly filled shell there are transitions (a weak and a strong one, depending on whether spin flip is involved or not) the energies of which are prevented from going to zero essentially only by the pairing gap. The effect begins to be of importance with the $4g_{9/2}$ level around $A = 80$. It is illustrated by a simple model in fig. 5. For the first excited state $S(= S^p + S^n)$ and thus the energy is largely determined by the low-energy unperturbed line, but B receives very substantial contributions from the higher lines.

For a more detailed study of the effect of the spread in the single-particle spectrum we go on to fig. 6. In fig. 6a all the low-energy single-particle

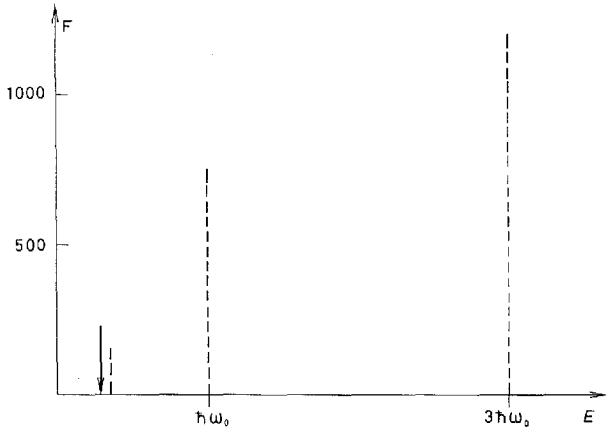

Fig. 5. Illustration of the influence of the strong transition inside the partly filled shell to the lowest resulting line for the nucleus $A,Z = 90,40$. The strengths F_1^p and F_2^p are placed in $\hbar\omega_0$ and $3\hbar\omega_0$, respectively, with the exception that the strong $3p_{3/2}-4g_{9/2}$ line is placed at the expected position 3.27 MeV $\simeq 1/3\hbar\omega_0$ (shown by dashed lines). The situation here is especially favourable to the low energy transition, since for this one the $u\ v$ factor in the numerator in S is almost equal to unity. (The transition goes from an almost filled to an almost empty level).

In the detailed calculation (sect. 15), the collective mode of lowest energy occurs at 2.61 MeV (shown by an arrow). If we use this energy in the model, $S_1^p = 434$ and $S_2^p = 90$. The contribution to S^p from the lowest-lying unperturbed line is 254. We can illustrate the influence of the higher-lying unperturbed lines on B in the following way. Let us first calculate B by taking only S^p and S'^p from the transition of lowest energy into account, subsequently by including all the $\Delta N = 1$ lines, and finally by also including the $\Delta N = 3$ lines (keeping E fixed). In this case, the ratio of B values is $1 : 2.9 : 4.2$. In the detailed calculation $S_1^p = 537$, which is more than found above, because of the influence of the broadening of the shells. The quantity S_2^p should be changed less. Using the value from above, $S_2^p/S_1^p \simeq 90/537 \simeq 17\,\%$, which should be a reasonable value.

transitions are placed as in a preliminary calculation, roughly equal to that in sect. 15. All the high-energy transitions are placed at $3\hbar\omega_0$. As a standard nucleus Sn^{116} is chosen.

Fig. 6b shows the picture when the octupole force is introduced. In the low-energy region two strong lines appear, one governed primarily by the transitions inside partly filled shells, and another one by the transitions between neighbouring shells. From table 1 it appears that these two lines contain about $10\,\%$ of the total B oscillator strength, i.e. the same amount as the line of the lowest energy in the simple harmonic oscillator picture in fig. 4.

In the medium region around $\hbar\omega_0$ many weak lines show up. In total they contain $23\,\%$ of the B oscillator strength, which is $5\,\%$ more than when $\varkappa_0 = 0$.

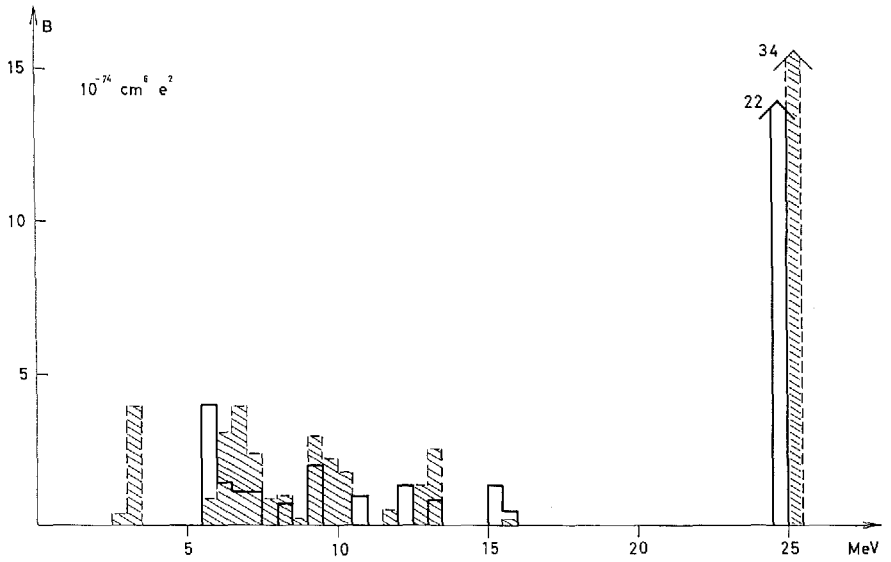

Fig. 6a.

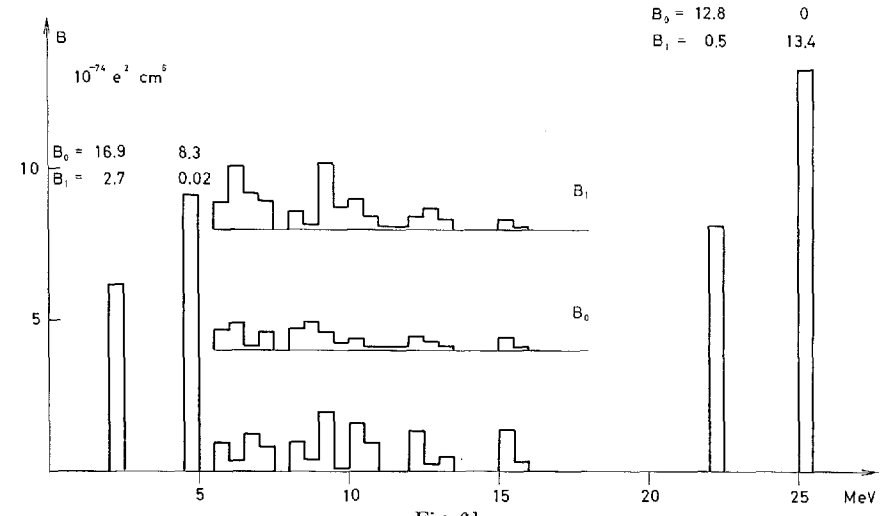

Fig. 6b.

Fig. 6. Histogram of the energy distribution of B values for Sn^{116}.

a) The unperturbed spectrum with the proton lines fully drawn and the neutron ones dashed. The $\Delta N = 3$ levels are concentrated in $3\hbar\omega_0$. The position of the $\Delta N = 1$ levels comes from a preliminary calculation and is somewhat different from the values used in section 15. The B value in a) is calculated with an effective charge e on all nucleons.

b) The spectrum when the isospin independent octupole force is introduced ($S = 0.578 \times A^{5/3}$, which corresponds closely to $S_1 = 0.45 \times A^{5/3}$ used below). For the medium region around $\hbar\omega_0$, histograms of B_0 and B_1 are inserted. For the strong lines above and below this energy region, B_0 and B_1 are written above the lines. B_1 and B_0 are in units of 10^{-74} cm^6.

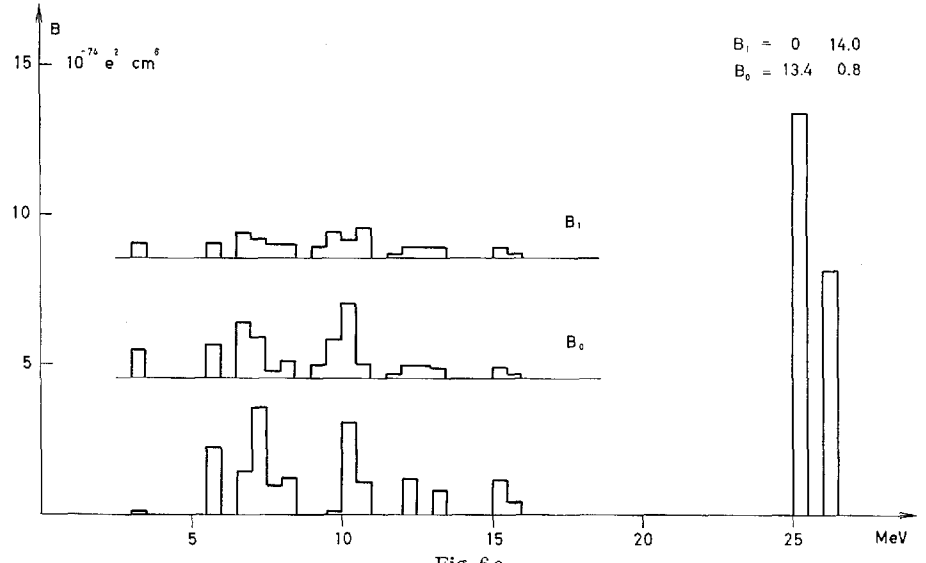

Fig. 6c.

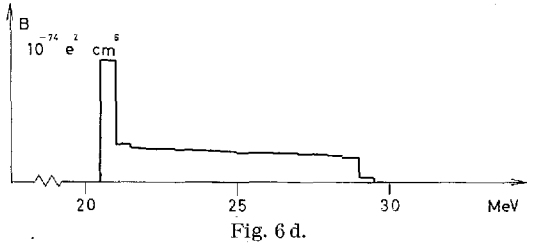

Fig. 6d.

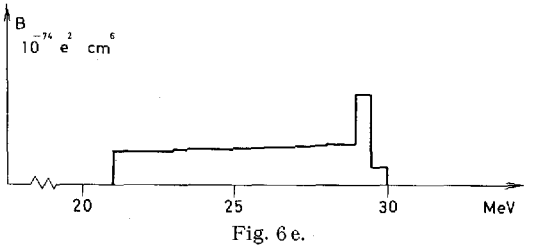

Fig. 6e.

Fig. 6. Histogram of the energy distribution of B values for Sn^{116}.

c) B, B_0 and B_1 for $\varkappa_1 = -$half the $\varkappa_0$ value from b) and $\varkappa_0 = 0$.
d) The spectrum in the $3\hbar\omega_0$ region when F_2 is smeared out between 2.5 $\hbar\omega_0$ and 3.5 $\hbar\omega_0$ and $\varkappa_0$ is the same as in b). (For computational reasons the region of proton F_2 lines is pushed down 0.2 MeV compared to the neutron F_2 region).
e) The change from d), when $\varkappa_1$ like in c) and $\varkappa_0 = 0$.

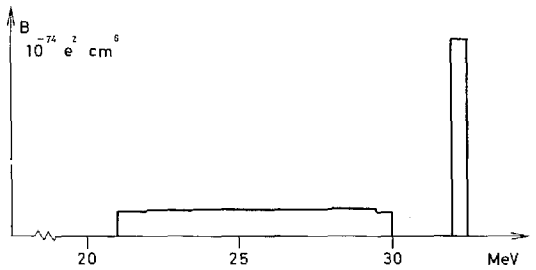

Fig. 6f.

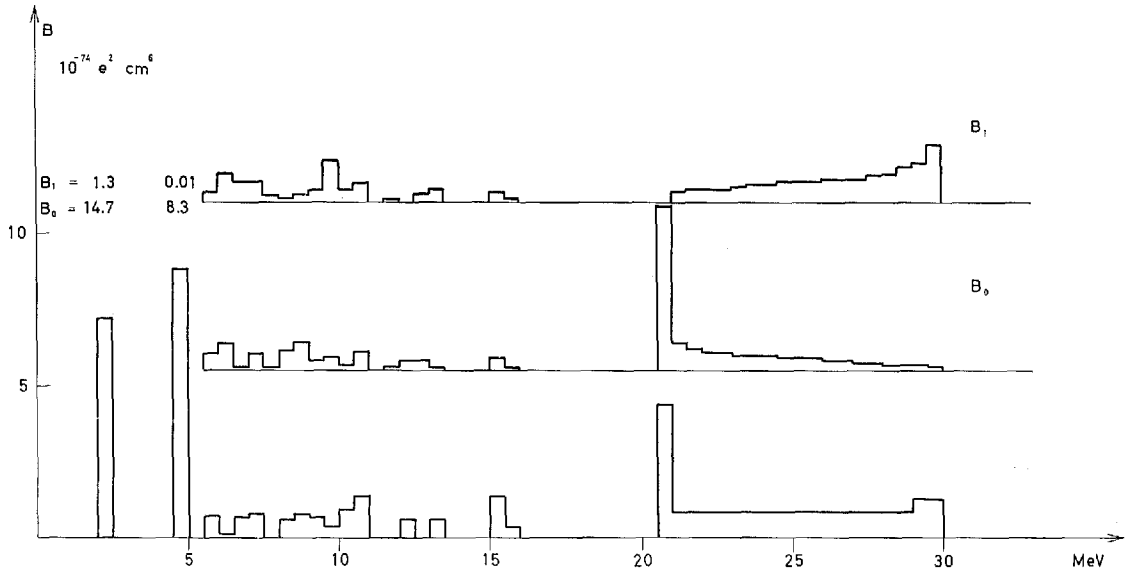

Fig. 6g.

Fig. 6. Histogram of the energy distribution of B values for Sn^{116}.

f) The change from d), when $\varkappa_0 = 0$ and $\varkappa_1$ four times stronger than in c).

g) Histograms of B, B_0 and B_1 when $\varkappa_0$ has the same value as in b) and $\varkappa_1 = -0.5\,\varkappa_0$. The unperturbed spectrum is for F_1 the same as in a) and for F_2 the same as in d).

Finally, we get two high-energy, strong lines. They are not realistic but appear because of the concentration of the F_2 transitions at $3\hbar\omega_0$.

To get some insight into the way in which smearing out of the $3\hbar\omega_0$ transitions affects the picture we consider a crude model, the main results of which are shown in figs. 6d, e and f (figs. 6e and 6*f* are discussed in sect. 8). The unperturbed $3\hbar\omega_0$ lines are distributed with constant density between $2.5\hbar\omega_0$ and $3.5\hbar\omega_0$. This change in the model from above affects the lines only slightly in the $\hbar\omega_0$ domain, and therefore they are not shown.

TABLE 1. Contributions (here called relative oscillator strengths) to the energy-weighted sum of B, B_0 and B_1 for the two low-lying strong levels in the resulting spectrum of Sn^{116} from the model of fig. 6 and for the two high-lying levels which occur when F_2 is concentrated at $3\,\hbar\omega_0$.

The data are given for a pure $\varkappa_0$ force (denoted $\varkappa_0$) (the force from fig. 6 b), for a mixed force with same $\varkappa_0$ and $\varkappa_1 = -0.5\,\varkappa_0$ (denoted $\varkappa_0+\varkappa_1$) (the force from fig. 6 g), for this value of $\varkappa_1$ and $\varkappa_0 = 0$ (denoted $\varkappa_1$) (force from fig. 6 c), and for $\varkappa_1$ four times greater and still $\varkappa_0 = 0$ (denoted $4\varkappa_1$). Finally, "none" means the sum fractions from the unperturbed spectrum, i.e. when $\varkappa_0 = \varkappa_1 = 0$.

levels	force	rel. B osc. str.	rel. B_0 osc. str.	rel. B_1 osc. str.
two low-energy strong levels	$\varkappa_0$	7 %	17 %	1 %
	$\varkappa_0+\varkappa_1$	8 %	17 %	½ %
two high-energy levels	$\varkappa_0$	67 %	64 %	80 %
	$\varkappa_1$	72 %	80 %	83 %
	$4\varkappa_1$	77 %	79 %	91 %
	$\varkappa_0+\varkappa_1$	67 %	64 %	83 %
	none	72 %	79 %	79 %

As was to be expected, the oscillator strength is pushed somewhat to the low-energy end of the region, where stronger lines are built up, while a great part is left as a rather constant background (fig. 6 d).

We note that the force is not able to form a very strong line in the gap between F_1 and F_2. This is partly due to a cancellation effect; the contributions to S from F_1 and F_2 have opposite signs. Attempts to press a greater part of the oscillator strength down from the $3\hbar\omega_0$ region does not result in the formation of a strong line in the gap, but makes the strength go further down to the $\hbar\omega_0$ region. If only the $3\hbar\omega_0$ unperturbed lines are included in the Sn spectrum, the $\varkappa_0$ value from fig. 6 d is just strong enough to place the resulting state of lowest energy at the edge of the F_2 region. When $\varkappa_0$ is made twice as large, the state comes down from 20.61 MeV to 17.95 MeV and the contribution to the total B oscillator strength increases from 21 % to 32 %. If $\varkappa_0$ is once more multiplied by two, we are very near unstability of the spherical shape of this fictive nucleus. The state appears at 7.63 MeV, but only contains 38 % of the B oscillator strength and 62 % are still left in the $3\hbar\omega_0$ region.

From the discussion above we expect the spectrum in a nucleus to consist of some few, strong lines of low energy (2–5 MeV) and many weak ones distributed rather uniformly in the $\hbar\omega_0$ and $3\hbar\omega_0$ regions.

When going from nucleus to nucleus the qualitative picture of the spec-

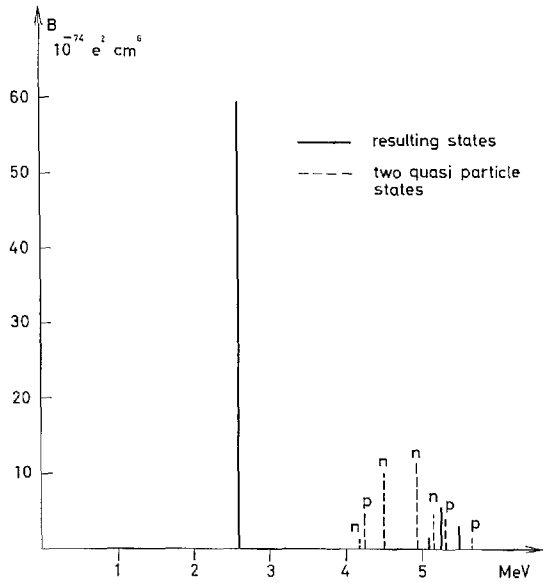

Fig. 7. The B values in the low-energy spectrum in $A,Z = 208,82$. Resulting lines fully drawn, unperturbed dashed. p and n denote proton and neutron two-quasiparticle excitations, respectively. The B values in the unperturbed spectrum are calculated by giving all particles effective charge e. Note that the proton lines of highest energy indicate the start of the "continuum" of states in the $\hbar\omega_0$ region.

The single-particle levels come from a preliminary calculation, using the same neutron levels as in case 9a and KSII proton levels (cf. sect. 15):

$g_{7/2}$: 0, $d_{5/2}$: 0.8, $h_{11/2}$: 2.1, $d_{3/2}$: 2.6 and $s_{1/2}$ 2.95 MeV. In this calculation $c_0 = 0.413$.

trum in these two regions should vary rather slowly, the variations being essentially brought about by the changes in intershell distances and the broadening of the shells.

The low-energy, strong states are expected to vary much more quickly in position and B value, since they are very dependent on the energy and the number of particles available for the transitions inside the partly filled shells. This is the reason why we concentrate on this part of the spectrum in the detailed investigation below.

The fine structure in the low-energy part of the unperturbed spectrum has a strong influence on the distribution of the oscillator strength among the very lowest-lying resulting states. We shall give some characteristic examples in concluding this survey of the qualitative features of the spectrum. The examples are chosen from the numerical calculation in sect. 15.

The general, well-known trend is that the level of lowest energy has a

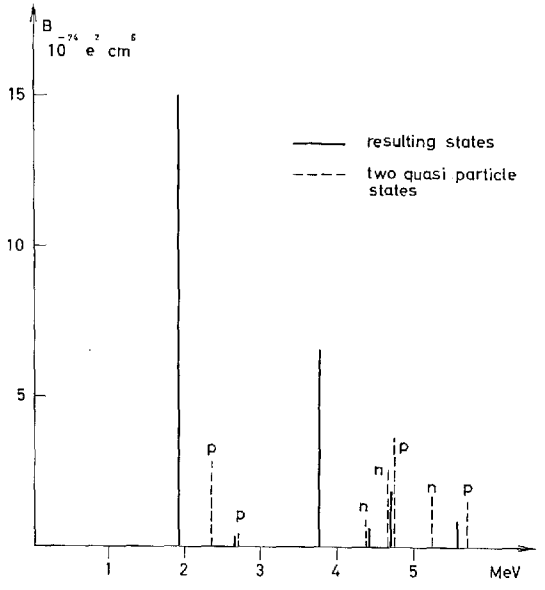

Fig. 8. The B values in the low-energy spectrum in $A,Z = 142,60$ (case 8a in section 15). Same notation as in fig. 7.

small $S' = S'^p + S'^n$ and thus a great B, whereas the opposite is true for the following ones.

An example is given by the double magic Pb^{208}, for which the lowest part of the spectrum is shown in fig. 7. In this and the following figures only the 6–10 lowest states are included. It should be kept in mind that the unperturbed lines of greatest energy in the figures are just the lowest ones of the numerous states forming almost a continuum up to 10–15 MeV, as shown in fig. 6.

For a non-magic nucleus the single-particle transitions inside partly filled shells in general all have energies well below the intershell transitions. This gives rise to a gap in which a collective state may appear, and thus the oscillator strength in the low-energy part of the resulting spectrum is in general split into two or more parts. Figs. 8 and 9 refer to a neutron-magic and a non-magic nucleus.

A special fine structure effect in the very lowest end of the spectrum is seen when the lowest unperturbed transition is weak (due to the uv factor or because spin flip is involved). This is illustrated by fig. 10.

Table 2 gives the contributions to the total B and B_0 oscillator strengths for the lowest states. We see that the strength in the low part of the spec-

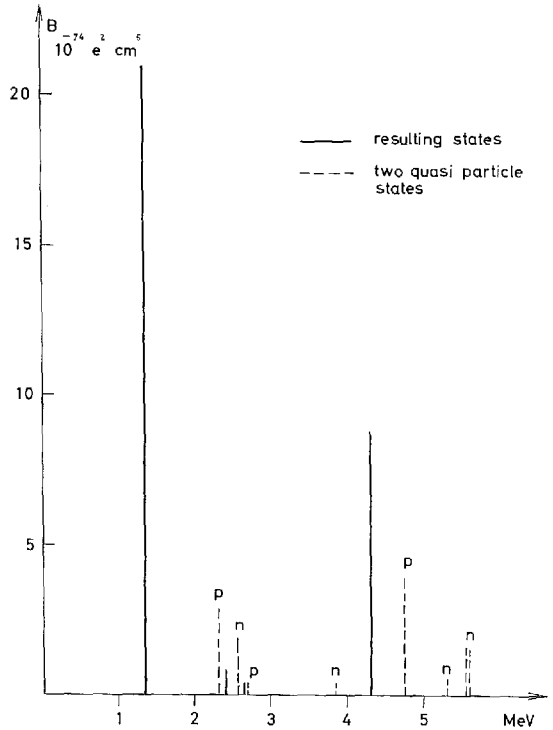

Fig. 9. The B values in $A,Z = 148,60$ (case 8a in sect. 15). Same notation as in fig. 7.

trum, is fairly constant, although it may be distributed in different ways among the lowest states. In $A,Z = 142,60$ the lowest level is moderately collective (closed neutron shell) and in $A,Z = 148,60$ it is very collective. (We note that the increase in B and decrease in E just compensate each other).

For the next nucleus in the table the lowest state is especially weak, while for $A,Z = 90,40$ the collective state is fairly high in energy and largely governed by the strong proton transition across the closed $Z = 40$ subshell. This gives rise to an especially great contribution to the B strength.

7. Examples of the isospin structure of the excited states

In this section we shall give examples of the isospin structure, i.e. the relative magnitude of B, B_0 and B_1, for the excited states which we find below, using the $\varkappa_0$ force. To start with the strong low-energy lines we see

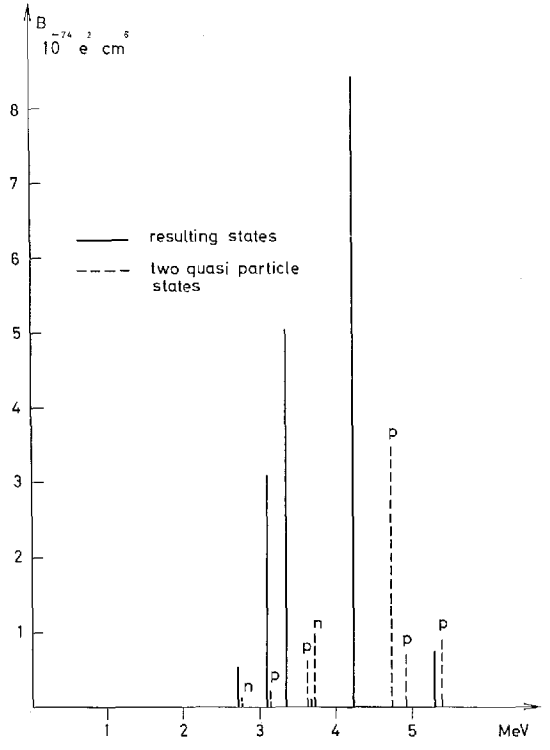

Fig. 10. The B values in $A,Z = 132,54$ (case 7b in section 15). Same notation as in fig. 7.

from tables 3 and 4 that B_0 is of the order of or greater than B, and $B_1 \ll B$. This means that the lines, as was to be expected, are fairly pure $\tau = 0$. This is the case even for single closed shell nuclei, where you might expect a greater $\tau = 1$ mixing.

The tables teach us further that even small $\tau = 1$ impurities are able to change the ratio of B_0 to B so that it differs considerably from unity. Because of the neutron excess, S^n for the lowest level is in general greater than S^p, and thus $B_0 \geq B$. Since for this level B_0 is never much smaller than B, it follows from the considerations in section 4 that it contains a greater part of the B_0 oscillator strength than of the B strength (see also table 2).

The levels in the $\hbar\omega_0$ region (fig. 6b), which although individually weak contain in total an appreciable part of the B oscillator strength, are very often of mixed $\tau = 0$ and $\tau = 1$ type ($B_0 \simeq B_1$). However, τ is less significant here. In the $3\hbar\omega_0$ region of fig. 6b we get a rather pure $\tau = 0$ state and a pure $\tau = 1$ state, due to the fact that we have concentrated

TABLE 2. Row I gives for some nuclei the relative contribution to the total B oscillator strength from the resulting level of lowest energy, and row II the contributions from the five states of lowest energy.

Rows III and IV give the same quantities for the B_0 strength.

The contributions to the B_1 strength are always very small.

A,Z	142,60 case 8a	148,60 case 8a	132,54 case 7b	90,40 case 3
I	2.5 %	2.5 %	1/4 %	5 %
II	6 %	5.5 %	7 %	8 %
III	5 %	8 %	1/2 %	7 %
IV	16 %	16 %	13 %	13 %

TABLE 3. E (in MeV), B (in $e^2\,10^4\,f^6$), B_0 and B_1 (in $10^4\,f^6$) for all the lowest lying resulting states for some nuclei, when a pure isospin-independent force is used. The data come from the general calculation in sect. 15, with the exception that for $A,Z = 120,50$ the proton transition $4g_{9/2} - 5h_{11/2}$ was placed 0.8 MeV higher.

$A,Z = 90,40$				$A,Z = 120,50$			
E	B	B_0	B_1	E	B	B_0	B_1
2.61	8.4	6.3	0.2	2.51	7.0	21	3.6
3.77	0.4	0.4	10^{-6}	3.31	5×10^{-2}	0.1	10^{-2}
4.23	1.7	2.2	0.04	4.48	6.2	7.6	8×10^{-2}
4.73	0.2	0.4	0.07	5.14	0.1	4×10^{-3}	10^{-2}
4.80	0.5	0.2	0.07	5.29	2.4	0.4	0.8
5.07	7×10^{-3}	0.8	0.7	5.65	5×10^{-2}	0.2	5×10^{-2}

$A,Z = 142,60$				$A,Z = 148,60$			
E	B	B_0	B_1	E	B	B_0	B_1
1.92	15	16	3×10^{-2}	1.36	21	46	4.8
2.65	0.4	0.5	9×10^{-3}	2.41	0.9	0.4	2.6
3.77	6.6	20	3.4	2.67	0.4	2×10^{-2}	0.2
4.44	0.6	0.5	10^{-2}	3.83	0.2	0.6	0.1
4.70	1.9	5×10^{-2}	1.3	4.30	8.8	12	0.2
5.12	3×10^{-3}	1.5	1.6	5.18	10^{-2}	4.2	3.8
5.56	0.8	3.2	0.7	5.35	0.1	1.7	1.0
				5.58	10^{-2}	5×10^{-2}	10^{-2}

TABLE 4. B_1/B_0 for the two strongest lines in the low-energy spectrum of some nuclei from case 8 a (see detailed calculation in sect. 15).

A,Z	138,56	140,58	142,58	142,60	144,60	146,60	148,60
lowest level.....	0.03	0.01	0.10	0.002	0.04	0.08	0.10
next, strong level ...	0.18	0.17	0.10	0.17	0.10	0.04	0.02

all the $3\hbar\omega_0$ transition strength on a single neutron and a single proton line. In a real case we would expect the $3\hbar\omega_0$ region to look somewhat like the $\hbar\omega_0$ one.

If F_2 is smeared out in the same way as in fig. 6d, a rather strong $\tau = 0$ state is formed at the low end and B_0 falls off when we go upwards, whereas B_1 is constant in the region. This result is, however, dependent on the model. Variations in the relative and absolute density of neutron and proton states may influence the picture considerably.

8. The possible existence of strong $\tau \simeq 1$ lines

As seen in sect. 5, we can in the case in which we use an isospin independent force primarily expect to treat the $\tau \simeq 0$ states correctly while the $\tau \simeq 1$ states are mainly determined by the magnitude of $\varkappa_1$. To get information on the distribution of the B_1 oscillator strength and the possible existence of strong $\tau \simeq 1$ states we therefore, in this section, study the spectrum of our standard nucleus Sn^{116} (fig. 6) when a pure $\varkappa_1$ force is used.

When F_2 is concentrated in $3\hbar\omega_0$, a strong $\tau \simeq 1$ line and a $\tau = 0$ line are formed in the high-energy end of the spectrum (fig. 6c). If $\varkappa_1$ is made four times stronger, the line of highest energy appears at 30.68 MeV with $(B, B_0, B_1) = (8.3, 0.6, 13.2)$. The influence of the $\Delta N = 1$ lines is very small. If they were left out, the $\tau = 0$ line would be unchanged, the $\tau \simeq 1$ line would be $10-15\,\%$ weaker. The oscillator strengths from table 1 show the expected variations. If the $3\hbar\omega_0$ lines are smeared out between $2.5\hbar\omega_0$ and $3.5\hbar\omega_0$ the oscillator strengths are practically unchanged, but the tendency to forming a distinct high-lying $\tau \simeq 1$ state is considerably weakened, as seen from figs. 6, e and f, especially if $\varkappa_1 = -0.5\varkappa_0$.

Of particular interest is the problem whether strong $\tau \simeq 1$ lines could be expected in the lower energy part of the spectrum. It is striking that in the present model no such lines appear in the gap between the $\Delta N = 1$ and the $\Delta N = 3$ excitations, not even when $\varkappa_1 = -2\varkappa_0$. This is due to

the same cancellation effect as considered in sect. 6 in connection with the investigation of the possible existence of states in the gap below the $3\hbar\omega_0$ region (for pure $\varkappa_0$ force), but the effect is even stronger here, since the density of the oscillator strength in the high-energy end of the unperturbed spectrum in the $\hbar\omega_0$ region is small, i.e. the levels are weaker and are more widely spread. We will study this point again below, using a $\varkappa_0+\varkappa_1$ force.

In the $\hbar\omega_0$ region many weak states, often of mixed isospin character, appear and even in the lowest part, where the nuclei show more individual trends, a study of some nuclei of different types has revealed no tendency to formation of stronger $\tau = 1$ states. We are led to conclude that, with the models and $\varkappa_1$ values which we have used, there is no pronounced tendency towards building up individual very strong $\tau = 1$ levels. Even in the $\Delta N = 3$ region the B_1 oscillator strength is expected to be smeared out over a broad energy interval, unless $\varkappa_1$ is very strong.

As mentioned above, the interaction matrix elements for the $\Delta N = 3$ transitions are less reliable than for $\Delta N = 1$, and this may give rise to modifications.

9. Modifications in the spectra, when $\varkappa_1 \neq 0$ is introduced

On the basis of the discussion of the simple examples in section 5 and the cases of pure $\varkappa_0$ and pure $\varkappa_1$ force (sects. 6 and 8) it is easy to understand the qualitative effects of an octupole coupling which contains both isoscalar and isovector components. An example is given in fig. 6g.

In the $3\hbar\omega_0$ region of the spectrum the B_0 oscillator strength is pushed downwards, B_1 upwards.

A concentration of B, coming from $\tau \simeq 0$ levels is formed in the low energy end and a concentration of B, coming from $\tau \simeq 1$ levels is formed at the high end. However, the tendency for forming a distinct, high-lying $\tau \simeq 1$ line is only weak. When $\varkappa_1 = -2\varkappa_0$, this is no longer correct. A line with $B = 7.74$, $B_1 = 10.72$ (same units as in fig. 6) is formed at 31.95 MeV, containing 32 % of the total B oscillator strength and 77 % of the B_1 strength. This is rather near to the results for a pure $\varkappa_1$ force. We note that this concentration is only reached when we use a $\varkappa_1$ value, which is very large compared to the tentative theroretical estimates. Table 1 gives relative oscillator strengths for different $\varkappa_1$ values in a spectrum in which F_2 is concentrated in $3\hbar\omega_0$. If F_2 is smeared out, the figures for B, B_0 and B_1 are practically unchanged in the $3\hbar\omega_0$ region.

TABLE 5. E, B and B_0 for some selected resulting states as discussed in the text. Units as in table 3. The data are given for pure $\varkappa_0$ force, for $\varkappa_0 + \varkappa_1$, where $\varkappa_1 = -\frac{1}{2}\varkappa_0$, and for $\varkappa_0 + \varkappa_1$ force with $\varkappa_1 = -2\varkappa_0$. The magnitude of $\varkappa_0$ is the same in all three cases.

The results for Sn^{116} are due to the same calculation as in table 3.

	$\varkappa_1 = 0$	$\varkappa_1 = -\frac{1}{2}\varkappa_0$	$\varkappa_1 = -2\varkappa_0$	Nucleus (A,Z)
E	2.26	2.45	2.65	116,50
B	5.7	6.8	8.0	lowest excited state
B_0.....	16	14	12	
E	2.61	2.63	2.66	90,40
B	8.4	8.0	7.6	lowest excited state
B_0.....	6.3	6.5	6.8	
E	1.36	1.50	1.61	148,60
B	21.0	21.5	21.6	lowest excited state
B_0.....	45.8	35.0	27.1	
E	4.65	4.65	4.66	116,50
B	9.0	8.7	8.5	next strong state
B_0.....	8.2	8.3	8.2	
E	4.30	4.31	4.32	148,60
B	8.8	9.2	9.6	next strong state
B_0.....	12.0	11	11	
E	4.70	4.75	4.79	142,60
B	1.9	1.1	0.5	
B_0.....	0.05	0.1	0.2	

In the medium region around $\hbar\omega_0$, the states are weaker since some $\tau = 0$ strength is sucked down by $\varkappa_0$ and some $\tau = 1$ strength upwards by $\varkappa_1$. If only the F_1 lines are included in the unperturbed spectrum, a calculation using the same values of $\varkappa_0$ and $\varkappa_1$ as in fig. 6g gives the perhaps somewhat surprising result that no strong $\tau \simeq 1$ line is formed above the F_1 lines. This reminds us of what happened when only F_2 was included. In sect. 6 we saw that then a rather strong force $\varkappa_0$ was needed to suck a greater part of the oscillator strength out of the unperturbed lines.

In the low-energy spectrum, the presence of $\varkappa_1$ tends to decrease B_1, and this may have considerable influence on B and B_0. A quantitative insight requires a more detailed study. For the resulting state of lowest energy the changes depend on 1) the relative magnitude of S^p and S^n, 2) whether the near-lying unperturbed modes are neutron or proton excitations. When $S^n > S^p, \varkappa_1$ tends to mix more proton motion into the state, B

increases and B_0 goes down (see the data for $A,Z = 116,50$ in table 5). The opposite trend is observed when $S^p > S^n$ (e.g. $A,Z = 90,40$). It may be noted that only few cases exist where $S^n < S^p (B_0 < B)$ for the lowest state.

Some modification arises from the low-lying modes. An example is $A,Z = 148,60$ (table 5). Here, $S^n > S^p$, and thus B increases when $\varkappa_1$ is introduced, but only very little, since the lowest and strongest unperturbed transition inside the partly filled shells is a proton one (fig. 9), the role of which is weakened by $\varkappa_1$.

In all the above mentioned cases $\varkappa_1$ makes the state less collective in the sense that E is increased. In $A,Z = 142,60$ we find an example where $B_0 \simeq B$ (the neutron excess and the closing of the neutron shell neutralize each other). Then E,B and B_0 are almost independent of whether $\varkappa_1 = 0$, $\varkappa_1 = -0.5\varkappa_0$ or $\varkappa_1 = -2\varkappa_0$ (table 6).

For the next strong excitation in the low-energy part of the spectra the rules from above may be used, but it may happen that B and B_0 both move up or move down, when $\varkappa_1$ is introduced. For the weaker levels one should be more careful by using simple arguments, since there is a strong dependence on the nearest unperturbed modes. Finally, table 5 gives an example (from $A,Z = 142,60$) of a line which is mainly of $\tau = 1$ character. (The line comes between a proton and a near-lying neutron mode). When the $\tau = 1$ part of the excitation is shifted to higher energy, B decreases strongly.

10. Simultaneous adjustment of $\varkappa_0$ and $\varkappa_1$

When fitting the experimental energies by an isospin independent octupole-octupole force we make of course a systematic error. In this section we shall sketch briefly how our results would have been changed if a fit to experimental energies had been made by some general $\varkappa_0, \varkappa_1$ mixture.

When, for the lowest state, B and B_0 are different as, e.g., for $A,Z = 116,50$ we see from table 6 that we are able to make very great variations in B and B_0, by keeping the energy fixed and varying $\varkappa_0$ and $\varkappa_1$ simultaneously. This is not possible, however, when $B_0 \simeq B$ as is the case for the next, strong state in $A,Z = 116,50$ or for the lowest excitation in $A,Z = 142,60$. For the energies we obtain the result that states with great difference between B and B_0 move upwards relative to the states for which B and B_0 are equal, when $\varkappa_1$ is introduced. An example is given in fig. 11. By applying these simple rules it is easy to predict the variations and we have not gone further into a systematic study.

TABLE 6. E, B, B_0, B_1 and b in the same units as in table 3 for the two strongest, low-energy lines in some selected nuclei for different values of $\varkappa_1$. For $\varkappa_1 \neq 0$ we have chosen $\varkappa_0$ to give the lowest-lying resulting state approximately the same energy as when $\varkappa_1 = 0$.

$A,Z = 88,38$ case 4a			
$\varkappa_1 = 0$ $c_0 = 0.48$	E	2.74	4.63
	B	6.2	1.4
	B_0	4.9	3.7
	B_1	0.07	0.5
	b	0	0
$\varkappa_1 = -0.5\,\varkappa_0$ $c_0 = 0.48$	E	2.75	4.70
	B	6.0	1.9
	B_0	5.1	3.4
	B_1	0.03	0.2
	b	0.04	0.13
$\varkappa_1 = -2\varkappa_0$ $c_0 = 0.48$	E	2.77	4.76
	B	5.8	2.4
	B_0	5.3	3.1
	B_1	0.01	0.05
	b	−0.08	0.25
$A,Z = 142,60$ case 8a			
$\varkappa_1 = 0$ $c_0 = 0.45$	E	1.92	3.77
	B	15	6.6
	B_0	16	20
	B_1	0.03	3.4
	b	0	0
$\varkappa_1 = -0.5\,\varkappa_0$ $c_0 = 0.45$	E	1.92	3.89
	B	15	8.5
	B_0	16	16
	B_1	0.01	1.3
	b	0.02	0.14
$\varkappa_1 = -2\varkappa_0$ $c_0 = 0.45$	E	1.92	4.00
	B	15	9.9
	B_0	15	13
	B_1	0.003	0.3
	b	0.03	0.28
$A,Z = 116,50$ case 6			
$\varkappa_1 = 0$ $c_0 = 0.45$	E	2.20	4.23
	B	6.9	7.5
	B_0	18	4.6
	B_1	2.5	0.4
	b	0	0
$\varkappa_1 = -0.5\varkappa_0$ $c_0 = 0.43$	E	2.18	4.20
	B	11	6.6
	B_0	20	4.7
	B_1	1.3	0.2
	b	0.13	−0.09
$\varkappa_1 = -2\varkappa_0$ $c_0 = 0.41$	E	2.16	4.17
	B	17	5.5
	B_0	22	4.6
	B_1	0.4	0.04
	b	0.24	−0.18
$A,Z = 112,48$ case 5b			
$\varkappa_1 = 0$ $c_0 = 0.45$	E	2.15	3.82
	B	9.1	6.3
	B_0	17	1.8
	B_1	1.1	1.4
	b	0	0
$\varkappa_1 = -0.5\varkappa_0$ $c_0 = 0.435$	E	2.14	3.93
	B	12	4.5
	B_0	18	1.6
	B_1	0.5	0.7
	b	0.09	−0.33
$\varkappa_1 = -2\varkappa_0$ $c_0 = 0.42$	E	2.13	4.04
	B	15	2.1
	B_0	18	1.1
	B_1	0.1	0.1
	b	0.17	−0.72

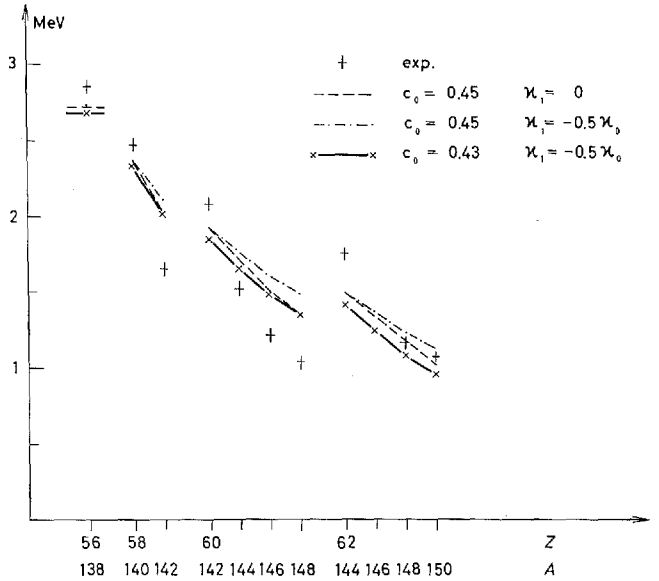

Fig. 11. Experimentally and theoretically determined values of the lowest resulting energy in nuclei in case 8a from section 15. The theoretical values are calculated for different $\varkappa_0$ and $\varkappa_1$. c_0 is defined by $S_1 = 7/\varkappa_0 = c_0 \times A^{5/3}$ where $\varkappa_0$ is the effective force constant as discussed in sections 13 and 14. A is the atomic number.

Only one comment is left. As will be discussed below, it is almost always possible for $\varkappa_1 = 0$ to use a smoothly varying $\varkappa_0$ in different regions of the periodic table. An exception is e.g. the nucleus $A,Z = 90,40$, for which a somewhat smaller $\varkappa_0$ is needed to reproduce the experimental energy. As seen above, the theoretically determined energy is practically unchanged when $\varkappa_1 \neq 0$ is introduced (since $B \lesssim B_0$). Thus, $\varkappa_1 \neq 0$ cannot provide a greater $\varkappa_0$.

11. Influence of $\varkappa_1$ on inelastic scattering

In the preceding sections we have discussed the influence of $\varkappa_1$ on B and B_0 which two quantities are relevant in Coulomb excitations and in the scattering of isospin-zero particles, respectively.

For some few examples, table 6 gives the quantity b, defined in sect. 4, especially connected to scattering, e.g. of protons or neutrons.

For $\varkappa_1 = 0$, b vanishes, but already for $\varkappa_1 = -0.5\varkappa_0$, in some cases it is so large that it should influence the relative cross section considerably. E.g. for $|b| = 0.1$, the relative cross section for inelastic proton and α

particle scattering should differ by 20 %. From a comparison of the results in the table with those from the detailed calculation (tables 21 to 36) it is easily seen where the greatest effects are expected.

12. The collective character of the states

The amount of collectiveness in the excitation can be demonstrated, e.g., by comparing B with the single-particle estimate $B_{\text{s.p.}}$ (table 7). It may be

TABLE 7. The ratio for some selected nuclei of the predicted B value (from the detailed calculation) to the single-particle value, using for this last one the estimate $B_{\text{s.p.}} = 0.416\, A^2 e^2\, 10^{-78}\ \text{cm}^6$.

case	1	2a	3a	5a	6	7a	7b	7c
A,Z	60,28	88,38	96,42	110,48	116,50	124,52	124,52	124,52
$B/B_{\text{s.p.}}$	16	24	23	14	12	6	3	17

case	8a	8a	8c	8c	9a
A,Z	140,58	150,62	140,58	150,62	208,82
$B/B_{\text{s.p.}}$	13	35	20	45	33

mentioned that, when the single-particle transition of lowest energy goes from an almost filled to an almost empty level, every one of the particles gives a contribution to B, which thus may be large without any coupling between the excitations. More detailed information on the states is obtained from a study of the relative magnitude of the amplitudes for different two-quasiparticle creations and annihilations in the resulting excitation $p(\alpha,j_1,j_2)$ and $q(\alpha,j_1,j_2)$ introduced in sect. 3.

If $\varkappa_1 = 0$ but $\varkappa_0 \neq 0$ they are given by (ref. 1)

$$p(\alpha,j_1,j_2) = \frac{1}{(S'(\hbar\omega_\alpha))^{1/2}} \frac{\langle j_2 || i^3 Y_3 \left(\frac{r}{a}\right)^3 || j_1 \rangle (u_{j_1} v_{j_2} + v_{j_1} u_{j_2})}{E(j_1) + E(j_2) - \hbar\omega_\alpha}, \qquad (12.1)$$

$$q(\alpha,j_1,j_2) = \frac{1}{(S'(\hbar\omega_\alpha))^{1/2}} \frac{\langle j_2 || i^3 Y_3 \left(\frac{r}{a}\right)^3 || j_1 \rangle (u_{j_1} v_{j_2} + v_{j_1} u_{j_2})}{E(j_1) + E(j_2) + \hbar\omega_\alpha}, \qquad (12.2)$$

where $\hbar\omega_\alpha$ is the energy of the state, and

$$S'(\hbar\omega_\alpha) = S'^{p}(\hbar\omega_\alpha) + S'^{n}(\hbar\omega_\alpha). \tag{12.3}$$

When $\hbar\omega_\alpha$ is not very near to the energy of any of the unperturbed modes, many of these contribute to the state with comparable amplitudes. Because of the denominators the amplitudes for quasiparticle annihilation are much smaller than for quasiparticle creation, unless $E(j_1) + E(j_2) \gg \hbar\omega_\alpha$. This condition is fulfilled when the level is pushed far down from the unperturbed

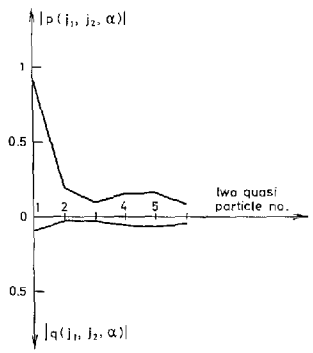

Fig. 12a.

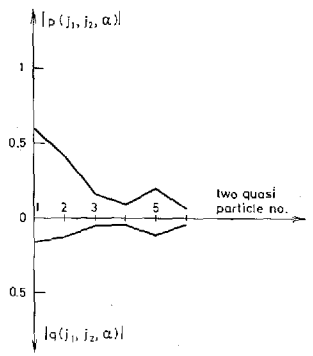

Fig. 12b.

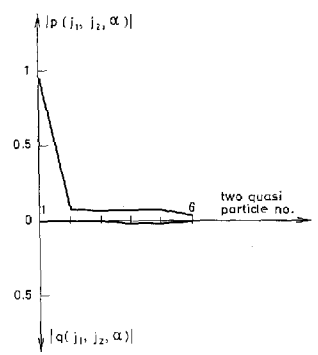

Fig. 12c.

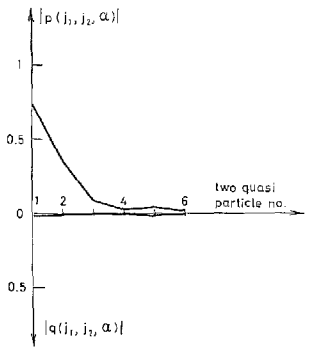

Fig. 12d.

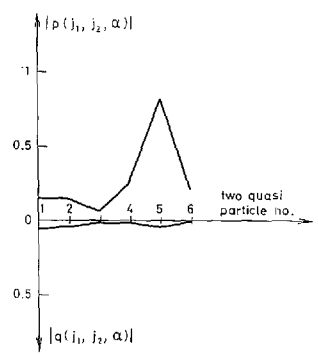

Fig. 12e.

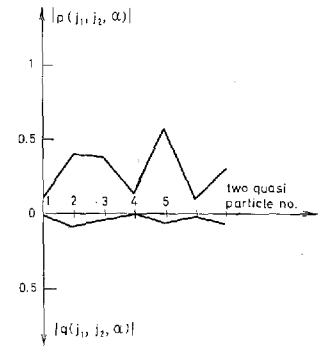

Fig. 12f.

Fig. 12. The numerical value of the two-quasiparticle amplitudes $p(\alpha, j_1, j_2)$ and $q(\alpha, j_1, j_2)$ (p up q down) from the 6 or 7 unperturbed lines of lowest energy
a) to the lowest lying collective level in $A,Z = 142,60$ (case 8a).
b) to the lowest lying collective level in $A,Z = 148,60$ (case 8a).
c) to the lowest lying collective level in $A,Z = 132,54$ (case 7b).
d) to the second resulting level in $A,Z = 148,60$ (case 8).
e) to the fifth resulting level in $A,Z = 148,60$ (case 8a).
f) to the third resulting level in $A,Z = 116,50$ (case 6, a preliminary calculation).

energies towards zero, or when considering contributions from higher lying transitions.

For the state of lowest energy the amplitude $p(\alpha,j_1,j_2)$ has the same sign as the reduced matrix element times the uv factor. This means that it has the same sign as the annihilation term in the two-quasiparticle interaction (ref. BM). In this sense there is a special coherence in the lowest state. This coherence is also demonstrated by the fact that all contributions to B have the same sign, S^p only contains positive terms.

For the other states the denominator in $p(\alpha,j_1,j_2)$ is negative for contributions from unperturbed modes at lower energy and positive for contributions from unperturbed modes at higher energy.

Then, some cancellation effect arises (cf. the discussion in sects. 6 and 8 of the vanishing of the lines in the gap between the $\Delta N = 1$ and the $\Delta N = 3$ transitions).

In fig. 12 the numerical values of the amplitudes for the lowest resulting state are given for a medium collective (a), a strongly collective (b), and a weakly collective case (c). For (c) the nearest unperturbed mode dominates completely. In (a) $p^2 - q^2$ from the lowest unperturbed excitation is $\simeq 85\,\%$, while in (b) the contribution from the six lowest ones is about $54\,\%$. Thus, $46\,\%$ is left for contributions from the remaining part of the levels in the unperturbed spectrum. In (d) and (e) we consider the 2^{nd} and the 5^{th} resulting state from the same nucleus as in (b). (d) is a rather weak state where $S_p < 0$ because it lies just above a strong proton line. (e) is the second, strong state in the spectrum. Another example of this kind is (f).

13. The renormalization procedure

As mentioned above all the single-particle transitions in principle are taken into account when the resulting energies and transition probabilities are calculated. Thus, no concept of effective charge is introduced.

The contributions from the $\Delta N = 3$ excitations are evaluated in the simple harmonic oscillator model. Such an approximative treatment may be justified by the fact that S_2, the $\Delta N = 3$ part of S, always plays a minor role in comparison to that of S_1. When going to the highest end of the periodic table this changes somewhat, but still in ^{208}Pb $S_1 > 2S_2$, although the double closed shells allow no transitions of very low energy in S_1.

When performing the calculation we found it convenient to work with a renormalized force constant $\varkappa_{\text{eff}}$ defined by

$$\frac{7}{\varkappa_{\text{eff}}} = S_1 (= S - S_2). \tag{13.1}$$

The resulting energies are thus obtained as the solutions to this equation, neglecting the energy variation of S_2. This should be a good approximation, when the low-energy states are considered.

To calculate B we added to S_1^p the quantity $S_2^p = 0.05\, A^{5/3}$ which value was found to be a good approximation from ^{16}O to ^{208}Pb.

For $S' = S^{p'} + S^{n'}$ we simply used S_1' since the difference is very small and of no importance, when the uncertainties in the treatment are remembered. In the calculation of B_1 and B_0 we used values of S_2, quoted in sect. 14.

14. The parameters

The nuclei which we have considered are divided into regions (cases) as shown below. In each of these regions G was chosen as $20/A_0$ where A_0 is some representative atomic number in the region. This standard value is pretty near to that which has been used before in spherical nuclei (refs. 4 and 12).

An exception is made for the region $28 \leq Z \leq 50$. Here, KISSLINGER and SORENSEN (ref. 12) have found that G_p (G for protons) should be $26/A$ to give the right quasiparticle energies. We have made calculations for both values of G_p and find the best results with the high one. (For further details: see below).

The shell-model levels $\varepsilon(j)$ have been taken from ref. (13) except for the partly filled shells for which the level separations were obtained from KS I and KS II or from stripping and pick-up experiments (for details, see below). Since one of the weakest points in the treatment is the poor knowledge of the exact value of $\varepsilon(j)$s, we have in several cases made calculations with different level schemes.

In our treatment we have looked apart from short range neutron-proton interactions. Experimentally it is found that sometimes there are rather strong shifts in the single-particle levels, e.g., so that the neutron level with $j = l - \frac{1}{2}$ moves down in energy when the lower spin-orbit partner is filled by the protons (ref. 14). By using a simple δ-function force it has been possible to describe this effect (ref. 15), but the explanations are still rather tentative, and a survey including satisfactory quantitative predictions over

a wider region of the periodic table does not exist. In some cases where experiments indicate the existence of this effect, it is taken into account.

Since many parts of the residual interaction are not explicitely included in our Hamiltonian, we should not be surprised to see how the theoretically or experimentally determined effective locations of the levels change from region to region of the periodic table.

There is little direct evidence concerning the separation of levels in different shells. In our calculation the distance from the "center of gravity" of the partly filled shell to the centers of gravity in the shells above and below have been chosen to be approximately the same as in the simple shell-model calculation (ref. 13), but sometimes, when the shell is almost filled or almost empty, we have tried to reproduce approximately the distances corresponding to the strongest, low energy transitions across the shells. It is clear that the uncertainty here suggests to take the energies and B values of the states in the 3–5 MeV region as even more tentative and preliminary results than those for the resulting state of lowest energy.

In the determination of the $\varkappa$ variation we started by estimating S_2/A from the simple harmonic oscillator model, giving points on a line 0.027 A within 5 %. The experimental energies were inserted in S_1 to give some experimental value of the effective force constant (13.1). Smoothe curves were drawn for $7/\varkappa_{\text{eff}} A = S_1/A$ and $7/\varkappa A = S/A$. As we could perhaps have expected, none of these curves could be fitted by a simple power dependence of A, but to a good approximation $7/\varkappa_{\text{eff}}$ could in the different regions of the periodic table be given by a variation like $A^{5/3}$. Then all the calculations were run again, using

$$\frac{7}{\varkappa_{\text{eff}}} = S_1 = c_0 \frac{A^{5/3}}{\text{MeV}}. \tag{14.1}$$

The details are discussed in section 15. In most cases $c_0 = 0.45$ was chosen. This value corresponds to a force constant, given by

$$\frac{7}{\varkappa} = 0.45 \frac{A^{5/3}}{\text{MeV}} + 0.027 \frac{A^2}{\text{MeV}} \tag{14.2}$$

(cf. equation (13.1)).

Since S_2 varies somewhat more strongly with A than S does, $S_1 = S - S_2$ was a little lower in the heaviest nuclei ($c_0 = 0.404$ for Pb).

For the lighter nuclei the situation was unclear, but S_1 may have a variation like A^2.

The $A^{5/3}$ variation of $\varkappa$ is somewhat slower than expected from the simple scaling argument in sect. 2. Whether this points to a real effect is difficult to say, in view of uncertainties in S_2 due to the meager knowledge of the high lying unperturbed modes, and in view of uncertainties in S_1 which is strongly influenced by the two-quasiparticle excitations of lowest energy.

15. The calculation and the results

In our treatment we shall neglect the pairing interaction between neutrons and protons. Thus, it is essential that there is a reasonably large distance between their Fermi levels; therefore we have not considered nuclei with $28 < Z < 40$ when $28 < N < 40$, whereas we have investigated nuclei with Z and N at each side of the subshell at 40 and nuclei, where the proton shell between 50 and 82 is almost empty and the same neutron shell is almost filled.

For each value of N and Z and for the possible, different level schemes the BCS equations (2.4) and (2.5) were solved and the values for $u(j)$, $v(j)$ and $E(j)$ inserted into the eigenvalue equation for $\hbar\omega_\alpha$ (3.13). For some of the nuclei λ and Δ are given in tables 8 to 19. The distances from some levels in the partly filled shell to a level in the shell above and the shell below is given in table 20.

TABLE 8. λ and Δ for case 1.

	$N = 30$	$N = 32$	$N = 34$	$N = 36$
λ.....	−0.32	0.131	0.594	1.079
Δ	0.810	1.048	1.152	1.142

TABLE 9. λ and Δ for case 2 a.

	$Z = 30$	$Z = 32$	$Z = 34$	$Z = 36$	$Z = 38$
λ.....	−0.560	−0.125	0.339	0.842	1.457
Δ	0.89	1.153	1.270	1.107	1.018

	$N = 40$	$N = 42$	$N = 44$	$N = 46$	$N = 48$
λ.....	2.670	3.138	3.496	3.818	4.123
Δ	0.650	0.833	0.884	0.828	0.650

TABLE 10. λ and Δ for protons from case 2 b.

$N = 40$:	$Z = 30$	$Z = 32$	$Z = 34$	
λ.....	−0.645	−0.205	0.257	
Δ	0.991	1.303	1.467	

$N = 42$:	$Z = 32$	$Z = 34$	$Z = 36$	
λ.....	−0.263	0.178	0.667	
Δ	1.215	0.972	0.958	

$N = 44$:	$Z = 32$	$Z = 34$	$Z = 36$	
λ.....	−0.349	0.082	0.570	
Δ	1.168	1.289	1.306	

$N = 46$:	$Z = 32$	$Z = 34$	$Z = 36$	$Z = 38$
λ.....	−0.429	−0.013	0.465	1.111
Δ	1.082	1.182	1.169	1.093

$N = 48$:	$Z = 34$	$Z = 36$	$Z = 38$	
λ.....	−0.116	0.364	1.060	
Δ	1.114	1.082	0.963	

$N = 50$:	$Z = 36$	$Z = 38$		
λ.....	0.259	1.017		
Δ	0.955	0.760		

TABLE 11. λ and Δ for cases 3 a and 4 a.

	$Z = 38$	$Z = 40$	$Z = 42$	$Z = 44$
λ.....	1.435	2.293	2.858	3.286
Δ	0.848	0.835	0.996	1.039

TABLE 11 (continued).

$Z = 40$:	$N = 52$	$N = 54$	$N = 56$
λ.....	−0.227	0.132	0.766
Δ	0.518	0.617	0.569

$Z = 42$:	$N = 52$	$N = 54$	$N = 56$	$N = 58$
λ.....	−0.242	0.119	0.685	1.189
Δ	0.534	0.653	0.687	0.968

$Z = 44$:	$N = 52$	$N = 54$	$N = 56$	$N = 58$	$N = 60$
λ.....	−0.244	0.097	0.577	1.010	1.317
Δ	0.521	0.651	0.727	0.940	1.095

TABLE 12. λ and Δ for case 5 a.

	$Z = 46$	$Z = 48$	$N = 56$	$N = 58$	$N = 60$	$N = 62$	$N = 64$	$N = 66$	$N = 68$
λ.....	3.586	3.868	0.171	0.501	0.850	1.215	1.655	2.062	2.364
Δ	0.749	0.591	0.759	0.799	0.838	0.836	0.841	0.947	1.032

TABLE 13. λ and Δ for neutrons from case 5 c.

	$N = 56$	$N = 58$	$N = 60$	$N = 62$	$N = 64$	$N = 66$	$N = 68$
λ.....	−0.093	0.150	0.415	0.726	1.131	1.529	1.833
Δ	0.898	0.957	0.971	0.942	0.914	0.988	1.057

TABLE 14. λ and Δ for neutrons from case 6.

	$N = 64$	$N = 66$	$N = 68$	$N = 70$	$N = 72$	$N = 74$
λ.....	1.199	1.700	2.012	2.277	2.520	2.746
Δ	0.606	0.756	0.854	0.901	0.912	0.889

TABLE 15. λ and Δ for case 7 a.

	$Z = 52$	$Z = 54$	$Z = 56$	$Z = 58$
λ.....	0.241	0.425	0.616	0.818
Δ	0.504	0.674	0.774	0.828

	$N = 68$	$N = 70$	$N = 72$	$N = 74$	$N = 76$	$N = 78$	$N = 80$
λ.....	1.548	1.740	1.930	2.120	2.313	2.507	2.704
Δ	1.051	1.032	0.992	0.928	0.835	0.706	0.516

TABLE 16. λ and Δ for protons from case 7 b.

	$Z = 52$	$Z = 54$	$Z = 56$	$Z = 58$
λ.....	−0.310	−0.095	0.143	0.414
Δ	0.438	0.569	0.631	0.657

TABLE 17. λ and Δ for neutrons from case 7 c.

	$N = 68$	$N = 70$	$N = 72$	$N = 74$	$N = 76$	$N = 78$	$N = 80$
λ.....	2.040	2.290	2.519	2.731	2.931	3.122	3.307
Δ	0.745	0.797	0.815	0.800	0.749	0.655	0.491

TABLE 18. λ and Δ for case 8 a.

	$Z = 56$	$Z = 58$	$Z = 60$	$Z = 62$	$N = 84$	$N = 86$	$N = 88$
λ.....	0.154	0.421	0.704	0.985	−0.469	−0.275	−0.006
Δ	0.530	0.538	0.549	0.514	0.533	0.733	0.877

TABLE 19. λ and Δ for case 9 b.

	$Z = 76$	$Z = 78$	$Z = 80$
λ.....	2.709	3.055	3.283
Δ	0.139	0.233	0.152

	$N = 114$	$N = 116$	$N = 118$	$N = 120$	$N = 122$	$N = 124$
λ.....	1.546	1.716	1.887	2.056	2.227	2.444
Δ	0.721	0.665	0.604	0.529	0.425	0.256

TABLE 20. The energy difference between some level in the partly filled shells and a level in the shell above or below.

case	levels	energy (MeV)
1, protons and neutrons	$3f_{7/2}-3p_{3/2}$	2.6
	$4g_{9/2}-4g_{7/2}$	3.88
2a, protons	$2d_{3/2}-3f_{5/2}$	7.5
	$4g_{9/2}-4g_{7/2}$	2.4
2a, neutrons	$2d_{3/2}-3f_{5/2}$	7.5
	$4g_{9/2}-4g_{7/2}$	2.2
3, protons	$2d_{3/2}-3f_{5/2}$	7.5
	$4g_{9/2}-4g_{7/2}$	2.4
3, neutrons	$4g_{9/2}-4d_{5/2}$	2.9
	$5h_{11/2}-5f_{7/2}$	5.4
5b, protons	$3f_{7/2}-3f_{5/2}$	2.9
	$4g_{9/2}-4g_{7/2}$	2.4
5b, neutrons	$4g_{9/2}-4d_{5/2}$	3.6
	$4s_{1/2}-5f_{7/2}$	4.9
6, neutrons	$4g_{9/2}-4d_{5/2}$	3.4
	$5h_{11/2}-5f_{7/2}$	3.6
7a, protons	$4g_{9/2}-4d_{5/2}$	3.0
	$4s_{1/2}-5f_{7/2}$	4.44
7a, neutrons	$4g_{9/2}-4g_{7/2}$	3.2
	$4s_{1/2}-5f_{7/2}$	5.7
8a, protons	$5h_{11/2}-5f_{7/2}$	5.4
	$4g_{9/2}-4g_{7/2}$	2.2
8a, neutrons	$5p_{1/2}-6g_{9/2}$	2.3
	$4s_{1/2}-5f_{7/2}$	4.67
9b, protons	$4s_{1/2}-5h_{9/2}$	4.26
	$4g_{9/2}-4g_{7/2}$	2.1
9b, neutrons	$5p_{1/2}-6g_{9/2}$	3.6
	$4s_{1/2}-5f_{7/2}$	4.95

The number of terms in S_1 was between 54 and 96, greatest in the heaviest nuclei.

The calculation was performed on a GIER computing machine with programs written in ALGOL.

In general the ten lowest resulting energies have been calculated. In tables 21 to 36 we report all those which seem to be of interest with special emphasis on those excitations which have significant values of B or B_0. In figures 13 to 20 we give the energy of the lowest mode and compare with the experimental data. When experimental B values are available, we also give the theoretical results.

A very large part of the experimental information comes from an article by HANSEN and NATHAN (ref. 16). The B values, given by these authors, were derived from inelastic α scattering experiments, assuming pure Coulomb excitation. However, it appears that owing to the fact that the energy of the α particles comes near to the Coulomb barrier, penetration becomes important, and the real B values are smaller by a factor two or three in most cases (an exception seems to be the $A \sim 145$ region, cf. ref. 48). Therefore only the energies from ref. 16 are given below.

Case 1: $Z = 28$.

In this region the proton shell is closed, and the situation could be expected to be somewhat similar to *Sn* where a strong line appears just below the energy of the proton transitions between the shells. Such a line is only seen for the heaviest isotopes.

For neutron number = 30, the neutron fermi energy lies below the lowest level in the partly filled shell, the neutron transitions are rather high in energy, and most of the available oscillator strength is concentrated on one level. The calculations were done with the KS II neutron levels: $f_{5/2}$:0, $p_{3/2}$:0, $p_{1/2}$:3 and $g_{9/2}$:4 MeV and with the KS I levels 0.78, 0, 1.56 and 4.52 MeV. Since COHEN, FULMER and MCCARTHY found good experimental agreement with the last level scheme (ref. 17) we only report the results which have been obtained when using this scheme. For the KS II single particle energies there is an accidental degeneracy which can give rise to special phenomena in the figures. Apart from this, the results from the two calculations are not very different.

In recent (d,t) experiments, the results of which were published when our calculation was finished, FULMER and DALHNICK (ref. 18) find good agreement with KS I, only the $p_{1/2}$ level should perhaps come at 1.12 MeV.

Since the proton shell is closed, the lowest resulting states are essentially governed by the strong neutron transition $p_{3/2} - g_{9/2}$ and the weak $f_{5/2} - g_{9/2}$ transition. The proton transitions coming up from the (sd)-shell are rather weak and not very low energetic. The most important proton excitation is $f_{7/2} - g_{9/2}$ which is of medium strength. If we change the intershell distance $f_{7/2} - p_{3/2}$ from 2.6 MeV, the value we have used, to 4 MeV, as supposed by

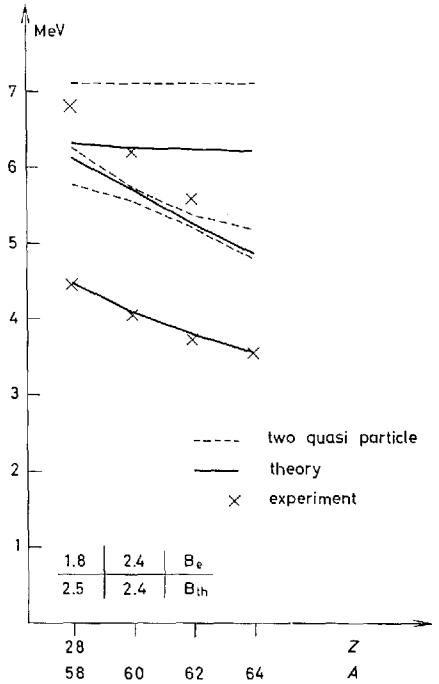

Fig. 13. The lowest-lying theoretical and experimental energies and B values for the Ni group (case 1), $c_0 = 0.39$. The dashed lines indicate the two-quasiparticle energies. The experimental data are taken from different authors (ref. 34).

KS II, the B value in $A,Z = 58,28$ is diminished by a factor of 2, whereas in 64,28 it goes down by a factor $\frac{4}{3}$. The energy is 0.5 MeV greater in the lightest nucleus, 0.1 in the heaviest one. This great influence, especially on the B values, is not very surprising, since mainly the protons contribute here. The $\tau = 0$ part of B is less affected.

The best fit to the energies was reached by $c_0 = 0.39$, for which the energies are plotted in fig. 13. This value does not lie on the smooth curve for S_1 discussed in sect. 14, and therefore another calculation was run, using $c_0 = 0.435$. In table 21 the lowest energy is given for $c_0 = 0.435$ and energies for all the stronger lines for $c_0 = 0.39$.

The theory indicates the existence of one or two higher-lying excitations of apprcciable strength and in some cases such levels are found, but the agreement between theory and experiment is poor, perhaps because of uncertainties in the shell-model levels.

The B values of the lowest level are rather well reproduced by theory. We note that when we extend the $f_{7/2} - p_{3/2}$ distance towards the KS II value,

TABLE 21. The first row gives energy, B and B_0 for the state of lowest excitation energy for case 1, $c_0 = 0.435$. The following rows contain data for the most strongly excited, low-lying states in case 1, when $c_0 = 0.39$.
For units, see caption to table 3.

A,Z:	58,28			60,28			62,28			64,28		
E, B, B_0:	4.84	1.8	2.5	4.46	1.7	2.9	4.19	1.6	3.3	3.95	1.5	3.5
	4.47	2.5	3.3	4.07	2.4	3.9	3.82	2.3	4.4	3.57	2.3	4.8
	6.13	0.6	0.3	6.25	1.2	0.6	6.26	1.4	0.8	6.21	1.5	1.0
	6.31	0.2	0.1	7.30	0.2	3×10^{-2}	7.33	0.2	4×10^{-2}	7.33	0.2	5×10^{-2}
	7.24	0.2	10^{-2}									

B passes the experimental figure. As it was to be expected, $S^p < S^n$ for the lowest level and $B_0 > B$ as discussed before. When the number of neutrons increases, the lowest resulting level is pressed down, away from the lowest proton mode; B decreases and B_0 goes up.

Note added in proof: A new investigation of the Ni spectra has recently been planned in Paris. Partly inspired by this experiment we have performed two more calculations to see how the results are changed when other single particle shell model level schemes are used: (b) proton levels $f_{7/2}$: -3, $p_{3/2}$:0, $f_{5/2}$:0.8, $p_{1/2}$:2.2 and $g_{9/2}$:3.0 MeV, neutron levels $f_{7/2}$: -4, $p_{3/2}$:0, $f_{5/2}$:0.77, $p_{1/2}$:1.12 and $g_{9/2}$:4.0 MeV, $G_n = 24/A$. (c): The $g_{9/2}$ neutron level placed at 3 MeV, the other levels unchanged from (b). $G_n = 24/A$. In both cases $c_0 = 0.39$. The results are presented in tables 21 b and 21 c.

TABLE 21 b. Energy, B and B_0 (in same units as in table 3) for the strongest, low energy excitations in case 1 b, when $c_0 = 0.39$.

A,Z:	58,28			60,28			62,28			64,28		
E, B, B_0:	4.57	3.3	3.1	4.31	3.3	3.9	4.04	3.2	4.7	3.77	3.2	5.4
	6.55	0.006	0.2	6.23	0.1	0.06	6.04	0.4	0.003	5.92	0.6	0.01
	7.40	0.2	0.09	7.35	0.3	0.2	7.33	0.3	0.3	7.25	0.3	0.5
	7.95	0.1	0.4	8.00	0.2	0.4	7.94	0.1	0.5	7.73	10^{-3}	0.3

TABLE 21 c. Energy, B and B_0 (in the same units as in table 3) for the strongest, low energy excitations in case 1 c, when $c_0 = 0.39$.

A,Z:	58,28			60,28			62,28			64,28		
E, B, B_0:	4.34	3.1	3.3	4.03	3.0	4.0	3.78	2.9	4.6	3.61	2.9	5.2
	6.12	0.2	0.01	5.91	0.4	10^{-2}	5.84	0.7	0.05	5.79	0.8	0.1
	7.15	0.2	0.4	7.25	0.3	0.4	7.28	0.3	0.4	7.27	0.3	0.5
							7.79	0.01	0.4	7.79	0.2	0.5

Case 2: $28 < Z < 40$; $40 \leq N \leq 50$

Here rather many neutrons (or rather neutron holes) are available in the unfilled shell for the lighter isotopes whereas there are only few protons. The B values are low in the beginning and increase with increasing atomic number. There is some tendency for giving a line in the gap above the transitions inside partly filled shells, but the stronger proton transitions between the shells are rather high in energy and do not contribute much to the low-energy spectrum.

Calculations were made for (a) the KS I proton levels $f_{5/2} = 0$, $p_{3/2} = 0.6$, $p_{1/2} = 1.8$ and $g_{9/2} = 3.4$ MeV and $G_p = 26/A$. Neutron levels from KS II: $f_{5/2} = 0$, $p_{3/2} = 0.3$, $p_{1/2} = 2.5$ and $g_{9/2} = 3.6$ MeV. (b) neutron levels like in (a), proton levels which are almost equal to the KS II ones: $p_{3/2}$:0, $p_{1/2}$:1.8, $g_{9/2}$:2.8 and $f_{5/2}$: $-0.6 + (50 - N) \times 0.1$ MeV where N is the neutron number, $G_p = 26/A$. In both cases $c_0 = 0.45$ was used. The lowest proton and neutron two-quasiparticle excitations are the weak $f_{5/2} - g_{9/2}$ and the strong $p_{3/2} - g_{9/2}$ transition. When going from (a) to (b) the $p_{3/2}$ $g_{9/2}$ distance which represents the strong proton transition inside the shell is constant, and thus the (a) and (b) results are rather similar. The differences arise from the fact that in (b) the $f_{5/2}$ proton level is placed above $p_{3/2}$ and is populated less for the lower values of the neutron number. Therefore the strong $p_{3/2} - g_{9/2}$ transition has the greatest uv factor in (b), and B is larger. In tables 22 and 23 we give the results for cases (a) and (b). The lowest level was discussed above. For the second level, given in table 22, S^n is small, because we have just passed a neutron excitation. Thus in most cases $B > B_0$.

Some of the lines of higher energy are rather mixed in isospin character ($B_0 \simeq B_1 >> B$), indicating that the line is primarily due to neutron excitations. The experimental material is very meager. For the lighter nuclei Darcey gives energies below the theoretically predicted values and with slower variation.

For $A,Z = 88,38$ the energy is rather well reproduced by the (a) calculation, but B is too small by 30 % (see also the results from case 3).

Case 3: $Z = 40, 42$; $50 \leq N \leq 82$. ($A,Z = 88,38$ is also included).

In this region, we start with a relative large lowest energy in $A,Z = 90,40$, having a closed neutron shell and closed proton subshell, but B is large since the transition across the proton subshell is strong. When more neutrons enter, the energy goes down. The quantity B is almost constant and is spread a little over the lowest levels.

We used the KS I proton levels (as in case 2a), and neutron levels based on stripping experiments (ref. 19) $d_{5/2}$:0, $s_{1/2}$:1.7, $g_{7/2}$:2.6, $d_{3/2}$:2.7 and

TABLE 22. Energy, B and B_0 for the low-energy, stronger levels in case 2 a, $c_0 = 0.45$. Same units as in table 3.

A,Z:	70,30			72,32			74,32		
E, B, B_0:	2.54	1.4	4.4	2.51	2.0	5.0	2.84	2.0	5.2
	5.05	0.5	0.4	4.75	1.1	0.5	4.78	1.0	0.4
	5.28	0.7	0.7	5.63	0.2	0.8	5.67	0.3	1.0

A,Z:	76,32			78,32			74,34		
E, B, B_0:	3.13	2.1	5.2	3.29	1.9	4.9	2.42	3.2	6.1
	4.79	0.8	0.3	4.22	0.3	0.5	4.41	0.3	0.3
	5.62	0.3	1.1	5.46	0.1	0.9	5.60	0.4	1.1
							6.35	0.5	0.3

A,Z:	76,34			78,34			80,34		
E, B, B_0:	2.72	3.3	6.3	3.01	3.4	6.2	3.17	3.2	5.9
	4.44	1.2	0.2	4.43	0.7	0.2	4.17	0.6	0.4
	5.65	0.6	1.3	5.59	0.5	1.5	4.53	0.6	0.04
							5.42	0.3	1.3

A,Z:	82,34			78,36			80,36		
E, B, B_0:	3.19	2.7	5.4	2.44	5.7	7.8	2.67	5.7	7.4
	4.16	1.5	1.2	3.92	0.6	10^{-4}	5.46	1.3	1.8
	5.18	0.07	0.9	5.51	1.4	1.7			

A,Z:	82,36			84,36			86,36		
E, B, B_0:	2.82	5.6	7.1	2.89	5.2	6.8	2.85	4.6	6.5
	5.31	0.9	1.7	3.87	0.5	0.2	3.73	1.1	0.3
				4.58	0.03	0.6	4.69	0.2	1.7
				5.11	0.3	1.0	6.00	0.5	0.3
				6.13	0.7	0.2			

A,Z:	84,38			86,38			88,38		
E, B, B_0:	2.46	8.0	8.2	2.54	7.6	7.9	2.55	7.1	7.8
	5.14	1.6	1.6	4.53	0.3	1.1	4.59	0.7	2.3
				4.94	0.5	0.8	5.50	0.6	0.06
				5.77	0.5	0.02			

TABLE 23. Energy, B and B_0 for the level of lowest excitation energy in case 2 b, $c_0 = 0.45$. The following levels are rather weak and not very different from case 2 a. Same units as in table 3.

A,Z:	70,30			72,32			74,32		
E, B, B_0:	2.41	2.1	5.2	2.33	3.1	6.2	2.65	3.2	6.2
A,Z:	76,32			78,32			74,34		
E, B, B_0:	2.97	3.0	6.0	3.16	2.7	5.5	2.25	4.4	7.2
A,Z:	76,34			78,34			80,34		
E, B, B_0:	2.54	4.5	7.2	2.82	4.4	6.9	3.00	4.1	6.4
A,Z:	82.34			78,36			80,36		
E, B, B_0:	3.08	3.5	5.8	2.41	6.1	8.2	2.64	6.1	7.8
A,Z:	82,36			84.36			86,36		
E, B, B_0:	2.75	5.9	7.2	2.81	5.4	6.7	2.77	4.8	6.4
A,Z:	84.38			86,38			88,38		
E, B, B_0:	2.51	7.6	7.9	2.49	7.3	7.4	2.37	7.0	7.1

$h_{11/2}$: 2.8 MeV. Two calculations were run. a) $G_p = 26/A$ and b) $G_p = 20/A$. The neutron single-particle energies might be somewhat uncertain. There is some indication of a rather strong movement of the $g_{7/2}$ neutron level (ref. 20). Therefore this level is lowered by 0.4 MeV in $Z = 42$.

When neutrons are added to $N = 50$, the strong neutron transition $d_{5/2} - h_{11/2}$ is populated and goes rapidly down in energy. At $N = 56$ there is a minimum for the collective energy. After that the transition goes up, and the weak $g_{7/2} - h_{11/2}$ transition becomes the lowest one. The proton excitations have higher energy, and the uv factor in the numerator in S goes down (to 0.7) with increasing Z. To fit the experimental energy, $c_0 = 0.48$ was needed, which is greater than in the neighbouring cases. In fig. 15 the results are given for $Z = 40$ when using $c_0 = 0.45$. From the previous discussion we remember that we are not able to fit the energies with a lower c_0 value, if $\varkappa_1 < 0$ is introduced.

For $Z = 40$ the lowest level of the lightest nuclei has $S^p > S^n$ and thus

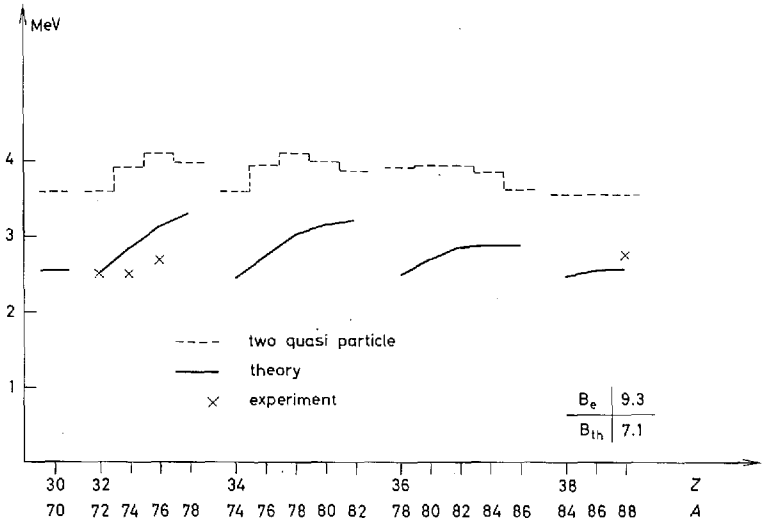

Fig. 14. The lowest-lying theoretical and experimental energies and B values for case 2a. The experimental data for $A,Z = 88,38$ are due to HELM (ref. 35). The other ones come from an experiment by W. DARCEY (ref. 36).

TABLE 24. Energy, B and B_0 for the low-energy, stronger excitations in cases 3a and 4a, $c_0 = 0.45$. Same units as in table 3.

A,Z:	88,38			90,40			92,40		
E, B, B_0:	2.74	6.2	4.9	2.61	8.4	6.3	2.37	9.1	9.3
	4.63	1.4	3.7	4.23	1.7	2.2	4.36	1.8	1.3
	4.80	1.5	2.7	4.80	0.5	0.2	5.19	0.3	1.3
				5.06	7×10^{-3}	0.8			
A,Z:	94,40			96,40			92,42		
E, B, B_0:	2.03	9.3	13	1.62	9.8	17	2.93	9.2	7.1
	3.31	0.7	0.02	3.21	1.5	0.07	4.06	0.9	1.0
	4.40	1.9	1.1	4.41	1.9	1.1	4.28	0.8	1.0
	5.24	0.4	1.1	5.27	0.6	1.5	4.80	0.6	1.0
							5.07	0.01	0.9
A,Z:	94,42			96,42			98,42		
E, B, B_0:	2.63	9.0	9.7	2.26	8.6	12	1.92	8.7	15
	4.12	0.6	0.3	3.54	1.4	0.07	3.49	2.1	0.3
	4.36	1.4	1.0	4.12	0.6	0.2	4.13	0.5	0.2
	5.19	0.3	1.4	4.39	1.6	0.9	4.40	1.7	0.9
				5.26	0.7	1.5	5.29	0.8	1.7

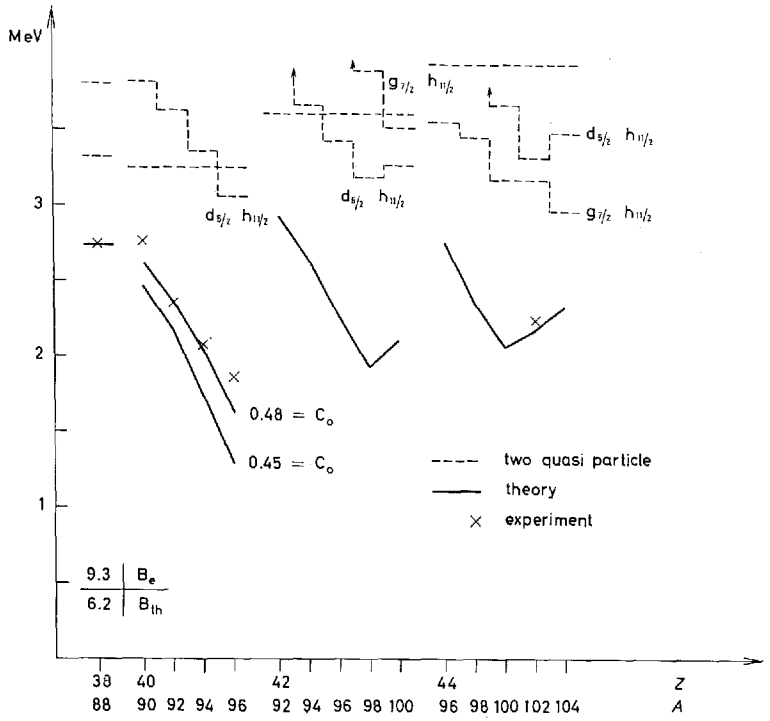

Fig. 15. Energies and B values for cases 3 and 4, where $d_{5/2}$ $h_{11/2}$ and $g_{7/2}$ $h_{11/2}$ denote the energy of the two-low lying neutron quasiparticle excitations. The theoretical energies are calculated with $c_0 = 0.48$. For $Z = 40$ the results for $c_0 = 0.45$ are shown. The experimental energies are due to HANSEN and NATHAN (ref. 16). For $A,Z = 88,38$ see caption to fig. 14.

TABLE 24 (continued).

A,Z:	100,42			96,44			98,44		
E, B, B_0:	2.11	8.8	15	2.76	8.1	9.7	2.36	7.6	12
	3.55	1.5	0.06	3.75	2.2	0.5	3.74	3.1	0.8
	4.43	1.7	0.8	4.29	1.6	1.1	4.31	1.8	1.1
	4.77	5.6	0.3	5.00	0.3	0.5	5.02	0.4	0.6
	5.37	1.4	1.6				5.44	10^{-5}	0.6

A,Z:	100,44			102,44			104,44		
E, B, B_0:	2.06	7.6	14	2.17	7.7	14	2.32	7.5	14
	3.75	3.0	0.8	3.79	2.9	0.6	3.82	2.4	0.4
	4.33	2.0	1.1	4.36	2.1	1.0	4.38	2.2	0.9
	4.72	0.5	0.4	4.73	0.6	0.4	4.74	0.7	0.4
	5.03	0.6	0.6	5.05	0.7	0.6	5.06	0.9	0.6

TABLE 25. Energy, B and B_0 for the lowest excitation, case 3 b and 4 b, $c_0 = 0.45$. Same units as in table 3.

A,Z:	88,38			90,40			92,40		
E, B, B_0:	2.26	6.0	4.4	2.10	9.9	7.0	1.92	11	10
A,Z:	96,40			96,40			92.42		
E, B, B_0:	1.64	13	15	1.28	15	21	2.29	9.3	6.5
A,Z:	94,42			96,42			98,42		
E, B, B_0:	2.12	11	9.5	1.87	12	13	1.60	12	17
A,Z:	100,42			96,44			98,44		
E, B, B_0:	1.77	12	17	2.48	9.6	9.7	2.17	9.5	12
A,Z:	100,44			102,44			104,44		
E, B, B_0:	1.91	9.5	15	2.02	9.5	15	2.16	9.4	15

$B_0 > B$. This is changed when the neutron number grows, and for some nuclei $B_0 \simeq 2B$. The smaller G_p in case b results in smaller collective energy but causes no major changes in B. We note that the theory predicts the existence of some higher-lying collective states.

Case 4: $Z = 44$.

The levels are the same as in case 3, only the neutron $g_{7/2}$ is lowered still further and the splitting in the neutron states changes a bit because of the variation in A.

The neutron levels are: $d_{5/2}$: 0, $s_{1/2}$: 1.6, $g_{7/2}$: 1.8, $d_{3/2}$: 2.6 and $h_{11/2}$: 2.7 MeV. For the discussion, see case 3.

Case 5: $Z = 46$ and 48.

When passing on to this region there are still fewer proton holes in the partly filled shell, and the available oscillator strength is not concentratedon the lowest excitation. A number of level schemes was studied. We shall only mention three:

a) the same proton levels as in case 3 a.
$G_p = 26/A$.

Neutron levels experimentally found by CUJEC (ref. 21) in stripping experiments in *Pd* $g_{7/2}$:0, $d_{5/2}$:1, $s_{1/2}$:2.5, $h_{11/2}$:2.9 and $d_{3/2}$:3.1 MeV.

b) same proton levels as in a) $G_p = \frac{26}{A}$.
KS I neutron levels:
$d_{5/2}$:0, $g_{7/2}$:0.22, $s_{1/2}$:1.9, $d_{3/2}$:2.2, and $h_{11/2}$:2.8 MeV.

c) proton levels like in a) $G_p = \frac{26}{A}$, neutron levels from a tentative interpretation of a (d,p) and (d,t) experiment in Cd by ROSNER (ref. 45).
$d_{5/2}$:0, $g_{7/2}$:0.2, $h_{11/2}$:2.25, $s_{1/2}$:2.25 and $d_{3/2}$:2.85 MeV.
This scheme is in fair agreement with the experimental (d,p) results, obtained by SILVA and GORDON (ref. 46) who find $g_{7/2}$ to be placed less than 0.4 MeV above $d_{5/2}$. KS II assumes this distance to be more than 1 MeV.

In a) there is a rather strong variation in the lowest neutron two-quasiparticle energies. The transition $d_{5/2} - h_{11/2}$ has the lowest energy, which varies much as λ passes $d_{5/2}$. In addition, the uv factor varies from 0.4 to 1. This causes a rapid variation in the resulting energy. This variation is not found in b) or c), since here the $d_{5/2} - h_{11/2}$ uv factor only varies from 0.6 to 0.9 and the two-quasiparticle energy changes more slowly. The lowest unperturbed energy appears about 0.5 MeV lower in c) than in b). The

TABLE 26. Energy, B and B_0 for the low-energy, stronger excitations in case 5 a, $c_0 = 0.45$. Same units as in table 3.

A,Z:	102,46			104,46			106,46		
E, B, B_0:	2.95	11	11	2.71	8.6	10	2.29	7.1	11
	4.11	1.7	0.5	3.71	2.8	0.7	3.66	4.3	1.5
	5.25	0.2	1.3	4.07	1.9	0.9	4.07	2.0	1.0
				5.28	0.3	1.2	5.30	0.4	1.2

A,Z:	108,46			110,46			106,48		
E, B, B_0:	1.86	7.0	13	1.60	7.4	16	2.73	8.9	11
	3.65	4.9	1.8	3.65	5.1	2.0	3.76	4.7	1.4
	4.07	2.2	1.1	4.07	2.3	1.2	5.23	0.5	1.2
	5.31	0.5	1.1	5.33	0.5	1.1			

TABLE 26 (continued).

A,Z:	108,48			110,48			112,48		
E, B, B_0:	2.33	7.2	11	1.19	7.0	13	1.65	7.2	15
	3.71	6.5	2.3	3.70	7.4	2.9	3.70	7.8	3.2
	5.25	0.5	1.1	5.25	0.6	1.0	5.48	0.2	1.0

A,Z:	114,48			116,48					
E, B, B_0:	1.77	7.5	16	1.99	7.6	16			
	3.46	1.7	1.2	3.62	4.2	2.3			
	3.75	6.8	2.6	3.83	4.0	1.2			
	5.51	0.5	1.1	5.53	0.7	1.0			

TABLE 27. Energy, B and B_0 for the low-energy, strong excitations in case 5 b, $c_0 = 0.45$. Same units as in table 3.

A,Z:	102,46			104,46			106,46		
E, B, B_0:	2.67	11	13	2.53	11	14	2.38	10	15
	4.16	2.1	0.4	3.82	1.1	0.03	3.79	1.8	0.2
				4.14	2.3	0.5	4.13	2.5	0.7

A,Z:	108,46			110,46			106,48		
E, B, B_0:	2.22	9.5	16	2.10	9.1	17	2.57	11	14
	3.76	2.6	0.5	3.74	3.3	0.8	3.95	3.4	0.4
	4.12	2.6	0.9	4.11	2.6	1.0			

A,Z:	108,48			110,48			112,48		
E, B, B_0:	2.42	10	15	2.27	9.6	16	2.15	9.1	17
	3.90	4.5	0.8	3.85	5.5	1.3	3.82	6.2	1.7

A,Z:	114,48			116,48					
E, B, B_0:	2.22	9.7	18	2.35	10	19			
	3.85	5.9	1.6	3.89	5.3	1.3			

TABLE 28. Energy, B and B_0 for the low-energy, stronger excitations in case 5 c, $c_0 = 0.45$. Same units as in table 3.

A,Z:	102,46			104,46			106,46		
E, B, B_0:	2.38	9.6	13	2.20	9.1	14	2.03	8.8	15
	3.72	2.8	0.6	3.71	3.4	0.8	3.70	3.9	1.1
	4.08	2.0	0.8	4.08	2.2	0.9	4.09	2.3	1.0

TABLE 28 (continued).

A,Z:	108,46			110,46			106,48		
E, B, B_0:	1.88	8.4	16	1.82	8.1	16	2.25	9.2	14
	3.68	4.5	1.4	3.68	4.8	1.7	3.78	5.7	1.6
	4.09	2.4	1.1	4.09	2.5	1.2			

A,Z:	108,48			110,48			112,48		
E, B, B_0:	2.08	8.8	15	1.94	8.4	16	1.88	8.1	16
	3.76	6.5	2.0	3.75	7.2	2.5	3.74	7.6	2.8

A,Z:	114,48			116,48					
E, B, B_0:	2.06	8.1	16	2.31	8.4	16			
	3.77	7.3	2.6	3.81	6.7	2.2			

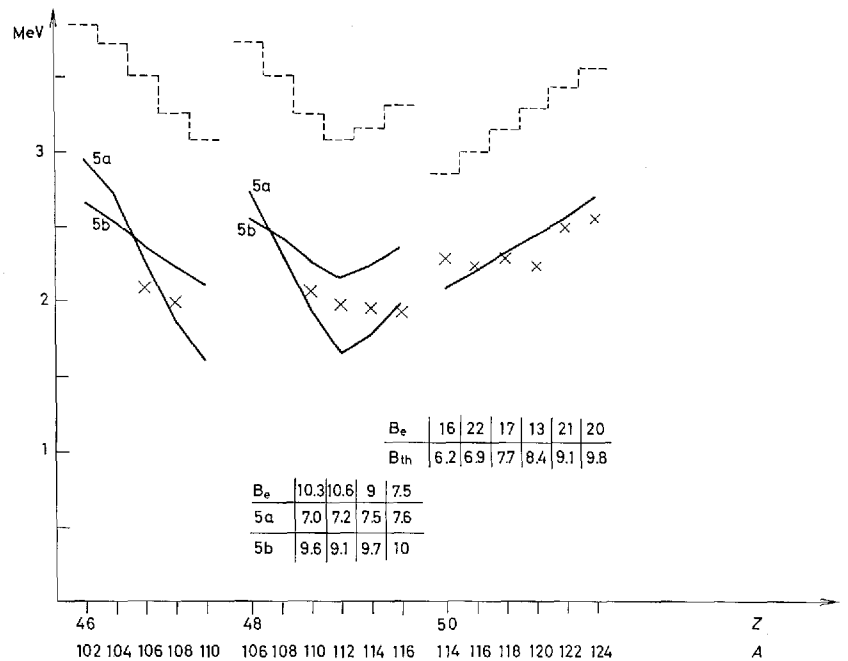

Fig. 16. Theoretically and experimentally determined energies and B values for cases 5a and 5b and for case 6. In 5, the quasiparticle energies are from case a. For cases 5, experimental data are available from HANSEN and NATHAN (ref. 16), from M. SAKAI et al. (ref. 37), and from MCGOWAN et al. (ref. 38). The experimental values for case 6 come from LEMBERG et al. (ref. 39).

Experiments by HANSEN and NATHAN for the nuclei in case 6 give the same energies except for Sn^{120} where they find an energy of perhaps 2.40 MeV. Their B values are a factor of 3 greater than the experimental ones given in the figure.

proton Fermi energy is higher than the energy of the levels in the partly filled shell. The lowest proton transition becomes high in energy and the uv factor is only 0.5 for $Z = 46$ and 0.25 for $Z = 48$. This means that the transitions from $p_{1/2}$ and $g_{9/2}$ to the next shell become important. The result is a strong, higher-lying 3^- state, for which $B > B_0$ while $B < B_0$ for the resulting level of lowest energy.

When comparing the results with the experimental data it is seen that none of the level schemes, which we tried, could give the correct trend in the energies and B values. Still, something seems to be missing to give the right variation with A. Therefore, further experimental studies of the location of the single-particle levels would be interesting.

Case 6: $Z = 50$.

The *Sn* region has been discussed above, especially in relation to fig. 6. We have seen how the closed proton shell gives rise to a higher-lying strong line.

Since the proton shell is closed, we used for the proton single-particle levels the Nilsson values (ref. 13) with the exception that $5h_{11/2}$ was placed in the middle of the 50–82 shell, just as in case 7 and as in the Mottelson-Nilsson paper (ref. 13). The energies are the following:

$3f_{7/2}$: −2.1, $3p_{3/2}$: 0, $3f_{5/2}$: 0.7, $3p_{1/2}$: 1.4,
$4g_{9/2}$: 3.7, $4d_{5/2}$: 7.1, $4g_{7/2}$: 7.4, $4s_{1/2}$: 9.1,
$4d_{3/2}$: 9.2 and $5h_{11/2}$: 8.4 MeV.

The neutron levels were taken from KS I:

$d_{5/2}$: 0, $g_{7/2}$: 0.22, $s_{1/2}$: 1.9, $d_{3/2}$: 2.2, $h_{11/2}$: 2.8 MeV.

Calculations have also been performed for another neutron level scheme, proposed by COHEN and PRICE on the basis of a stripping experiment (ref. 22). Since, however, they give a poorer fit to experimental energies, and since after publication the measurements have been reinterpreted (ref. 23) so that the level scheme comes much closer to KS I, the results of this calculation are not reported.

The two neutron transitions in the partly filled shell are the weak $g_{7/2} - h_{11/2}$ and the strong $d_{5/2} - h_{11/2}$, which lies a little higher. The energies of both transitions go up and the uv factor down, when A increases.

The transitions from the closed proton shell give rise to the second strong line. The line of lowest energy has $B_0/B \simeq 2.5$ due to the small S^p because of the closed shell, whereas the higher lying strong line has $B_0/B < 1$.

TABLE 29. Energy, B and B_0 for the low-energy, stronger excitations in case 6, $c_0 = 0.45$. Same units as in table 3.

A,Z:	114,50			116,50			118,50		
E, B, B_0:	2.11	6.2	15	2.20	6.9	18	2.31	7.7	20
	4.24	7.8	4.5	4.23	7.5	4.6	4.22	6.9	4.6
	5.44	1.4	2.9	5.31	0.5	2.4	5.14	0.02	1.6
							5.57	1.4	1.0
A,Z:	120,50			122,50			124,50		
E, B, B_0:	2.43	8.4	22	2.56	9.1	24	2.70	9.8	26
	4.20	6.2	4.5	4.19	5.3	4.2	4.18	4.2	3.5
	5.01	0.05	1.0	5.44	0.8	1.9	5.34	0.4	1.9
	5.52	1.3	1.6						

Some of the levels of higher energy have very different values of B_0 and B. In some cases $B \ll B_0$ because the line is a rather pure neutron one.

The energies are in good agreement with the results of LEMBERG et al. and of HANSEN and NATHAN (see fig. 16), but the B values are smaller by a factor 2 or more than the Lemberg ones.

It is noteworthy that this large discrepancy appears just in *Sn* where, as mentioned above, B_0/B is extraordinarily great and thus the introduction of an isospin dependence in the octupole-octupole force will have especially large effects on B. However, we see from tables 5 and 6 that an unexpected large value of $-\varkappa_1/\varkappa_0$ is needed to reproduce the experimental B value completely.

It is rather unsatisfactory that the proton single-particle levels come just from a simple shell-model calculation. Because of the uncertainty in the position of the proton $5h_{11/2}$ level we have performed a calculation with the energy of this level increased by 0.8 MeV. Some results are given in tables 3 and 5. The shift in the $5h_{11/2}$ single-particle energy causes considerable changes, especially for the higher-lying, strong excitation, since the $4g_{9/2} - 5h_{11/2}$ proton transition (energy 4.7 MeV) is one of the strongest ones in the low-energy spectrum.

Preliminary results from inelastic α scattering by FARAGGI et al. (ref. 24) indicate the possible existence of a second, strong 3^- state around 5 MeV in A,Z = 122,50 and 124,50, the intensity being however much lower than when exciting the lowest octupole state.

It is interesting to note that from the calculation B should be roughly equal for the higher lying state and for the lower lying one, while B_0, which is the relevant quantity in α scattering, should be much smaller. Recently,

ALLAN et al. (ref. 25) have by means of inelastic proton scattering found a possibly collective level in $A,Z = 116,50$ and 118,50 around 3.9 MeV with unknown spin and parity. For the heavier *Sn* isotopes this level has disappeared, at least in the region below 4.7 MeV. It would be interesting to study the possible relationship between this state and the states found by FARAGGI et al.

Case 7: $50 < Z < 82$, $50 < N \leq 82$.

As mentioned in connection with fig. 10, there are here only few protons and few neutron holes in the partly filled shells and the oscillator strength in the low-energy spectrum is spread over several levels. Three level schemes were used, viz.

a) protons: $g_{7/2}$:0.8, $d_{5/2}$:0.8, $h_{11/2}$:2.4, $d_{3/2}$:3.13 and $s_{1/2}$:3.36 MeV; neutrons: $d_{5/2}$:0, $g_{7/2}$:1, $h_{11/2}$:1.66, $s_{1/2}$:2.1 and $d_{3/2}$:2.37 MeV.

b) same level scheme as in a), but the proton $g_{7/2}$ is lowered to 0 MeV.

c) protons like in a), neutrons like in case 6.

The proton levels in a) were chosen on the basis of a suggestion by KISSLINGER (ref. 26) and are almost identical to the KS II levels. The neutron levels in a) come from a stripping experiment in the $N = 82$ region (ref. 27). There is rough agreement between this neutron level scheme and single-particle energies, found by JOLLY in (d,p) and (d,t) experiments in *Tl* (ref. 47).

In case b) we only changed the position of the proton $g_{7/2}$ level in order to investigate how this modifies the picture. The two level schemes a) and c) are really different, and we report in detail the results for both with the aim to demonstrate the influence of changing the single-particle parameters.

The main difference between the "a-neutron levels" found by experiment in the end of the region and the *c* levels, which fitted the quasiparticle energies nicely in *Sn*, is that $h_{11/2}$ in the last case is placed at the top of the shell, so that the neutron transitions from $d_{5/2}$ and $g_{7/2}$ are allowed by the uv factor, whereas in the first case $h_{11/2}$ as well as $d_{5/2}$ and $g_{7/2}$ are almost

TABLE 30. Energy, B and B_0 for the low-energy, stronger excitations in case 7 a, $c_0 = 0.45$. Same units as in table 3.

A,Z:	120,52			122,52			124,52		
E, B, B_0:	1.93	7.3	14	2.09	5.7	11	2.24	4.2	7.7
	2.36	2.1	3.2	2.47	3.1	5.1	2.58	4.8	6.5
	4.19	7.8	5.8	4.23	8.3	6.0	4.24	8.7	6.3
	5.31	1.8	0.7	5.32	1.7	0.6	5.12	0.2	1.5
							5.35	1.3	0.2

TABLE 30 (continued).

A,Z:	126,52			128,52			130,52		
E, B, B_0:	2.39	3.2	5.5	2.54	3.0	4.8	2.68	4.8	6.1
	2.68	5.4	6.3	2.76	4.9	4.8	2.81	2.5	2.0
	3.15	0.2	1.8	3.31	0.8	3.5	3.52	1.9	5.1
	4.24	8.9	6.7	4.24	9.1	7.4	4.21	8.9	8.1
	5.20	1.0	2.1	5.22	1.4	2.4	5.20	1.3	2.8

A,Z:	124,54			126,54			128,54		
E, B, B_0:	2.01	9.7	15	2.16	8.8	12	2.30	8.6	11
	2.41	2.8	2.9	2.48	3.5	3.2	2.56	3.2	2.5
	4.35	7.6	5.9	4.37	8.0	6.2	3.17	0.1	1.9
	5.53	1.9	1.0	5.53	1.8	0.9	4.37	8.3	6.6
							5.55	1.4	0.5

A,Z:	130,54			132,54			134,54		
E, B, B_0:	2.42	9.5	11	2.49	10	11	2.52	11	11
	2.65	1.6	0.9	3.56	1.0	3.5	3.81	1.7	4.4
	3.35	0.5	2.8	4.33	8.7	8.5	4.28	8.4	9.8
	4.36	8.5	7.3	5.40	1.4	4.0	5.33	0.8	4.6
	5.40	1.3	3.2						

A,Z:	136,54			130,56			132,56		
E, B, B_0:	2.53	11	11	2.15	13	15	2.24	14	13
	4.12	10	17	2.52	1.2	0.5	3.37	0.3	2.6
	5.19	0.1	3.7	3.17	0.1	2.0	4.46	8.2	7.3
	6.08	0.2	2.1	4.71	7.9	6.5	5.52	0.5	3.0
				5.75	2.0	1.6	5.76	1.4	1.0

A,Z:	134,56			136,56			138,56		
E, B, B_0:	2.29	14	13	2.32	14	13	2.32	14	13
	3.58	0.6	2.9	3.83	1.0	3.1	4.24	9.5	16
	4.43	8.4	8.5	4.37	8.5	10	5.26	3×10^{-3}	3.4
	5.56	1.2	5.4	5.44	0.5	5.5	5.82	1.4	0.4
							6.13	0.01	1.7

TABLE 30 (continued).

A,Z:	136,58			138,58			140,58		
E, B, B_0:	2.11	16	15	2.13	16	15	2.13	17	15
	3.59	0.5	2.7	3.84	0.7	2.6	4.33	9.3	16
	4.51	8.3	8.5	4.45	8.5	11	5.29	3×10^{-3}	3.0
	5.66	0.8	5.9	5.51	0.3	5.5	5.98	1.5	2.0
				6.04	1.1	0.5			

TABLE 31. Energy, B and B_0 for the lowest line in case 7 b, $c_0 = 0.45$. Same units as in table 3.

A,Z:	120,52			122,52			124,52		
E, B, B_0:	2.00	4.8	11	2.15	3.1	7.3	2.29	1.9	4.5

A,Z:	126,52			128,52			130,52		
E, B, B_0:	2.43	1.2	2.7	2.58	0.8	1.7	2.74	0.5	1.1

A,Z:	124,54			126,54			128,54		
E, B, B_0:	2.16	3.1	6.9	2.30	1.9	4.3	2.43	1.2	2.7

A,Z:	130,54			132,54			134,54		
E, B, B_0:	2.58	0.8	1.7	2.74	0.5	1.2	2.93	0.5	1.0

A,Z:	136,54			130,56			132,56		
E, B, B_0:	3.08	3.0	3.4	2.42	1.8	2.5	2.57	1.4	2.5

A,Z:	134,56			136,56			138,56		
E, B, B_0:	2.73	1.6	2.5	2.88	5.0	5.6	2.90	5.6	5.8

A,Z:	136,58			138,58			140,58		
E, B, B_0:	2.53	9.7	9.5	2.56	9.9	9.3	2.56	10	9.8

TABLE 32. Energy, B and B_0 for the low-energy, stronger excitations in case 7 c, $c_0 = 0.45$. Same units as in table 3.

A,Z:	120,52			122,52			124,52		
E, B, B_0:	2.12	11	20	2.26	11	20	2.41	11	18
	4.26	7.4	4.7	4.28	7.4	4.6	3.12	0.05	1.8
	5.09	0.1	1.5	5.15	0.5	1.9	4.30	7.4	4.6
	5.40	1.3	0.01				5.19	0.9	2.1

A,Z:	126,52			128,52			130,52		
E, B, B_0:	2.54	11	16	2.64	9.5	13	2.71	8.3	10
	3.21	0.6	3.8	3.34	1.7	6.4	3.51	3.0	8.4
	4.31	7.3	4.6	4.31	7.1	4.7	4.30	6.7	4.8
	5.21	1.2	2.3	5.21	1.3	2.5	5.20	1.2	2.9
				5.72	5×10^{-4}	2.1	5.71	3×10^{-3}	2.1

A,Z:	124,54			126,54			128,54		
E, B, B_0:	2.09	15	21	2.21	14	19	2.32	14	17
	3.05	0.01	1.2	3.14	0.05	2.4	3.26	0.4	3.9
	4.39	7.0	4.8	4.41	7.1	4.9	4.42	7.1	5.0
	5.25	0.1	2.0	5.33	0.6	2.7	5.38	1.0	3.2
	5.60	1.4	0.1						

A,Z:	130,54			132,54			134,54		
E, B, B_0:	2.40	13	15	2.47	12	13	2.52	11	11
	3.41	1.0	5.3	3.58	1.7	6.1	3.77	1.9	5.1
	4.41	7.1	5.3	4.40	7.0	5.7	3.88	1.2	2.8
	5.39	1.3	3.6	5.38	1.2	4.1	4.36	6.7	6.4
							5.34	0.9	4.7

A,Z:	136,54			130,56			132,56		
E, B, B_0:	2.55	10	9.8	2.12	16	18	2.20	15	16
	4.17	10	16	3.29	0.4	4.0	3.44	0.8	4.8
	5.27	0.4	4.8	4.50	7.0	5.2	4.50	7.1	5.6
	5.81	0.1	1.2	5.50	0.6	3.7	5.54	1.0	4.8
				5.84	1.0	0.07			

TABLE 32 (continued).

A,Z:	134,56			136,56			138,56		
E, B, B_0:	2.27	15	14	2.31	14	13	2.35	13	12
	3.62	1.1	4.8	3.80	0.8	2.7	4.29	9.7	15
	3.74	1.1	1.4	3.90	1.3	3.5	5.36	0.2	5.2
	4.48	7.1	6.3	4.44	7.2	7.5	5.67	0.5	1.0
	5.52	1.0	5.4	5.46	0.6	5.6			

A,Z:	136,58			138,58			140,58		
E, B, B_0:	2.07	17	16	2.12	17	15	2.16	16	14
	3.63	0.9	4.0	3.81	0.5	1.8	4.38	9.4	15
	3.75	0.4	1.7	3.91	1.1	3.6	5.41	0.08	4.9
	4.54	7.2	6.6	4.50	7.4	8.1	5.71	0.4	2.2
	5.61	0.6	5.8	5.52	0.3	5.5			
				5.83	0.5	1.8			

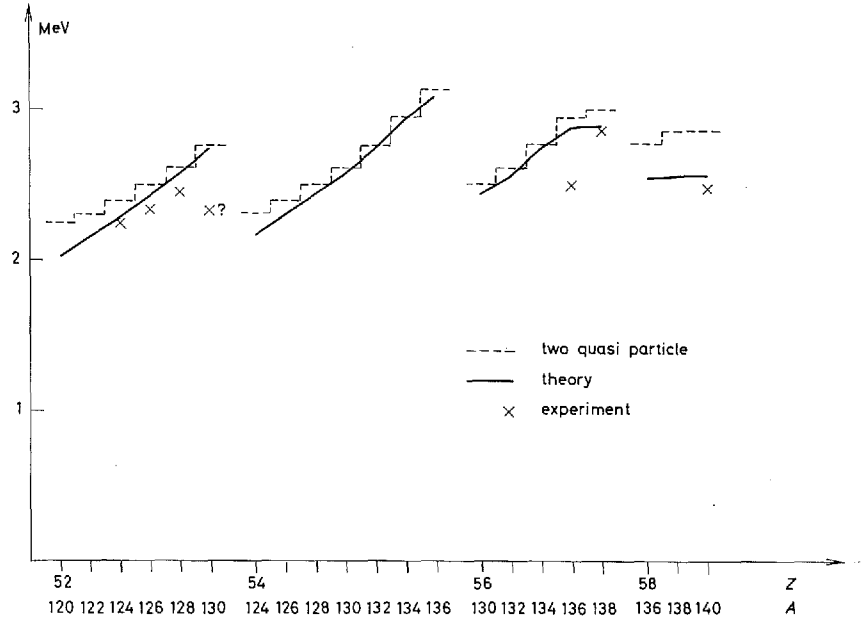

Fig. 17. Energies for case 7b. The experimental points are due to HANSEN and NATHAN (ref. 16). Recent experiments (ref. 40) indicate a possible existence of 3^- states in the following nuclei:
$A,Z = 130,56 : E = 1.80$ MeV, $A,Z = 132,56 : E = 2.06$ MeV,
$A,Z = 134,56 : E = 2.37$ MeV.

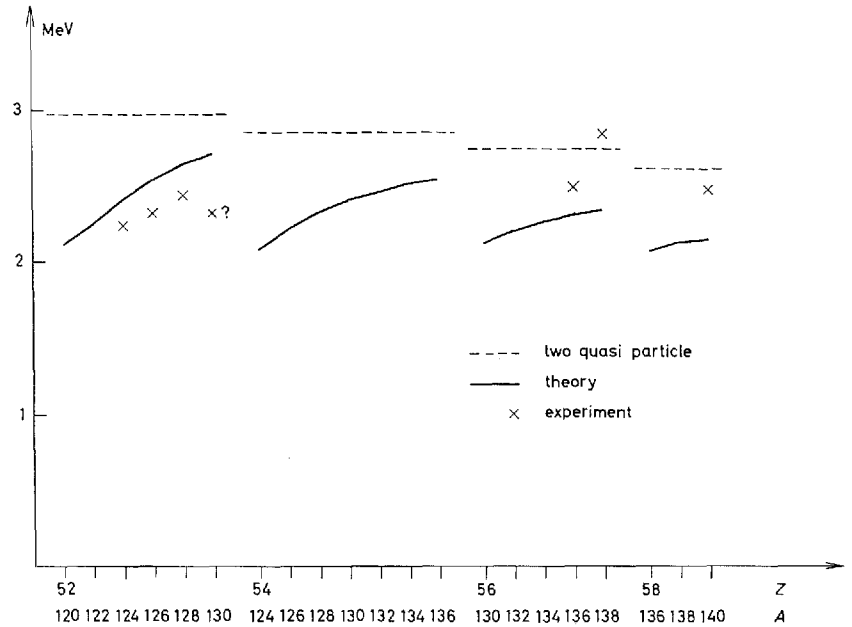

Fig. 18. Energies for case 7c. When comparing this and fig. 17 we see that now the lowest lying proton transition comes below the neutron ones. As discussed in the text, this causes great changes.

filled. Therefore, all the transitions inside partly filled shells are rather weak in case a) for Z just above 50. In case b) this is even more pronounced, since here the strong proton transition $d_{5/2}$–$h_{11/2}$ has a very small uv factor (both levels are almost empty). As seen from fig. 17, the lowest resulting state in b) almost sticks to the two-quasiparticle energy.

The trend in the B values follows from the above mentioned facts. In a) the oscillator strength in the lowest part of the spectrum is spread over more levels, and in b) the lowest line is especially weak, as seen from fig. 10. Following, in table 31, the isotopes with $Z = 56$ for case b), we see a bump in the B values at $A = 136$. The reason is that the lowest neutron two-quasiparticle energy here is increased so much that it comes pretty near to the lowest proton excitation, and thus S^p goes up.

In c) the resulting state of lowest energy is always the strongest one. For the following states there is often an appreciable difference between B and B_0. Still, for the strong ones, $B_0 > 3B_1$.

The experimental results by HANSEN and NATHAN (giving $B = 45$ for $A,Z = 124,52$ and $128,52$) might perhaps be taken as an indication that the

c) levels are most reliable at least in the beginning of the region, but the experimental information is very incomplete. Recent experiments by GERSCHEL et al. (see caption to fig. 17), indicate a possible existence of 3^- states, which show a more rapid energy variation than the theoretically calculated ones. A confirmation of the results would be very interesting.

We note that we are here in a region, where some of the nuclei might be fairly near to (or even have) non-spherical equilibrium shape (ref. 28). This will of course influence the spectra.

Case 8: $50 < Z < 82$, $82 \leqslant N$

(below the region of stable quadrupole deformation).

Here, relatively few particles are available in the partly filled shells, and above the lowest resulting state a strong octupole excitation is formed, largely governed by the intershell transitions, as shown in figs. 8 and 9. We report the results arising from three different level schemes:

a) protons: $g_{7/2}$:0, $d_{5/2}$:0.8, $h_{11/2}$:2.4, $d_{3/2}$:3.13, $s_{1/2}$:3.36; neutrons: $f_{7/2}$:0, $p_{3/2}$:0.83, $i_{13/2}$:1.36, $f_{5/2}$:1.88, $h_{9/2}$:1.9, $p_{1/2}$:2.25 MeV.
b) the neutron level $i_{13/2}$ changed to 0.75 MeV.
c) neutron levels as in a). The proton level $h_{11/2}$ changed to 3.2 MeV.

The proton levels come from a modification of a suggestion by KISSLINGER for $A \simeq 200$ and are almost identical to the KS II levels. In case c) we studied the influence of placing the proton level $h_{11/2}$ between $d_{3/2}$ and $s_{1/2}$, where the neutron $h_{11/2}$ lies in case 5. The neutron levels are due to COHEN, FULMER and MCCARTHY (ref. 27). They do not find the $i_{13/2}$ level, which in a) and b) is placed in two different positions.

The second position reproduces the $f_{7/2} - i_{13/2}$ distance in KS II. On the other hand, they use values which are greatly deviating from ours, especially by placing the $h_{9/2}$ level 0.72 MeV below $f_{7/2}$. For the three cases $c_0 = 0.45$, $c_0 = 0.47$ and $c_0 = 0.41$, respectively, were used (see comment below).

Another calculation was run, using the proton levels from case a) and neutron levels, partly based on a suggestion by KISSLINGER: $f_{7/2}$:0, $h_{9/2}$:0.2, $i_{13/2}$:1.5, $p_{3/2}$:1.75, $f_{5/2}$:2.3, $p_{1/2}$:2.9 MeV. The results from this calculation are the same as those from case a) for $N = 82$. For the greater Ns the energies are just a little higher; they are not reported.

For case a) the lowest proton transitions are the weak $g_{7/2} - h_{11/2}$ and the strong (for $Z > 56$ lower lying) $d_{5/2} - h_{11/2}$, the uv factor of which changes

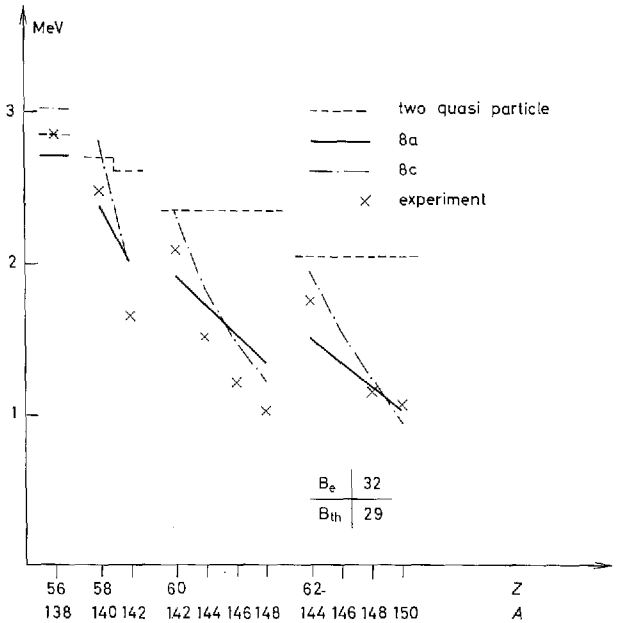

Fig. 19. Energies for case 8a with $c_0 = 0.45$ and for case 8c with $c_0 = 0.41$. "Two-quasiparticle" refers to the lowest lying two-quasiparticle energy in case 8a. The experimental points are due to HANSEN and NATHAN (ref. 16) and E. VEJE (ref. 48) (the B value).

from 0.2 at $Z = 56$ to 0.8 at $Z = 62$. The neutron transitions are the weak $i_{13/2} - h_{11/2}$ with a small uv factor and the strong $f_{7/2} - i_{13/2}$ with a uv factor varying from 0 to 0.72.

Figs. 8 and 9 illustrate how the picture changes when going away from the closed neutron shell. The most remarkable feature is the drop in the energies, caused by the increasing strength of the low-energy neutron lines, which lie above the proton two-quasiparticle excitation of lowest energy.

In case c) the proton quasiparticle energies are increased. This gives the neutron variation a greater influence, but causes an overestimate of the high energies. Changing two protons into two neutrons, i.e. going from $A,Z = 142,58$ to 142,60 or from 148,60 to 148,62 gives experimentally, like in case c), that the energy of the lowest 3^- state goes up, whereas the opposite is true for a). In this sense b) is a little better than a).

For the excitation of lowest energy the neutron excess gives rise to $B_0 > B$, i.e. $S^n > S^p$, even when the neutron shell is closed. The contributions from S_2 are partly responsible for this. For $A,Z = 142,60$ S_1^p is somewhat greater than S_1^n.

TABLE 33. Energy, B and B_0 for the low-energy, stronger excitations in case 8 a, $c_0 = 0.45$. Same units as in table 3.

A,Z:	138,56			140,58			142,58		
E, B, B_0:	2.72	7.8	11	2.38	11	14	2.02	11	23
	2.97	2.6	4.3	3.71	6.7	19	2.67	1.7	0.1
	3.67	5.6	17	4.69	1.8	0.03	3.98	7.8	16
	4.69	1.8	0.02	5.70	0.01	1.8	5.24	0.1	1.8
	5.66	0.03	2.4	5.83	0.03	1.7			

A,Z:	142,60			144,60			146,60		
E, B, B_0:	1.92	15	16	1.72	17	26	1.52	19	36
	3.77	6.6	20	4.03	7.6	16	4.06	1.2	2.5
	4.70	1.9	0.05	5.26	0.03	1.7	4.22	7.5	12
	5.12	0.01	1.5	5.61	0.9	1.8	5.10	0.01	1.9
	5.56	0.8	3.2						

A,Z:	148,60			144.62			146,62		
E, B, B_0:	1.36	21	46	1.51	21	21	1.35	25	32
	4.30	8.8	12	3.81	6.8	20	2.44	0.04	2.7
	5.18	0.01	4.2	4.70	1.8	0.05	4.06	7.7	16
	5.35	0.1	1.7	5.12	3×10^{-3}	1.5	5.71	0.4	3.0
				5.63	0.5	4.7	5.80	0.5	2.3

A,Z:	148,62			150,62			
E, B, B_0:	1.19	29	44	1.04	33	57	
	2.34	0.03	2.6	2.29	0.2	2.4	
	4.07	0.8	1.8	4.32	8.9	12	
	4.24	7.9	12	5.19	0.01	4.2	
	5.85	1.0	3.6	5.36	0.01	2.1	

Above the transitions inside the partly filled shells there is a rather strong line for which B is only a fraction of B_0 in the neutron magic nuclei. (The transition is governed largely by the neutron transitions).

When we had finished our above mentioned calculations, a new neutron level scheme became available, based on a tentative and preliminary interpretation of some experimental results due to YANG et al. (ref. 29):

$$f_{7/2}{:}0,\ p_{3/2}{:}1.2,\ h_{9/2}{:}1.7,\ f_{5/2}{:}1.9 \text{ and } i_{13/2}{:}2.0 \text{ MeV}.$$

TABLE 34. The first row gives E, B and B_0 for the lowest excited state from case 8 b, $c_0 = 0.47$, and the second row those for the same state in case 8 c, $c_0 = 0.41$. Same units as in table 3.

A,Z:	138,56			140,58			142,58		
E, B, B_0:	2.74	6.4	9.2	2.41	9.9	12	1.84	7.2	19
	3.03	17	35	2.82	17	29	1.99	11	29

A,Z:	142,60			144,60			146,60		
E, B, B_0:	1.96	13	15	1.66	14	24	1.45	15	33
	2.37	20	29	1.84	17	37	1.49	21	50

A,Z:	148,60			144,62			146,62		
E, B, B_0:	1.32	17	42	1.56	19	19	1.36	22	30
	1.23	25	66	1.95	27	33	1.57	28	47

A,Z:	148,62			150,62					
E, B, B_0:	1.18	25	41	1.06	28	52			
	1.24	33	65	0.97	41	90			

They did not see the $p_{1/2}$ level which we then placed at 2.3 MeV. The precise location of this level should have only a very small influence on the resulting spectrum.

When using this level scheme and the a) protons, the energy for the lowest state was changed by less than 0.1 MeV, the variation with neutron number N being a little slower than in a). The B values were increased by 10–20 %. For the higher lying strong, resulting states the changes were rather small. The main difference from a) to this case is that c_0 was changed from 0.45 to 0.43 to obtain the best energy fit.

Another calculation was performed with the Yang et al. data and protons from case c). When c_0 is chosen to fit the lowest resulting energy in A,Z = 150,62, ($c_0 = 0.393$), the agreement with experiment becomes poorer than in c) (less steep variation of energy), especially for the $Z = 60$ nuclei. B is increased by 10–20 %.

As seen above, in this region we have had some difficulties in fitting $\varkappa$. By just a small change in c_0 we are able to bring the lowest resulting state in A,Z = 150,62 down to zero energy. This warns us to be suspicious on the validity of our simple treatment. It is a well-known trend from the

quadrupole case that, when the resulting state is pressed far down from the lowest two-quasiparticle mode, the simple quasi-boson treatment breaks down. Anharmonicity effects and the Pauli principle should possibly have been taken into account. For the octupoles the situation should in general be better (the excitations are not so collective), one of the exceptions perhaps being just the nuclei below the rare-earth deformed region. It should be further stressed that the approximation of neglecting coupling between quadrupole and octupole vibrations might be especially bad here, near the domain of stable quadrupole deformation, where the 2^+ vibrations are very strong and of low energy.

Case 9: $Z \leq 82$, $N \leq 126$,
(above the region of stable quadrupole deformation).

In this final case only few proton and neutron holes in the partly filled shells are available. A higher lying state is formed, stronger than the lowest resulting mode.

Two level schemes were used:

a) neutron levels suggested by KISSLINGER (ref. 26) (almost identical to KS II) $h_{9/2}$:0, $f_{7/2}$:0.2, $i_{13/2}$:0.92, $p_{3/2}$:1.65, $f_{5/2}$:1.98, $p_{1/2}$:2.55 MeV; proton levels from calculations on Pb^{208} by GILLET et al. (ref. 30) $g_{7/2}$:0, $d_{5/2}$:1.69, $h_{11/2}$: 2.34, $d_{3/2}$:3.83, $s_{1/2}$:4.18 MeV.

b) same neutron levels, proton levels from a recent experiment by NATHAN (ref. 31) $g_{7/2}$:0, $d_{5/2}$:1.73, $h_{11/2}$:2.06, $d_{3/2}$:3.05 and $s_{1/2}$:3.40 MeV.

The single-particle energies in the neutron shell above the partly filled shell are taken from a report on stripping experiments (ref. 32).

The proton energies above the partly filled shell are the values used by GILLET et al. (refs. 33 and 30). The other single-particle energies come from the simple shell-model calculations (ref. 13) as explained before. The a) calculation was performed especially with the aim to compare it with the calculation by GILLET et al. (ref. 30).

The neutron single-particle energies are not exactly equal to the Gillet ones, but the differences are so small that it might be reasonable not to take them into account.

The transitions inside the partly filled shells are for the protons the weak $g_{7/2}\ h_{11/2}$ and the strong $d_{5/2}\ h_{11/2}$ transition and for the neutrons the weak $h_{9/2}\ i_{13/2}$ and the strong $f_{7/2}\ i_{13/2}$ transition, but all the contributing levels are almost filled. This is especially pronounced for the protons where the uv factor is very near to zero.

TABLE 35. Energy, B and B_0 for the low-energy, stronger excitations in case 9 a, $c_0 = 0.413$. Same units as in table 3.

A,Z:	192,76			192,78			194,78		
E, B, B_0:	2.49	3.0	15	2.21	4.7	20	2.48	4.2	18
	4.53	13	51	4.45	20	38	4.31	21	50
	5.55	5.9	16	5.05	1.7	15	5.54	5.1	13

A,Z:	196,78			198,78			196,80		
E, B, B_0:	2.76	4.4	18	3.03	5.6	23	2.47	6.1	21
	4.10	20	57	3.88	19	60	4.08	28	50
	5.38	3.4	12	5.18	1.5	8.1	5.69	1.0	10

A,Z:	198,80			200,80			202,80		
E, B, B_0:	2.74	6.6	22	3.00	9.4	31	3.19	21	67
	3.93	28	58	3.75	24	59	3.60	7.9	22
	5.34	3.9	9.1	5.18	1.8	8.1	3.66	4.7	12

A,Z:	204,80			202,82			204,82		
E, B, B_0:	3.13	34	112	2.96	16	43	3.10	33	88
				3.65	29	58	3.57	9.8	21
				5.87	1.8	11	5.77	1.1	10

A,Z:	206,82			208,82					
E, B, B_0:	3.01	45	125	2.79	49	147			

The greatest role is played by the strong transitions between the shells, giving a rather low-lying and strong octupole state in the doubly magic Pb^{208} (fig. 7).

For the lower A values, there is a strong higher-lying 3^-, whereas the lowest one is rather weak and near to the two-quasiparticle energy. Because of the neutron excess and the weakness of the proton transitions inside the partly filled shell, B for the lowest state is smaller than B_0.

One more calculation was run, using the a) neutron levels and proton levels from KS II:

$$g_{7/2}:0,\ d_{5/2}:0.8,\ h_{11/2}:2.1,\ d_{3/2}:2.6 \text{ and } s_{1/2}:2.95 \text{ MeV}.$$

TABLE 36. Energy, B and B_0 for the low-energy, stronger excitations in case 9 b, $c_0 = 0.404$. Same units as in table 3.

A,Z:	192,76			192,78			194,78		
E, B, B_0:	1.64	0.9	1.2	2.16	7.5	25	2.32	4.2	9.6
	2.47	4.0	18	4.38	26	48	2.48	2.9	14
	4.41	18	58	5.04	1.2	11	4.22	25	56
	5.46	2.0	3.2	5.63	5.4	7.3	5.50	6.1	12
	5.52	4.3	10	5.79	0.8	3.0			

A,Z:	196,78			198,78			196,80		
E, B, B_0:	2.34	2.3	4.0	2.34	2.1	3.6	2.43	8.7	27
	2.74	5.3	21	3.00	8.0	30	4.00	33	57
	3.99	23	60	3.78	21	61	5.40	4.5	4.6
	5.34	4.1	11	5.16	1.7	7.7	5.67	0.9	6.9
	5.86	2.8	3.6	5.68	4.3	4.7			

A,Z:	198,80			200,80			202,80		
E, B, B_0:	2.69	9.9	28	2.77	2.9	6.4	2.77	3.0	6.8
	3.84	31	63	2.96	12	37	3.10	28	82
	5.30	4.8	9.1	3.67	25	58	3.57	8.3	21
				5.15	2.4	8.0	3.65	1.6	3.7
							4.98	0.7	5.2

A,Z:	204,80			202,82			204,82		
E, B, B_0:	2.76	6.5	17	2.90	24	59	2.98	44	109
	3.01	34	109	3.57	28	53	3.54	8.0	16
	4.62	4.0	0.4	5.02	4.6	3.8	4.93	2.3	4.7
	5.39	4.2	5.3	5.80	2.9	8.5	5.72	1.8	9.2

A,Z:	206,82			208,82			
E, B, B_0:	2.85	53	140	2.62	58	165	
	4.59	4.2	0.1	4.56	4.3	0.4	
	4.80	0.3	3.3	5.08	2.4	1.1	
	5.44	1.5	3.5	5.46	1.9	2.5	
	5.68	0.8	5.2				

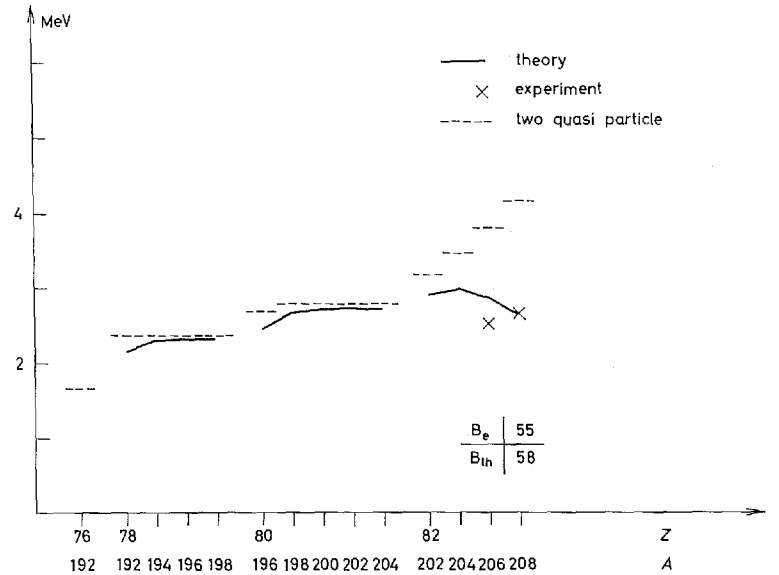

Fig. 20. The lowest lying energy, B value and two-quasiparticle energy for the nuclei in case 9b, where $c_0 = 0.404$. The experimental values come from ref. 41 and ref. 49.

Although the proton energies are quite different from those above, the resulting states are only affected little, especially the state of lowest energy. The quantity c_0 was 0.413 in a) and 0.404 in b). The results are given in tables 35 and 36.

In Pb^{208} the agreement between theory and experiment is quite satisfactory, but it must be remembered that c_0 is chosen lower than in the other cases.

If $\varkappa_1 < 0$ is used B will exceed the experimental value since $B_0 > B$.

Comparison with the calculation by GILLET et al.

As mentioned above, we are able to compare our results with those obtained by GILLET et al. (ref. 30) in Pb^{208} when using a spin and isospin dependent force in which the radial dependence is of Gaussian type in the distance between the two nucleons. In table 37 and table 38 we quote the amplitudes p and q for quasiparticle pair creation and annihilation, respectively, from the lowest neutron and proton modes to the lowest resulting state. It is remarkable that all the amplitudes except those for the neutron $5f_{5/2}$ $6s_{1/2}$ quasiparticle excitation have the same sign for the two quite different forces.

TABLE 37. For GILLET's calculation (ref. 30) and for the calculation from case 9 a, the table gives E, $p = p(\alpha, j_1, j_2)$ and $q = q(\alpha, j_1, j_2)$ for the lowest neutron particle-hole excitations, contributing to the first octupole excitation in Pb^{208}. E is the energy for the relevant particle-hole excitation.

Since there is some difference between GILLET's phase convention (ref. 42) and ours, the sign for our amplitudes p and q in this table is changed to be in agreement with GILLET's choice of phase.

transition	GILLET			this calculation		
	E	p	q	E	p	q
$5f_{5/2}$–$6g_{9/2}$	4.01	0.19	0.03	4.17	0.21	0.04
$5p_{3/2}$–$6g_{9/2}$	4.34	−0.42	−0.07	4.50	−0.50	−0.12
$5f_{5/2}$–$6i_{11/2}$	4.80	0.39	0.07	4.94	0.41	0.12
$5p_{1/2}$–$6d_{5/2}$	5.02	0.08	0.02	5.16	0.23	0.07
$5f_{5/2}$–$6d_{5/2}$	5.59	0.06	0.02	5.73	0.11	0.04
$5f_{7/2}$–$6g_{9/2}$	5.78	−0.20	−0.06	5.95	−0.09	−0.03
$5p_{3/2}$–$6d_{5/2}$	5.92	−0.05	−0.02	6.06	−0.15	−0.06
$5f_{5/2}$–$6s_{1/2}$	6.04	−0.08	−0.04	6.20	0.12	0.04
$5p_{1/2}$–$6g_{7/2}$	6.14	0.17	0.04	6.07	0.20	0.07
$5f_{5/2}$–$6g_{7/2}$	6.71	0.13	0.05	6.64	0.15	0.06
$5d_{3/2}$–$6f_{5/2}$	6.93	0.05	0.02	6.69	0.11	0.04

TABLE 38. E, p and q for the lowest proton particle-hole excitations contributing to the first octupole state in Pb^{208}. For further explanation, see caption to table 37.

transition	GILLET			this calculation	
	E	p	q	p	q
$4d_{3/2}$–$5h_{9/2}$	4.61	−0.47	−0.08	−0.33	−0.08
$4s_{1/2}$–$5f_{7/2}$	5.16	0.37	0.08	0.22	0.07
$4d_{3/2}$–$5f_{7/2}$	5.51	−0.15	−0.04	−0.11	−0.03
$4d_{5/2}$–$5h_{9/2}$	6.75	−0.07	−0.02	−0.06	−0.02
$4d_{3/2}$–$5p_{3/2}$	7.26	−0.13	−0.05	−0.09	−0.04
$4s_{1/2}$–$5f_{5/2}$	7.56	−0.15	−0.06	−0.10	−0.04
$4d_{5/2}$–$5f_{7/2}$	7.65	0.14	0.06	0.10	0.05
$5h_{11/2}$–$6i_{13/2}$	7.72	−0.17	−0.07	−0.17	−0.08
$4d_{3/2}$–$5f_{5/2}$	7.91	−0.10	−0.04	−0.08	−0.04

Concerning their magnitudes, there is also a quite strong correlation. The most interesting feature is that the Gillet neutron amplitudes in general are a little smaller than our amplitudes, whereas the proton ones are about 50 % greater.

This is consistent with the result that GILLET et al. reach 60 % of the experimental B value (which is only known $\pm$ 30 %, ref. 41) without using any renormalization of the charge. If we took only the $\Delta N = 1$ transitions into account (keeping the resulting energy constant) B would go down with a factor of two.

A stronger influence from the proton excitations on the lowest resulting level is obtained when an isospin dependent force is introduced. Thus, when $\varkappa_1 = -0.5\varkappa_0$ is used and $\varkappa_0$ is changed to give approximately the same energy as when $\varkappa_1 = 0$, the B value is increased by 50 %, which means that it becomes greater than the experimental value. ($c_0 = 0.38$, $\varkappa_1 = -0.5\varkappa_0$ gives $E = 2.83$ MeV, $B = 72$.)

16. Concluding remarks

The most striking feature we meet when we start the numerical calculations is the very great sensitivity of the results to the energies of the shell-model levels inside the partly filled shells, and the incomplete and partly contradictory information which is available concerning these energies.

It looks as if one may sometimes take different shell-model level schemes for all of which it is possible to argue reasonably well, and obtain very different quantitative pictures for the lowest part of the resulting spectrum, especially for the B values. This should be kept in mind, when our conclusions are studied.

When the number of experimental results increases, and when more modes of excitation are to be described from the same quasiparticle energies, we may get a better insight into the variation of $\varepsilon(j)$, and then also into the precise validity of the theory.

The fitting of the octupole force constant

For simplicity reasons a major part of the calculation was made, using an isospin independent octupole force constant.

In general it has been possible to fit the experimental energies of the lowest resulting excitation reasonably well with a smoothly varying $\varkappa$. In the *Ni* region we had to use a value which was a few percent larger, and in *Zr* a value which was a few percent smaller. Although difficult to say definitely (cf. sect. 14) there seems to be some tendency for a weaker $\varkappa$ variation with A than obtained by a simple scaling argument (cf. sect. 2).

This might be taken as an indication that the surface region of the nucleus should have a stronger weight than assumed by our simple Hamiltonian.

The magnitude and variation of $\varkappa$ are in general agreement with the parameters used by SOLOVIEV et al. (ref. 3), although some details are different. E.g. they take only part of the single-particle levels into account. When more and more levels are included, their $\varkappa$ value approaches our value (ref. 43).

They also use another (slower) A variation inside each of the two regions of deformed nuclei around $A \sim 180$ and $A \sim 240$, whereas the variation from the first region to the second is approximately the same as our overall variation.

From the calculations on quadrupole vibrations (ref. KS II) it is well known that when the lowest resulting energy is pressed far down from the lowest two-quasiparticle excitation, the fitting of $\varkappa$ becomes very difficult. Even a small change in $\varkappa$ may bring the resulting energy down to zero.

This indicates that the simple quasiboson approximation breaks down. When the state is very collective, the Pauli principle and various anharmonicities should presumably have been taken into account (ref. 44).

Since the octupole vibrations are only moderately collective, the simple theory should work better for these than for the quadrupoles.

An exception is perhaps the nuclei just below the deformed rare-earth region where the nuclei seem to be able to undergo octupole deformation rather easily. However, there is in this case a great uncertainty in the single-particle energies, and a definite conclusion is difficult.

The general distribution of oscillator strength

From the calculation it appears that the octupole-octupole force sucks $5-10\,\%$ of the total B oscillator strength down and places it on some few, strong lines in the lowest part of the spectrum. While B for these lines varies quickly, $B \times E$ shows a much slower variation.

The rest of the oscillator strength is distributed in the $\hbar\omega_0$ and $3\hbar\omega_0$ regions. In the present model it will not be concentrated to any high degree at some few levels but is spread rather smoothly over large energy intervals. One of the more interesting results is that very strong lines just below or above the $3\hbar\omega_0$ region can hardly be expected, but it should be stressed that we have used a crude model and parameters which are not very well

known. There is especially poor knowledge about the energy distribution of the unperturbed excitations in the $3\hbar\omega_0$ region.

The influence of the shell structure is clearly seen. E.g. the low-energy part of the oscillator strength in the typical case is split into two parts because of an energy gap in the unperturbed spectrum. This gap appears just above the two-quasiparticle excitations inside partly filled shells.

It is worthwhile to note that the octupole excitation of lowest energy in some sense only represents a fine structure in the resulting spectrum, although it has been the subject of almost all theoretical and experimental investigations and is the most easily observed. The fine structure occurs because the spin-orbit splitting pushes a level down, so that some particles outside the core may change orbit almost without change in energy and make large octupole moments. An essential part of the oscillator strength is left on higher levels.

The low energy part of the spectrum

From the calculation it is seen that the energy of the lowest resulting state very intimately follows the variations in energy and strength of the very lowest two-quasiparticle modes. By studying the single-particle level scheme and the filling of the levels it is possible in a very simple way to understand the variations in position and strength of the strong excitations of low energy.

The few measured B values are reproduced by the calculation, in general within 30 %.

This is the best we could expect from the simple theory.

We may stress that the calculation has been performed without introducing any effective charge. If the $3\hbar\omega_0$ unperturbed transitions were not included, the B values would be about a factor of two smaller. Some uncertainty is introduced in B by simply using harmonic oscillator values for the strength and energy of the high-lying transitions.

There is some indication that the theory systematically underestimates the B value and it is not difficult to find possible reasons for this. One is that an isospin independent octupole force is used. We have seen how in almost all cases introduction of an isovector component leads to an increase in the resulting B value. We have not gone into a systematic study but may mention that in the Sn region where the discrepancies between theory and experiment for the B values are especially great, introduction of $\varkappa_1 \neq 0$ will have an especially large effect. Another possible reason is the systema-

tic error due to the use of the same harmonic oscillator potential for protons and neutrons. Thus, because of the neutron excess, the protons are kept too close to the nuclear centre and contribute too little to the transition moments. Finally, it is a more trivial possibility that a somewhat stronger pairing force should have been used. This would give higher two-quasi-particle energies. To reproduce the experimental energies a stronger octupole-octupole force should be used, the state would be more collective, i.e. B greater.

The isospin properties

In the calculation it has been found that the low-energy strong excitations to a good degree are of $\tau = 0$ type, although $\tau = 1$ impurities may give rise to interesting effects, e.g. so that the "strength" of the excitation depends of whether it is measured with the help of inelastic scattering of protons,or with α scattering or with Coulomb excitation. For the models which we have used, and for $\varkappa_1$ values from a tentative theoretical estimate, there is no strong tendency towards concentrating the $\tau = 1$ oscillator strength on a single level.

When using a pure $\varkappa_0$ force we make a systematic error, which however should be small, when the energies of the strong excitations of low energy are considered. For B there may be a more significant change when $\varkappa_1$ is introduced, as mentioned above.

It is very difficult to determine the strength of the $\tau = 1$ part of the long-range force. One possibility might be to study the ratio of isospin flip to non-isospin flip in the excitation of 3^- states by inelastic nucleon scattering. Another one is to study relative cross sections for inelastic scattering processes, using particles with different isospins and exciting different 3^- levels in the same nucleus.

It should be less rewarding to study, e.g., the lowest 3^- state in neighbouring nuclei, since the change in isospin character with a change in the atomic number is not very rapid.

Acknowledgements

The author is indebted to many guests and members of the staff of the Niels Bohr Institute, University of Copenhagen, for valuable comments and discussions. He especially wants to thank Drs. O. NATHAN and O. HANSEN

for stimulating discussions on the experimental aspects, professors L. KISSLINGER and V. GILLET for comments on the energies of the single-particle levels, and professor S. YOSHIDA for the explanation of some points in his calculation of quadrupole and octupole vibrations (ref. 1).

Also remarks from mag. scient. J. P. BONDORF are much appreciated. Primarily, however, the author feels very indebted to professor A. BOHR for his kind interest and many valuable discussions and suggestions concerning this work.

References

1. S. YOSHIDA: Nucl. Phys. **38**, 380 (1962).
2. M. KOBAYASI and T. MARUMORI: Progr. Theor. Phys. **23**, 387 (1960);
   R. ARVIEU and M. VENERONI: Compt. Rend. **250**, 992, 2155 (1960);
   A. BOHR and B. MOTTELSEN: Lectures on Nuclear Structure and Energy Spectra, to be published; in the following called BM.
3. V. G. SOLOVIEV: Phys. Lett. **6**, 126 (1963).
   V. G. SOLOVIEV, P. VOGEL and A. A. KORNEICHUK: Preprint, Dubna 1964;
   LU YANG, V. G. SOLOVIEV, P. VOGEL and A. A. KORNEICHUK: Preprint, Dubna 1964;
   D. BÉS: Nucl. Phys. **49**, 544 (1963);
   E. R. MARSHALEK: Thesis, UCRL 10046 (1962);
   E. R. MARSHALEK and O. RASMUSSEN: Nucl. Phys. **43**, 438 (1963); cf. also ref. 6.
4. L. KISSLINGER and R. A. SORENSEN: Revs. Mod. Phys. **35**, 853 (1963); in the following called KS II.
5. S. T. BELYAEV: Mat. Fys. Medd. Dan. Vid. Selsk. **31**, no. 11 (1959).
6. For a presentation of the theory and the approximations involved, see, e.g., A. M. LANE: Nuclear Theory, Benjamin, New York 1964, or BM or KS II.
7. See, e.g., G. E. BROWN: Lectures on Many-Body Problems, Nordita 1962, or G. E. BROWN: Unified Theory of Nuclear Models, North Holland Publishing Company, Amsterdam 1964.
8. A. M. LANE and J. M. SOPER: Phys. Lett. **1**, 28 (1962).
9. D. ROBSON: Phys. Rev. **137**, B 535 (1965).
10. L. A. SLIV: Private communication.
11. O. NATHAN and S. G. NILSSON: Collective Nuclear Motion and the Unified Model; in Alpha, Beta and Gamma Ray Spectroscopy, Ed. Kai Siegbahn, North Holland Publishing Company, Amsterdam 1965.
12. L. S. KISSLINGER and R. A. SORENSEN: Mat. Fys. Medd. Dan. Vid. Selsk. **32**, no. 9 (1960); in the following called KS I.

13. S. G. Nilsson: Mat. Fys. Medd. Dan. Vid. Selsk. **29**, no. 16 (1955);
B. Mottelson and S. G. Nilsson: Mat. Fys. Skr. Dan. Vid. Selsk. **1**, no. 8 (1959).
14. B. L. Cohen: Phys. Rev. **127**, 597 (1962).
15. L. Silverberg: Arkiv för Fysik **20**, 341 (1962) and private communication.
16. O. Hansen and O. Nathan: Nucl. Phys. **42**, 197 (1963).
17. B. L. Cohen, R. A. Fulmer, and A. L. McCarthy: Phys. Rev. **126**, 698 (1962).
18. R. H. Fulmer and W. W. Dalhnik: Nuclear Structure Studies in the Ni Isotopes with (d, t) reactions, preprint, March 1965.
19. B. L. Cohen: Phys. Rev. **125**, 1358 (1962).
20. B. L. Cohen: Phys. Rev. **127**, 597 (1962).
21. B. Cujec: Phys. Rev. **131**, 735 (1963).
22. B. L. Cohen and R. E. Price: Phys. Rev. **121**, 1441 (1961).
23. B. Cujec: Private communication.
24. H. Faraggi et al.: Phys. Lett. **13**, 244 (1964);
H. Faraggi: Private communication.
25. D. L. Allan et al.: Nucl. Phys. **66**, 481 (1965).
26. L. Kisslinger: Private communication.
27. R. A. Fulmer: A. L. McCarthy and B. L. Cohen: Phys. Rev. **128**, 1302 (1962). They do not see the $d_{5/2}$ level but expect it to at least 0.6 MeV below $g_{9/2}$.
28. E. Marshalek, L. W. Person and R. K. Sheline: Revs. Mod. Phys. **35**, 108 (1963).
29. F. C. Yang, P. R. Christensen, B. Herskind and R. Borchers: Private communication.
A later interpretation of the experimental data gives the following single-particle energies: $f_{7/2}$: 0, $p_{3/2}$: 0.89, $i_{13/2}$: 1.38, $p_{1/2}$: 1.61, $f_{5/2}$: 1.91 and $h_{9/2}$: 2.00 MeV.
30. V. Gillet, A. Sanderson and A. Green: Phys. Lett. **11**, 44 (1964).
31. S. Hinds et al.: Phys. Lett. **17**, 302 (1965).
32. B. L. Cohen and Paresh Mukherjee: Phys. Rev. **127**, 1284 (1962).
33. V. Gillet: Private communication.
34. M. Crut et al.: Nucl. Phys. **17**, 665 (1960);
H. W. Broek: Phys. Rev. **130**, 1914 (1963);
K. Matsuda: Nucl. Phys. **33**, 536 (1962);
H. Crannel et al.: Phys. Rev. **123**, 923 (1961);
cf. also the references in ref. 1 and ref. 11.
35. R. H. Helm: Phys. Rev. **104**, 1466 (1956).
36. W. Darcey: Private communication and Proceedings of the Paris Conference 1964, Centre National de la Recherche Scientifique, Paris 1965.
37. M. Sakai et al.: Phys. Lett. **8**, 197 (1964).
38. F. K. McGowan, R. L. Robinson, P. H. Stelson and J. L. C. Ford: Nucl. Phys. **66**, 97 (1965).
39. D. Alkazov, J. P. Gangrinskij, J. K. Lemberg, J. I. Udralov: Tibilsi Conference, Februar 1964.
40. R. A. Ricci: Private communication;
G. Gerschel et al.: Proceedings of the Paris Conference 1964, Centre National de la Recherche Scientifique, Paris 1965.
41. H. Crannel et al.: Phys. Rev. **123**, 923 (1961).

42. V. GILLET and N. VINH MAU: Nucl. Phys. **54**, 321 (1964).
43. P. VOGEL: Private communication.
44. K. IKEDA, T. UDAGAWA and H. YAMAMURA: preprint;
B. SØRENSEN: Thesis, Copenhagen 1965.
45. B. ROSNER: Phys. Rev. **136**, B 664 (1964).
46. R. L. SILVA and G. E. GORDON: Phys. Rev. **136**, B 618 (1964).
47. R. K. JOLLY: Phys. Rev. **136**, B 683 (1964).
48. E. VEJE: to be published.
49. LANDOLT BÖRNSTEIN, Zahlenwerte und Funktionen, Neue Serie, Springer Verlag, Berlin 1961.
50. See, e.g., A. M. LANE: Nucl. Phys. **35**, 676 (1962).

Indleveret til Selskabet den 24. november 1965.
Færdig fra trykkeriet den 8. august 1966.